



TECHNISCHE
UNIVERSITÄT
WIEN

DISSERTATION

Optimizing geodetic VLBI schedules with VieSched++

Ausgeführt zum Zwecke der Erlangung des akademischen Grades eines Doktors
der technischen Wissenschaften unter Leitung von

Univ.Prof. Dipl.-Ing. Dr.techn. Johannes Böhm
E120-4

Department für Geodäsie und Geoinformation
Forschungsbereich Höhere Geodäsie

eingereicht an der Technischen Universität Wien
Fakultät für Mathematik und Geoinformation

von

Dipl.-Ing. Matthias Schartner BSc
Matr.-Nr.: 01127723

Wien, 17.12.2019

(Unterschrift Verfasser/in)

(Unterschrift Betreuer/in)

Acknowledgements

First of all, I would like to sincerely thank my supervisor, Prof. Johannes Böhm, without whom this thesis would not have been possible. Johannes supported me in all regards throughout my academic career. He gave me the freedom to follow my own ideas but was also giving me the right directions in case I needed them. For me, he was the best supervisor one can think of.

Another thank you goes to my colleagues from the TU Wien for their support, feedback, and fruitful discussions. Over the years, many of my colleagues became good friends, for which I am very grateful for. It was a pleasure to work in this excellent research group. The same holds for many of my international colleagues who welcomed me with open arms into their community. I would also like to thank my reviewers for their feedback and their ideas for improvement.

Moreover, I want to express my gratitude to all my friends and my family, who have always been there for me. Finally, my biggest thanks go to my girlfriend Laura, who supported me endlessly over the years. Thanks for your love, patience, encouragement, and support. I could not have done this without you.

Abstract

Very Long Baseline Interferometry (VLBI) is a technique that uses globally distributed radio telescopes to observe signals from extragalactic objects to measure their difference in arrival time at the telescopes by cross-correlation. Thereby, VLBI measures the positions and movements of these telescopes as well as the positions of the observed sources and orientation of the Earth in space. Since multiple stations have to observe the same radio sources simultaneously, an observing plan, the so-called schedule, has to be generated.

The generation of a geodetic VLBI schedule can be seen as an advanced optimization problem. It is necessary to optimize the time and observations of every telescope while many boundary conditions exist. A geodetic VLBI schedule is typically generated scan after scan by testing and evaluating all possibilities.

In this work, a general overview about VLBI scheduling is given followed by a discussion of the models and concepts which are used in existing scheduling software, such as subnetting, fillin-mode, and tagalong-mode. The main topic of this thesis is the development of a new VLBI scheduling software which is called VieSched++. The software is written in modern C++ for enhanced performance and uses an object-oriented software design. Every algorithm in VieSched++ is developed from scratch based on the knowledge gained through analyzing existing schedules and scheduling software. The design ideas of these algorithms are discussed in this work in all details.

Since VLBI scheduling is a complex task with many parameters and requirements interfering with each other, VieSched++ is designed to optimize schedules based on a brute-force approach, meaning, that it does not only generate one schedule for a session but is able to generate hundreds of schedules simultaneously by using different scheduling input parameters. These schedules can then be compared based on scheduling statistics or through Monte-Carlo simulations to pick the most appropriate schedule for the given session and scientific goal.

VieSched++ is already used to schedule multiple official observing programs for the International VLBI Service for Geodesy and Astrometry (IVS) and other parties. First results reveal a significant improvement in the accuracy of geodetic parameters during the analysis of sessions scheduled with VieSched++. It was possible to increase the number of observations for the T2 observing program by a factor of two to three and the schedules for the EURR&D program were also improved significantly. On average, the improvement in accuracy of the geodetic parameters is also a factor of two to three.

In summary, this work highlights the need to improve geodetic VLBI scheduling and reveals how this can be achieved.

Kurzfassung

Die Very Long Baseline Interferometry (VLBI) ist ein geodätisches Weltraumverfahren, welches global verteilte Teleskope benützt, um Signale von extragalaktischen Radioquellen zu beobachten. Durch die unterschiedlichen Ankunftszeiten der Signale an den Stationen, welche durch Kreuzkorrelation bestimmt werden, können die Positionen und Bewegungen der Teleskope sowie die Position von Radioquellen und die Orientierung der Erde bestimmt werden. Da mehrere Stationen gleichzeitig dieselbe Quelle beobachten müssen, ist es notwendig einen Beobachtungsplan zu erstellen.

Die Erzeugung eines solchen Beobachtungsplans kann als ein komplexes Optimierungsproblem betrachtet werden. Es müssen die Beobachtungszeiten und die Beobachtungsabfolge unter Einhaltung vieler Nebenbedingungen optimal angeordnet werden.

In dieser Arbeit wird das Problem des Erzeugens von VLBI Beobachtungsplänen erörtert und alle dafür nötigen Modelle und Algorithmen wie subnetting, fillin-mode und tagalong-mode erklärt. Der Hauptteil der Arbeit befasst sich mit der Entwicklung einer neuen, modernen Software namens VieSched++. Alle Algorithmen von VieSched++ wurden basierend auf Erfahrungen von anderen Softwarelösungen und Simulationen für diese Software neu entwickelt. Die Algorithmen werden im Detail erklärt und diskutiert.

Die VLBI Beobachtungspläne werden von vielen verschiedenen und miteinander verwobenen Parametern beeinflusst. VieSched++ versucht dabei, einen optimalen Parametersatz zu finden. Dafür erzeugt die Software viele verschiedene Beobachtungspläne mit unterschiedlichen Parametern. Diese Beobachtungspläne können in Folge basierend auf Monte-Carlo Simulationen verglichen werden.

VieSched++ wird bereits operationell für Beobachtungsprogramme des International VLBI Service for Geodesy and Astrometry (IVS) und für andere Anwendungen eingesetzt. Erste Resultate zeigen eine signifikante Verbesserung der Genauigkeit der geodätischen Parameter. Dabei wurde die Anzahl an Beobachtungen für das T2 Beobachtungsprogramm um einen Faktor von zwei bis drei erhöht. Außerdem wurde das EURR&D Beobachtungsprogramm signifikant verbessert. Im Durchschnitt wurden die Genauigkeiten um einen Faktor von zwei bis drei verbessert.

Zusammenfassend kann gesagt werden, dass sich diese Arbeit mit der Notwendigkeit des Verbesserns von geodätischen VLBI Beobachtungsplänen befasst und zeigt wie diese Verbesserungen erreicht werden können.

Contents

Acknowledgements	I
Abstract	II
Kurzfassung	III
List of Abbreviations	VIII
List of Figures	XII
List of Tables	XIII
1 Introduction	1
1.1 Scientific opportunities	2
1.2 Objectives and outline of this thesis	3
2 Very Long Baseline Interferometry (VLBI)	5
3 VLBI Scheduling	9
3.1 Master schedule	12
3.2 Sked	13
3.3 Sked catalogs	14
3.3.1 Station catalogs	15
3.3.2 Source catalogs	17
3.3.3 Observing mode catalogs	17
3.4 Antenna models	20
3.4.1 Cable wrap	22
3.4.2 Slew time	23
3.4.3 Horizon mask	24
3.4.4 Antenna sensitivity	25
3.5 Flux models	28
3.6 Required scan length	31
3.7 Special scheduling algorithms	33
3.7.1 Subnetting	33
3.7.2 Fillin-mode	35

3.7.3	Tagalong-mode	38
3.7.4	Extending observing time	39
4	Simulations and Analysis	42
4.1	Vienna VLBI and Satellite Software (VieVS)	42
4.1.1	Simulation setup	43
4.1.2	Analysis setup	43
5	VieSched++	45
5.1	Software design	45
5.2	Installation	45
5.3	General scheduling concept	46
5.3.1	Implementations of a scan	48
5.3.2	Scan generation	50
5.3.3	Possible scan start	51
5.3.4	Scan observing duration	52
5.3.5	Subnetting	53
5.3.6	Scan selection	55
5.3.7	Rigorous scan check	56
5.4	Optimization criteria and weight factors	56
5.4.1	Duration	58
5.4.2	Sky-coverage	59
5.4.3	Number of observations per scan	64
5.4.4	Idle time	64
5.4.5	Average observations per station	66
5.4.6	Average observations per sources	66
5.4.7	Average observations per baselines	67
5.4.8	Low elevation	68
5.4.9	Low declination	69
5.4.10	Other	70
5.5	Recursive scan selection	71
5.5.1	Concept	72
5.5.2	Fix scans a priori	74
5.5.3	Fillin-mode a posteriori	76

5.6	Multi-Scheduling feature	76
5.6.1	Multi-core support	78
5.6.2	Interaction with VieVS	79
5.7	Iterative source selection	79
5.8	Parameterization	82
5.8.1	Groups	83
5.8.2	Station based parameters	83
5.8.3	Source based parameters	86
5.8.4	Baseline based parameters	89
5.9	Astrometric optimization	90
5.9.1	Source selection	91
5.9.2	Calibration block	92
5.10	Custom Scan sequence	92
5.11	Scan alignment	93
5.12	Manual and multiple observing modes	95
5.12.1	Simple manual Observing mode	95
5.12.2	Advanced manual Observing mode	95
5.12.3	Mixed-mode observations	96
5.12.4	Multiple observing modes	96
5.13	Sky-coverage quantification	96
5.14	Output	99
6	Results	101
6.1	T2	101
6.1.1	Simulations	103
6.1.2	Real observations	106
6.2	EURR&D	109
6.2.1	Simulations	112
6.2.2	Real observations	113
6.3	INT3	115
7	VGOS simulation study	120
7.1	Optimizing through minimum slew distance	128
7.2	Optimizing through sky-coverage definitions	130

7.3 Optimizing through weight factors	132
8 Summary and Conclusion	134
9 Outlook	136
References	138

List of Abbreviations

- ASD** Allan Standard Deviation
- BBC** Base Band Converter
- CONT** Continuous VLBI Campaign
- CPU** Central Processing Unit
- CRF** Celestial Reference Frame
- DORIS** Doppler Orbitography and Radiopositioning Integrated by Satellite
- EOP** Earth Orientation Parameter
- GGOS** Global Geodetic Observing System
- GNSS** Global Navigation Satellite System
- GUI** Graphical User Interface
- ID** Identifier
- IERS** International Earth Rotation and Reference Systems Service
- IF** Intermediate Frequencies
- IVS** International VLBI Service for Geodesy and Astrometry
- NNR** No Net Rotation
- NNT** No Net Translation
- PWLO** Piece-Wise Linear Offsets
- SEFD** System Equivalent Flux Density
- SNR** Signal to Noise Ratio
- SLR** Satellite Laser Ranging
- SOFA** Standards of Fundamental Astronomy
- TRF** Terrestrial Reference Frame
- UT1** Universal Time
- UTC** Coordinated Universal Time
- VGOS** VLBI Global Observing System
- VieVS** Vienna VLBI and Satellite Software

VLBA Very Long Baseline Array

VLBI Very Long Baseline Interferometry

XML Extensible Markup Language

ccw counter-clockwise cable wrap

csv comma-separated values

cw clockwise cable wrap

n neutral cable wrap

vex VLBI experiment definition

List of Figures

1	Geometric principle of VLBI	6
2	Flowchart of general scheduling concept	10
3	Active VLBI stations participating in IVS sessions in 2019.	12
4	Organization of the sked catalogs	15
5	Antenna dish diameters	21
6	Antenna cable wrap	22
7	Antenna slew times	24
8	Antenna horizon mask	25
9	Antenna sensitivities	26
10	Elevation depending sensitivities	27
11	Flux density of source 0059+581 over time	28
12	Flux density model for source 3C274 - baseline length model	29
13	Flux density of source 0458-020 - elliptical gaussian model	30
14	Two components of the elliptical gaussian flux model of source 0458-020 . .	31
15	Required scan length for reaching target Signal to Noise Ratio (SNR) based on antenna System Equivalent Flux Density (SEFD) and source flux density	32
16	Schematic representation of subnetting	34
17	Concept of fillin-mode	36
18	Comparison of different fillin-mode approaches	38
19	Concept of tagalong-mode	39
20	Concept of extending observing time in case of available idle time	40
21	Flowchart of VieSched++ concept	47
22	Main components of a scan in VieSched++	49
23	Example of a subnetting situation	54
24	Available functions for calculation of sky-coverage saturation based on an- gular distance and time between two observations	61
25	Sky-coverage score examples based on combination of different transfer func- tion	63
26	Low elevation score function	69
27	Low declination score function	70
28	Concept of recursive scan selection	73
29	Recursive scan selection flowchart	75

LIST OF FIGURES

30	Iterative source selection flowchart	81
31	High and low elevation score functions during calibration blocks	92
32	Source sequence flowchart	93
33	Comparison of different scan alignment approaches	94
34	Sky-coverage score calculation flowchart	97
35	Sky coverage area distribution for 13, 25 and 37 areas	99
36	Antennas participating in recent T2 sessions	101
37	Simulated station coordinate repeatabilities of T2 sessions	104
38	Simulated Earth Orientation Parameter (EOP) repeatabilities of T2 sessions	105
39	Number of observations scheduled, correlated, recoverable and used for the T2 sessions	106
40	Formal errors of EOP estimates from T2 sessions	107
41	Formal errors of 3D-station coordinate estimates of T2 sessions	108
42	Antennas participating in recent EURR&D sessions	109
43	sky-coverage of selected stations of EURR&D sessions	111
44	Simulated EOP repeatabilities from EURR&D sessions	112
45	Simulated station coordinate repeatabilities of EURR&D sessions	113
46	Number of observations scheduled, correlated, recoverable and used for the EURR&D sessions	114
47	Formal errors of EOP estimates from EURR&D sessions	115
48	Formal errors of 3D-station coordinate formal errors of EURR&D sessions .	116
49	Antennas participating in recent INT3 sessions	117
50	Number of observations for INT3 sessions scheduled in 2018 and 2019 . . .	118
51	UT1 formal error accuracy for all intensive sessions	119
52	UT1 formal error accuracy for all INT3 sessions	120
53	VT9175 antenna network	121
54	Histogram of scheduling statistics for all generated schedules	123
55	Histogram of the time spent during the VLBI Global Observing System (VGOS) sessions for all generated schedules	124
56	Histogram of the estimated repeatabilities for geodetic parameters based on Monte-Carlo simulations	125
57	Number of observations versus sky-coverage score - geodetic results	127
58	Number of observations versus sky-coverage score - weight factors	128
59	Ratio of weight factors used to generate the VT9175 schedules	129

LIST OF FIGURES

60	Impact of different minimum slew distances on geodetic results	130
61	Impact of different sky-coverage definitions on geodetic results	131
62	Correlations between scheduling parameters including weight factors and sky-coverage definitions with geodetic results	133

List of Tables

1	List of IVS observing programs organized via the schedule master for the year 2019	13
2	List of all possible scans which are evaluated from a situation displayed in Figure 16 by using subnetting.	55
3	List and description of station based parameters	84
4	Constant station (overhead) times and cable wrap buffers	85
5	List and description of source based parameters	86
6	List and description of baseline based parameters	90
7	Scheduling statistics for T2 sessions	102
8	Scheduling statistics of EURR&D sessions	110
9	Number of stations per scan for EURR&D sessions	111
10	Antennas participating in VT9175 and their key attributes for scheduling. .	121
11	Key scheduling parameters used to generate the optimized schedule based on the results from the repeatabilities.	123

1 Introduction

Geodetic Very Long Baseline Interferometry (VLBI) is one of the four space geodetic techniques, together with Global Navigation Satellite System (GNSS), Satellite Laser Ranging (SLR), and Doppler Orbitography and Radiopositioning Integrated by Satellite (DORIS). It plays an important role in the realization of the Terrestrial Reference Frame (TRF) (Altamimi et al., 2016), in particular of its scale, and has the unique capability to determine the Celestial Reference Frame (CRF) at radio frequencies (Fey et al., 2015). Furthermore, it is widely used to determine the orientation of the Earth in space, which is critical for positioning and navigation, both on Earth and in space. Today it is the only technique capable of providing the full set of Earth Orientation Parameters (EOPs) consisting of the Earth rotation angle $dUT1$, two parameters for polar motion $[x_{pol}, y_{pol}]$, and two parameters for precession and nutation $[dX, dY]$ (Petit and Luzum, 2010). In particular, the direct determination of the precession/nutation parameters of the Earth as well as the Earth rotation angle is uniquely possible with VLBI (Schuh and Böhm, 2013). Additionally, interactions within the Earth system such as geodynamic and atmospheric parameters can be studied as well (Spicakova et al., 2010; Hobiger et al., 2006).

Due to the observing principle of VLBI it is necessary to synchronize observations between different antennas over the world. It must be ensured that multiple antennas observe the same source, which is typically an extragalactic radio source, simultaneously. Therefore, each VLBI session starts by generating an observing plan, the so-called schedule.

VLBI observations are organized in sessions. Typically, a VLBI session is either 1-hour or 24-hours long and a fixed set of multiple antennas are participating in each session. For sustainable resource management international collaborations such as the International VLBI Service for Geodesy and Astrometry (IVS) (Nothnagel et al., 2017) are organizing VLBI sessions globally using a so-called master schedule listing all VLBI sessions for the upcoming year.

The generation of geodetic VLBI schedules can be quantified as an advanced optimization problem. During the scheduling process, there is the freedom to select which extragalactic radio sources should be observed, in which sequence they should be observed and how many of the available antennas should observe them simultaneously. During a 24-hour session, the number of scans is around 1000 and around 100 sources are observed. Therefore, the number of possible schedules for a single session is incredibly high, see section 3, and by far outnumbers the number of atoms in the known universe. Since it is not

possible to test and evaluate all possible schedules, simplifications and generalizations are necessary to generate a schedule that is considered “good” within a reasonable amount of time. So far, the definition of a “good” schedule is mostly done based on the number of observations although other metrics, like the distribution of observations on the sky above a station, the so-called sky-coverage, is also known to significantly influence the quality of the result.

1.1 Scientific opportunities

Although optimizing a schedule directly influences the number and distribution of observations which are available during the analysis, little research work has been done during the last couple of years to improve scheduling.

If so, most of the research focused on improving the intensive schedules which are observed daily to measure $dUT1$, the difference between the Universal Time (UT1) defined through the Earth rotation and the Coordinated Universal Time (UTC) $dUT1 = UT1 - UTC$. Typically, only two stations are participating in these sessions and they only observe for one hour with low recording rate to reduce the time delay between the observations and the analysis providing a rapid estimation of $dUT1$. Multiple studies indicate that observations near the corners of the mutual visibility between the participating stations reduce the $dUT1$ formal errors for intensive sessions (Uunila et al., 2012). A lot of research focused on preselecting sources for intensive schedules intending to generate schedules with good sky-coverage while only observing strong sources and thus reducing the observing time per scan (Baver et al., 2012; Baver and Gipson, 2013, 2014, 2018; Gipson and Baver, 2016). Another intensive scheduling approach based on so-called “Impact-Factors” was developed by Leek et al. (2015). However, since intensive sessions are typically only one hour long and only consist of two stations, scheduling intensive sessions is very simple compared to scheduling a global 24-hour session. Furthermore, the goal of intensive sessions is clearly defined as measuring $dUT1$, while the goal of a 24-hour session can be more complex such as measuring all EOPs in conjunction with station coordinates and source positions. Therefore, intensive scheduling concepts and algorithms cannot be easily applied for 24-hour sessions.

With the development of the new VLBI Global Observing System (VGOS) with its fast slewing antennas, new demand on more research based on VGOS scheduling arose (Petra-chenko et al., 2009). A new source-based scheduling approach for VGOS was developed

by Sun et al. (2014) as part of their scheduling program “Vie_Sched”. Another approach based on dynamic scheduling is introduced by Lovell et al. (2016). However, optimizing VGOS scheduling is still an open research topic and improvements to existing scheduling programs are needed (Niell et al., 2018). Additionally, extensions to existing scheduling software are necessary to fully support the new observing modes used in VGOS.

Besides the rapid estimation of $dUT1$ during intensive sessions, the main VLBI products are EOP time series, as well as station and source coordinates provided through 24-hour sessions. Very little research has been done in optimizing the scheduling of these 24-hour sessions. Currently, almost all of these sessions are scheduled using the same software, called “sked” which is developed and maintained by the Goddard Space Flight Center’s IVS Analysis Center “GSFC”. Unfortunately, most schedules are simply generated by using the same parameters as always regardless of the antenna network and some schedulers spend very little effort in trying to optimize these schedules

1.2 Objectives and outline of this thesis

In this work, a new VLBI scheduling software called VieSched++ is presented. Similar as sked and Vie_Sched, VieSched++ uses a brute force approach to generate the schedules, see sections 3 and 5. Although some ideas are based on those two software packages, every algorithm and concept of VieSched++ is redesigned and written from scratch. In contrast to existing scheduling software, which inserts scans in sequential order into the schedule, VieSched++ provides a recursive scan selection which helps to minimize station idle time. Furthermore, it fully automates the optimization of schedules through another brute force approach of generating multiple schedules using varying parameters. Great care was taken to ensure a sophisticated definition of optimization conditions which are used to decide which scans should be selected in the schedule. The software is written in modern C++, reducing the run time of the generation of a schedule, which is problematic in other scheduling software like Vie_Sched.

1. INTRODUCTION

The main objectives of VieSched++ can be summarized as the following:

Requirements for VieSched++

- provide an easy-to-use software, which is flexible, powerful and generates high-quality schedules for intensive, 24-hour, and VGOS session.
- automate the optimization of VLBI schedules for any given network, source list, and scientific goal
- simplify interactions with existing VLBI software, in particular with Vienna VLBI and Satellite Software (VieVS), for selecting and comparing schedules based on Monte-Carlo simulations instead of scheduling statistics like number of observations
- high performance for a fast generation of schedules and possibility to carry out large-scale studies

Section 2 gives an introduction to the geodetic VLBI technique in general. Section 3 presents a detailed overview of VLBI scheduling as well as the general antenna (3.4) and source-based models (3.5) that are used. Furthermore, it discusses special scheduling concepts such as subnetting (3.7.1), fillin-mode (3.7.2) and tagalong-mode (3.7.3). Section 4 gives a short overview of the analysis of geodetic VLBI sessions and how these sessions can be simulated. This section focuses only on topics needed to understand this thesis and the upcoming results. In particular, it focuses on the VieVS package. Section 5 is the main part of this thesis. It lists the design concept of VieSched++ and gives a detailed explanation of the algorithms and models used in the software. Furthermore, it gives insight in parts of the implementations of scheduling in VieSched++ (5.3) as well as the parameters which can be used to fine-tune the generated schedules (5.8). It reveals how the scan selection during the scheduling process is done based on newly developed optimization criteria and weight factors (5.4). Main features such as the recursive scan selection (5.5) and the multi-scheduling feature (5.6) are discussed in detail. Finally, section 6 briefly summarizes improvements gained by changing the scheduling software to VieSched++.

2 Very Long Baseline Interferometry (VLBI)

In this section, a summary of the early history, as well as the basic concepts of VLBI, is provided. Further information about VLBI in general can be found in [Sovers et al. \(1998\)](#), [Campbell \(2000\)](#), [Kellermann and Moran \(2001\)](#), [Petrov et al. \(2009\)](#), [Nothnagel \(2019\)](#), and the references therein. More information about the history of VLBI can be found in [Schuh and Böhm \(2013\)](#).

The development of VLBI started in the mid-1960s by radio astronomers, see [Matveenko et al. \(1965\)](#) and [Broten et al. \(1967\)](#). It is an outgrowth of radio interferometry with cable connected antennas, which was made possible with the development of stable atomic time and frequency standards ([Moran et al., 1967](#)). Soon after VLBI was used by radio astronomers, the potential of VLBI was recognized for geophysical applications ([Gold, 1967](#); [Shapiro and Knight, 1970](#)) and first experiments were carried out ([Hinteregger et al., 1972](#); [Shapiro et al., 1974](#)).

Since the 1970s, the technique rapidly improved due to technological improvements like the wide spanned bandwidths made possible by the bandwidth synthesis technique ([Rogers, 1970](#)), low system temperature cryogenic receivers and dual-frequency observations to correct dispersive effects on the radio signal due to the Earth's ionosphere as well as due to improvements in data processing methods and physical models ([Petit and Luzum, 2010](#)). In the 1980s it was for the first time possible to estimate the length change of a transatlantic baseline over time ([Herring et al., 1986](#)). While the station coordinate accuracy was a few meters at the beginning, it is nowadays at the sub-centimeter level ([Schlüter and Behrend, 2007](#)).

VLBI measures the difference in arrival time of signals from objects, mostly extragalactic radio sources, in radio frequencies. Therefore, at least two stations have to observe the same source simultaneously. Since the extragalactic radio sources are very far away, up to billions of light-years, its radiation can be assumed to arrive as plane wavefronts on Earth and the direction to the source \vec{s}_0 becomes parallel for all ground-based stations. Thus, the geometric principle of VLBI reduces to a simple rectangular triangle. The observed difference in arrival time τ , defined as the difference between the arrival time of the signal between two stations 2 and 1 $t_2 - t_1$, can be expressed through the baseline vector \vec{b} between the two stations, the direction to the radio source \vec{s}_0 and the velocity of light c , see Figure

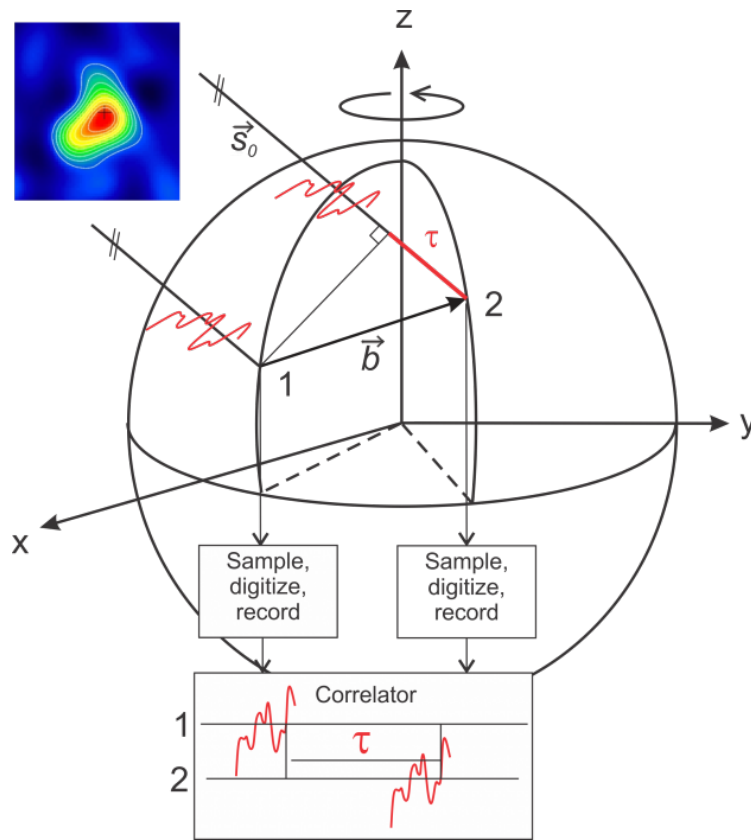


Figure 1: Geometric principle of VLBI (Schuh and Böhm, 2013).

1 and equation (1) (Campbell, 2000).

$$\tau = -\frac{\vec{b} \cdot \vec{s}_0}{c} = t_2 - t_1 \quad (1)$$

The observing principal highlights the necessity of organizing the VLBI observations via a schedule since two stations have to observe the same source simultaneously to form an observation. Typically, the necessary observing time is defined through a desired Signal to Noise Ratio (SNR) and is calculated based on the recording rate, the sensitivity of the two stations and the luminosity of the source, see section 5.3.4.

Often, more than two stations are observing the same source simultaneously leading to multiple observations. The sum of all simultaneously recorded observations of a source at a particular time is called a scan.

2. VERY LONG BASELINE INTERFEROMETRY (VLBI)

In geodetic VLBI, the signals of the observed radio sources are typically recorded in 16 individual channels, 6 within S-band (2.3 GHz) and 10 within X-band (8.4 GHz). The two frequency bands are necessary to correct dispersive effects on the radio signal due to the Earth's ionosphere. Since the luminosity of the source described through its signal flux density is very low, in the order of 1 Jansky ($1 \text{ Jy} = 1 \times 10^{-26} \frac{\text{W}}{\text{Hz m}^2}$), high recording rates or long observing times are needed. Today, the observing rate of standard SX observations vary between 128 Mbit/s and 1 Gbit/s and the observing times are between 30 and 600 seconds.

Around the beginning of the new millennium, the Global Geodetic Observing System (GGOS) (Plag and Pearlman, 2009) defined a major goal of providing a TRF with an accuracy of 1 millimeter in station position and stability of 0.1 millimeters per year. To reach this goal, considerations of a next-generation VLBI system, initially called VLBI2010 but later renamed to VGOS were carried out (Niell et al., 2005) and requirements were defined (Petrachenko et al., 2009). With the new VGOS, the frequency setup changed to observing channels between 2 and 14 GHz with very high data rates. Today, VGOS observations are recorded with 8 Gbit/s at 4 frequency bands and plans exist to move to 16 Gbit/s soon.

The observed signal is digitized, recorded on disks, marked with highly precise time-stamps provided through hydrogen masers and sent to the correlator. Today, some of the data can be sent via broadband internet links but since the amount of data is very large, in the order of multiple Terabytes, disks still have to be shipped from some locations.

At the correlator, the recorded signal from the antennas is combined pairwise producing an interference pattern as described in Sovers et al. (1998). The difference in arrival time τ can be estimated by comparing the recorded bitstreams at the two antennas $s_1(t)$ and $s_2(t)$ by using cross-correlation. The maximum of the cross-correlation function C_{12} is searched through shifting one of the bit-streams in time as shown in equation (2a) and equivalently in equation (2b) (Nothnagel, 2019).

$$C_{12}(\tau) = \frac{1}{T} \int_{-\infty}^{\infty} s_1(t) \cdot s_2^*(t - \tau) \cdot dt \quad (2a)$$

$$C_{12}(\tau) = \frac{1}{T} \mathcal{F}^{-1} \left(\mathcal{F}(s_1) \cdot \overline{\mathcal{F}(s_2)} \right) \quad (2b)$$

In equation (2a), T represents the averaging interval, the asterisk denotes the complex conjugate and τ corresponds to the difference in signal arrival times between the two

2. VERY LONG BASELINE INTERFEROMETRY (VLBI)

stations. In equation (2b), \mathcal{F} and \mathcal{F}^{-1} are the Fourier and inverse Fourier transforms and the long bar indicates the complex conjugate operator. Today, software correlators such as DiFX (Deller et al., 2007, 2011) are used in conjunction with high-performance computers to correlate VLBI data.

During the correlation process, amplitude and phase are determined for each frequency channel. In the so-called post correlation processing, the phase, group delay and phase rate are fitted to the phase samples from the various frequency channels, with the group delay being the prime observable in geodetic VLBI (Schuh and Böhm, 2013).

The resulting group delays can be analyzed by a least-squares parameter estimation algorithm or other methods like Kalman filters. For the parameter estimation, systematic effects presented in the raw observations have to be removed since they limit the accuracy of the results. One requirement for the least-squares parameter estimation is that the observation equation has to be linear. This is achieved by linearizing the VLBI observation equation by a first-order Taylor expansion. Precise a priori information is necessary for the Taylor expansion to work with sufficient accuracy. Based on the precise a priori information and by using models with the highest precision as described in the International Earth Rotation and Reference Systems Service (IERS) conventions (Petit and Luzum, 2010) the theoretical delay can be modeled and the parameters can be estimated. Since some effects are too variable and too hard to predict with sufficient accuracies, like the tropospheric wet delay and clock drifts, these parameters have to be estimated as well and cannot be modeled. More information about the analysis of VLBI sessions and the modeling of the theoretical delay is provided in Schuh and Böhm (2013).

3 VLBI Scheduling

Geodetic and astrometric VLBI sessions can be classified into three different groups: 24-hour SX sessions, 1 to 2-hour intensive sessions and 24-hour VGOS sessions. A fixed antenna network is assigned to each session and can be used for carrying out observations. One of the first tasks for every VLBI session is to generate a schedule. The scheduler has to decide which sources should be observed, how long to integrate and in which sequence the sources should be observed. Simplified speaking, a schedule is a list defining for each station which sources should be observed in which order and when the recording should start and stop. It also adds additional information on how the observations should be recorded, for example, which sample rate should be used and which frequencies should be observed.

A typical 24-hour VLBI session contains roughly 1000 scans. Considering a list of 300 sources which can be observed during a session, the total number of possible schedules can theoretically become 300^{1000} or 1.3×10^{2477} . However, for a typical 24-hour global VLBI session schedules are usually created using subnetting, see section 3.7.1, which means that two sources are simultaneously considered during the scheduling process, which increases the complexity of a schedule and leads to a total of $\left(\frac{300 \cdot 299}{2}\right)^{1000}$ or 5.7×10^{4651} possibilities. As a reference, the estimated number of atoms in the known universe is around 1×10^{80} .

Not all of these theoretically possible schedules are also practically possible because sources might not be above the horizon of multiple antennas at a time and other constraints need to be considered leading to a considerably smaller number of admissible schedules. However, the number of admissible schedules is still huge enough that it can be exploited for optimization.

Usually, a so-called scheduling software is used to prepare the schedule and automate this process. Only a handful of scheduling software exist which can generate VLBI schedules like sked (Vandenberg, 1999), sched (Walker, 2018), Vie_Sched (Sun, 2013) and VieSched++ (Schartner and Böhm, 2019c). Usually, the scheduling software is creating the schedule scan after scan, as indicated in Figure 2 (Gipson, 2016). It starts selecting scans at the beginning of a session and tests observations to every possible combination of sources at a specific time, compares them by some metrics and finally decides which scan is considered the best by these metrics and adds it to the schedule. After a scan is scheduled, the software moves on in time and the whole process starts over again by testing every possible next

3. VLBI SCHEDULING

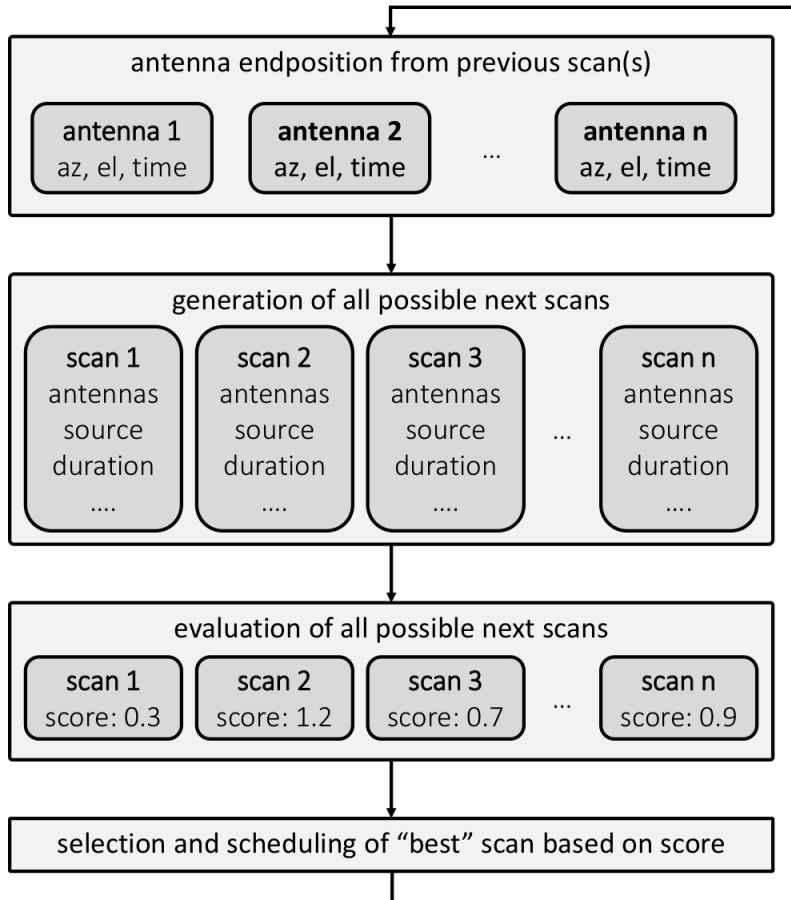


Figure 2: Flowchart of general scheduling concept based on the generation of schedules on a scan-by-scan basis

scan. This is repeated until the schedule is completed.

The tricky part is to decide which metrics should be used for comparison of individual scans. A rule of thumb for comparing VLBI sessions is *“a higher number of observations yields to a better schedule”* (Gipson, 2010). The idea behind this rule is, that a high number of observations increases the redundancy and averages out random errors. Another rule of thumb says *“the better the sky-coverage, the better the schedule”*. The idea behind this rule is, that evenly distributed observations help to estimate tropospheric delays, which are considered the dominating error source in VLBI (Böhm et al., 2006). Although both of these rules are true, the problem is that they are competing against each other.

Sky-coverage is considered good if within a certain time interval, like 30 minutes, the

3. VLBI SCHEDULING

station records observations at different azimuth and elevation angles. However, providing evenly distributed observations over the sky means that the station needs to slew a lot to reach these different angles. While a station is slewing, it is not possible to record observations leading to a lower number of scans and thus observations.

In contrast, if the goal is to schedule as many observations as possible, the station has to observe a lot. Since the observing time per scan is limited by the antenna System Equivalent Flux Density (SEFD), the source flux density, the recording mode, and the target SNR (see section 3.6) it is not possible to save time here, unless the observing mode is changed. The same is true for calibration time and necessary overhead time needed for field system commands which are usually fixed as well. The only available point where time can be saved is slew time. Therefore, if the goal is to schedule a high number of observations it is necessary to save time by minimizing the slew time as much as possible, leading to poor sky-coverage. One of the main challenges for generating optimized schedules is to find the sweet spot between a good sky-coverage and a high number of observations.

Another problem arises since a scheduling software is generating the schedules scan after scan by selecting the “best” scan at a certain time from a pool of possible scans. The problem is that all possible scans have to be compared with each other which is far from trivial. For example, time is one of the most critical factors for scheduling VLBI sessions and has to be considered during this comparison. It might be advantageous to not schedule the scan which would lead to the highest number of observations or best sky-coverage improvements if it would take too long to observe this scan. Often it is beneficial to select scans which are slightly worse in terms of their performance but can be observed faster. This could result in situations where scheduling a high number of slightly imperfect scans would lead to an overall improvement compared to scheduling a smaller number of perfect scans.

Together, these three quantities, namely the number of observations, the sky-coverage and the duration of a scan are the most important parameters a scheduling software has to keep in mind when comparing scans to generate a good schedule. These factors are used as optimization criteria during the scheduling process, see section 5.4. Every scan is given a score based on these and other optimization criteria and this score is further used as the metric to compare all possible scans at a certain time to pick the “best” one. One of the most challenging aspects while developing a scheduling software is to provide a sophisticated definition of these optimization criteria leading to a good scan selection.

3. VLBI SCHEDULING

3.1 Master schedule

Since VLBI is a global endeavor with stations and institutes working together all over the world, tasks have to be organized properly. In this activity, the IVS plays an important role. The IVS master schedule, or Masterfile, is a list of all geodetic and astrometric sessions within the IVS. Every session can be identified by unique experiment codes. Additionally, it includes the session start date, duration, participating stations as well as which institution is responsible for scheduling, correlation, and analysis of the session. The IVS master schedule is available at <https://ivscc.gsfc.nasa.gov/sessions/>. Currently¹ 184 24-hour sessions and 460 intensive sessions are organized via the master schedule for the year 2019 as well as bi-weekly VGOS experiments. The master schedule organizes activities of almost 50 stations including the Very Long Baseline Array (VLBA) visualized in Figure 3.

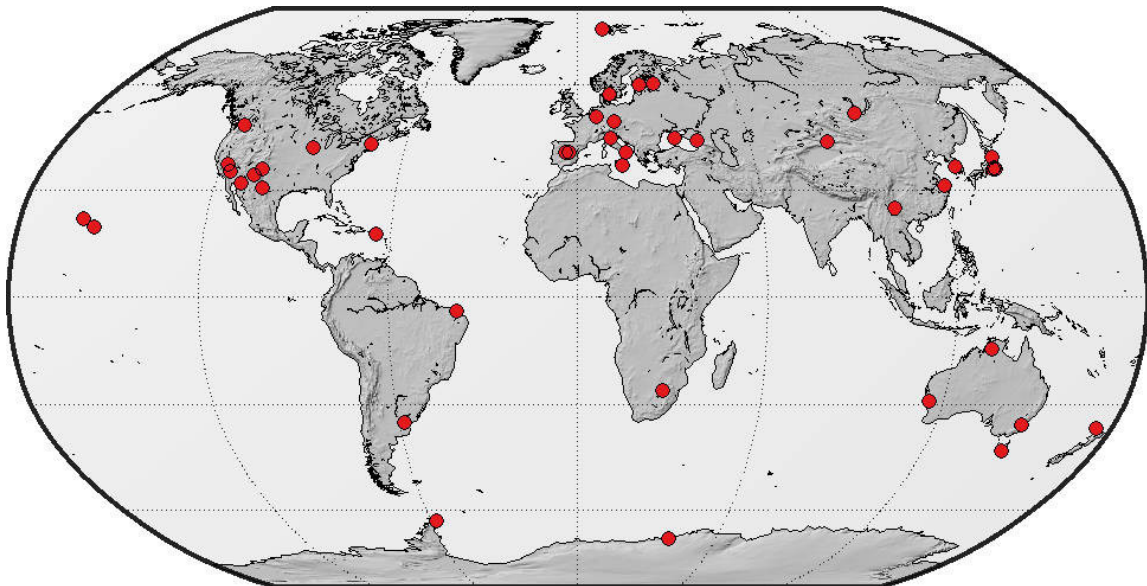


Figure 3: Active VLBI stations participating in IVS sessions in 2019 including the VLBA.

Table 1 lists the observing programs for the year 2019. On average a 24-hour session contains ≈ 10 stations. One exception are sessions focusing on the southern hemisphere, like AUA, CRDS and CRF sessions. Due to the lack of southern stations, which can also be seen in Figure 3, the average number of participating stations is considerably smaller. In contrast, typically more than 20 stations are participating per T2 session. Table 1 lists

¹checked at 25. April 2019

3. VLBI SCHEDULING

the average of all scheduled stations per session. However, oftentimes single stations can drop out of a session due to maintenance or technical problems leading to a lower average number of stations per session in reality.

Table 1: List of IVS observing programs organized via the schedule master for the year 2019. The top lists the 24-hour sessions while the bottom lists intensive sessions. In the session code, xx and xxx stands for a two or three digit consecutively increasing number while yy is the placeholder for the two digit year and doy is a placeholder for the day of the year.

Program	Code	duration [h]	#sessions	#stations
AOV	AOV xxx	24	12	9.1
APSG	APSG xx	24	2	10.0
AUS-AST	AUA xxx	24	12	5.8
IVS-CN	CN xxx	24	6	10.0
IVS-CRDS	CRD xxx	24	6	5.0
IVS-CRF	CRF xxx	24	6	6.2
EUROPE	EUR xxx	24	2	8.5
EURR&D	EURD xx	24	4	8.8
IVS-OHG	OHG xxx	24	6	8.7
IVS-R&D	RD $yyxx$	24	10	8.6
IVS-R1	R1 xxx	24	53	10.2
IVS-R4	R4 xxx	24	52	10.2
IVS-T2	T2 xxx	24	7	20.9
VLBA	RV xxx	24	6	14.0
IN1	I $yydoy$ or W $yydoy$	1 or 2	307	2.5
IN2	Q $yydoy$	1	104	2.0
IN3	Q $yydoy$	1	49	4.2

3.2 Sked

Sked is an interactive command-line program that helps prepare schedules for VLBI observing sessions (Vandenberg, 1997; Gipson, 2010, 2016). The software is developed and maintained by Goddard Space Flight Center. Currently, it is the most used scheduling software for geodetic VLBI. With sked, it is possible to

- enter an entire schedule interactively
- automatically let the software create a schedule

- edit an existing schedule
- list, check, evaluate and summarize a schedule.

In automatic mode, sked generates a schedule until the end time of the session is reached. New scans are added to the schedules scan-by-scan until the end of the last scan finishes later than the session end time (Gipson, 2016). Thereby, it schedules new scans in a strong sequential time ordering, meaning that the next scheduled scan is always occurring after the previous scan ends.

Sked calculated a source visibility table, which is a table that indicates which sources are visible by which station providing a list of possible scans. So-called “*major options*” together with the SNR targets determine which of the possible scans are generated and kept for further consideration. Major options can be the minimum angular distance between scans, the minimum angular distance of a source from the sun or the maximum allowable slew time of an antenna to the observed source. Afterwards, sked does an initial ranking either by comparing the covariance matrix of the observations or sky-coverage and is removing a certain percentage of low-quality scans. Finally, so-called “*minor options*” are used to assign a score to each scan based on some criteria like the number of observations per scan or the number of low observations at low elevation. The scan with the highest score is then selected and scheduled and the process is repeated until the end time is reached. A detailed description of sked and the sked commands can be found in Gipson (2016).

3.3 Sked catalogs

To create a VLBI schedule it is necessary to have access to information about the participating stations as well as about the observed sources and the observing mode which should be used. Most VLBI antennas are unique and they vary greatly in terms of slew speed (see section 3.4.2), cable wrap limits (see section 3.4.1) and sensitivity (see section 3.4.4). The same is true for sources. While some sources are very bright and compact some are faint and have significant structure (see section 3.5). Additionally, the recording hardware can be different at different stations. All this has to be considered during the generation of a schedule.

The information necessary to generate a schedule is bundled and updated in the so-called sked catalogs (Vandenberg, 1999). They are organized in three groups as indicated in Figure 4, catalogs related to stations (see section 3.3.1), sources (see section 3.3.2)

3. VLBI SCHEDULING

and observing mode (see section 3.3.3). A detailed description of the content of the sked catalogs and the entries is available in [Vandenberg \(1999\)](#).

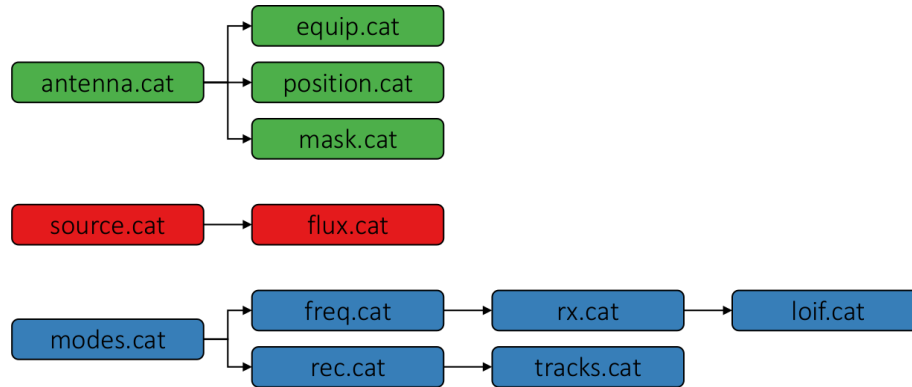


Figure 4: Organization of the sked catalogs.

The sked catalogs are de facto standard for creating geodetic and astrometric schedules within the IVS. They are maintained and updated by the Goddard Space Flight Center and serve as input for various scheduling software like sked, Vie_Sched and also VieSched++.

3.3.1 Station catalogs

Station dependent information is organized in four different catalogs connected via individual Identifiers (IDs) as indicated in the following box. A detailed description of the catalog entries can be found in [Vandenberg \(1999\)](#).

3. VLBI SCHEDULING

```
antenna.cat:
ID Name      Axis Offset Rate1 C1 Lim11 Lim12 Rate2 C2 Lim21 Lim22 Diam PO EQ MS
V WETTZELL AZEL 0.0 180.0 0 251.5 831.0 90.0 0 5.0 89.0 20.0 Wz 33 Wz

equip.cat:
Antenna      ID DAT_Name Heads Tape_len SEFD SEFD Equip
WETTZELL     33 WETTZELL 2x56000 17640 X 750 S 1115 DBBC MARK5B

position.cat:
ID Name      X (m)      Y (m)      Z (m)      Occ.Code Lon Lat Source
Wz WETTZELL 4075539.899 931735.270 4801629.351 72247801 347.12 49.15 GLB1069

mask.cat:
C Name      ID az1 e11 az2 ... eln-1 azn (step wise)
H WETTZ13N Wn 0 5 360
C Name      ID az1 e11 az2 ... eln-1 azn eln (line segments)
H HARTRAO Hh 0 7 90 9.5 100 7 110 8 120 7 300 9 320 9.5 330 9 350 7 360 7
```

antenna.cat This catalog holds information about antenna characteristics such as antenna mount, slewing speed along the individual axes, cable wrap limits per axes and antenna diameter. Additionally, it notes IDs which are used in the other station based catalogs for identification of corresponding elements.

equip.cat This catalog holds information on the equipment at a station. The corresponding entry for an antenna is identified via an ID defined in the antenna.cat. It lists which recorder and rack are used at each station as well as the SEFD information per band. Additionally, elevation dependent SEFD parameters (see section 3.4.4) can be listed.

position.cat The position catalog lists the geodetic earth-centered-earth-fixed coordinates per station. The corresponding entry for an antenna is identified via an ID from the antenna.cat file. For user convenience the geodetic west longitude and north latitude is listed as well.

mask.cat If necessary, this catalog defines a horizon mask for a station. The corresponding horizon mask of a station can be found via the ID from the antenna.cat file. There are two input formats available, one as a representation of a step function and one as a representation of line elements (see section 3.4.3). If an even number of parameters are

3. VLBI SCHEDULING

listed, the horizon mask is represented with line elements, an odd number indicates the representation as a step function.

3.3.2 Source catalogs

Source related information is organized in two individual catalogs and the source name serves as a link between those as indicated in the following box. A detailed description of the catalog entries can be found in [Vandenberg \(1999\)](#).

```
source.cat :
IAU-Name Common hh mm ss.ssss   sdd mm ss.sssss epoch Vel.  source
0059+581 $          01 02 45.762382 +58 24 11.13660 2000.0 0.0  ICRF2 def

flux.cat :
NAME Band Type Flux MajAx Ratio PA Off1 Off2
0059+581 X M 2.00 0.30 1.00 0. 0.0 0.0
0059+581 S M 2.13 1.50 1.00 0. 0.0 0.0
NAME Band Type Base1 Flux1 Base2 Flux2 ... Fluxn-1 Basen
3C274 S B 0 1.41 900 1.16 1530 0.92 2600 0.69 4420 0.45 7520 0.36 12800
3C274 X B 0 1.02 900 0.84 1530 0.65 2600 0.47 4420 0.41 7520 0.41 12800
```

source.cat This catalog lists source positions with right ascension and declination values of ≈ 700 sources. An additional catalog called “*source.cat.geodetic.good*” is also part of the official sked catalogs, which includes only ≈ 300 sources which are especially suitable for geodetic VLBI.

flux.cat This catalog holds source strength and structure information. There are two possible formats of how this information is provided, either as step function profiles as a function of the baseline length, indicated as type “*B*” or based on an elliptical Gaussian model indicated as type “*M*”, see section 3.5. The flux information is provided for each band individually.

3.3.3 Observing mode catalogs

Observing modes are organized via six different catalog files and linked through keywords as indicated in the following box. Previously, there have been seven catalog files including

3. VLBI SCHEDULING

hdpos.cat which is already deprecated since it is related to tape recording. A detailed description of the catalog entries can be found in [Vandenberg \(1999\)](#).

3. VLBI SCHEDULING

modes.cat:

Mode name **freq.cat** chan_bw samp_rate **rec.cat**
256-16(R1-R4) **GEOSX** 8.0 16.0 **00-16-0-1**

freq.cat:

Name Code Sub-groups **RXname**
GEOSX SX STD **SX_WIDE**

band	pol	sky_freq	SB	ChanID	BBC#	PCFreq
- X	R	8212.99	U	CH1	1	10000.0
- X	R	8252.99	U	CH2	2	10000.0

rx.cat:

RXname
SX_WIDE

Stn.Name	LOIFname
- WETTZELL	ODB_WIDE
- WETTZ13N	TWN_DBBC

rec.cat:

name
00-16-0-1

Stn.Name	HDpos	tracks.cat	Rec.Fmt.
- WETTZELL	MK3V-A	14U2L-1-1-B	Mk34
- WETTZ13N	MK3V-A	14U2L-1-1-B	Mk34
- BADARY	MK3V-A	14U2L-1-1-B	Mk34

loif.cat:

LOIF_name
TWN_DBBC

BBC/VC	IF	Band	Freq	SB
- 1	A1	X	7580	U
- 2	A1	X	7580	U
- 3	A1	X	7580	U

tracks.cat:

name fanout bits
14U2L-1-1-B 1 1

chan pass (us, ls, um, lm)

- 1	1(-1, 7)
- 2	1(0)
- 3	1(1)

3. VLBI SCHEDULING

mode.cat This is the top-level catalog for the observing modes including the name of the observing mode, the channel bandwidth and sample rate and keywords to *freq.cat* and *rec.cat*.

freq.cat This catalog lists frequency sequences and is linked via a keyword from the *modes.cat* catalog. Besides the sky frequency per channel, it lists which physical Base Band Converter (BBC) number is used per channel. It further defines the keyword for *rx.cat*.

rec.cat This catalog is linked via a keyword defined in *modes.cat*. It holds the recording mode information. It includes keywords for the tracks assignment information of each station defined in *tracks.cat*.

rx.cat This catalog is linked via a keyword defined in *freq.cat*. This catalog holds the receiver setup for each station. It defines the keyword for the *loif.cat* for each station.

tracks.cat This catalog includes the track assignments for each station and is referenced through a keyword from *rec.cat*.

loif.cat This catalog includes the local oscillator frequencies and Intermediate Frequencies (IF) setup. The setup is referenced through a keyword from *rx.cat*.

3.4 Antenna models

Nowadays, almost all antennas used by the IVS are Alt-Azimuth antennas, often also referred to as azimuth elevation or az-el antennas. From all antennas included in the 2019 master schedule, only two antennas are different, namely HARTRAO having an Equatorial mount and HOBART26 with a so-called XY mount. Antennas with Equatorial mounts have a polar axis parallel to the rotation axis of the Earth, and a declination axis while the XY mount has a horizontal fixed axis. The Equatorial mount is suited for easy tracking of radio sources, since the telescope only has to turn around one axis to follow a source, while the XY mount is built especially for spacecraft tracking since the maximum slew distance per angular distance occur near the horizon and not in the zenith as it is the case for Alt-Azimuth antennas [Salzberg \(1967\)](#).

3. VLBI SCHEDULING

The most used Alt-Azimuth design consists of one vertical azimuthal axis and a horizontal altitude/elevation axis. While this is the most symmetrical and thus most stable antenna mount type it is also easier to build than Equatorial or XY mounts. The downside of an azimuth elevation mount is, that real-time coordinate transformations are necessary to transform celestial equatorial source coordinates provided by right ascension and declination to local horizontal coordinates defined by azimuth and elevation. Additionally, it is necessary to slew the antenna around both axes simultaneously to track a source over the sky.

Many VLBI antennas are uniquely built and therefore their characteristics vary greatly. While some antennas have a dish diameter of only 6 meters others span up to 100 meters. Figure 5 displays the dish sizes of all S/X antennas included in the 2019 IVS master schedule up to 40 meters. Two stations, namely EFLSBERG with a 100-meter dish size and TIANMA65 with a 65-meter dish size are not shown. The high occurrence of 25-meter antennas is due to the VLBA.

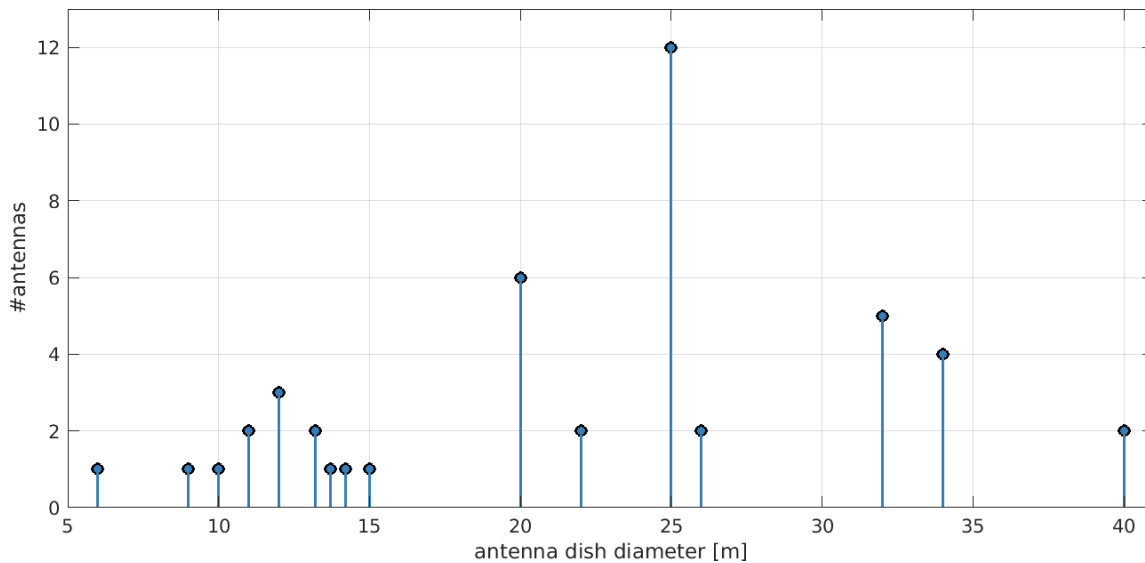


Figure 5: Dish diameter of all S/X antennas included in the IVS master schedule.

Since the antennas vary greatly in terms of size and thus slewing speed and sensitivity, it is necessary to provide unified models which are valid for all antennas.

3.4.1 Cable wrap

Cable wrap is only a concern for az-el antennas. The entire cable is viewed as a single continuous wrap which begins at a certain azimuth and proceeds clockwise through ever-increasing azimuths to the end of the cable (Gipson, 2016). Since the dish is rotating around an azimuthal axis while the cable is connected to equipment fixed at the ground, it is not possible for the stations to slew always in the same direction since the cable would twist around the mount. Therefore, it is necessary to monitor the cable wrap during scheduling to avoid the situation of a twisted cable wrap. If the total angular range is less than 360 degrees, there are no overlaps and the cable wrap position can be determined unambiguously. However, many az-el antennas have a cable wrap bigger than 360 degrees to allow more flexible scheduling and slewing. If this is the case, the unwrapped position of the cable wrap has to be monitored instead, see Figure 6.

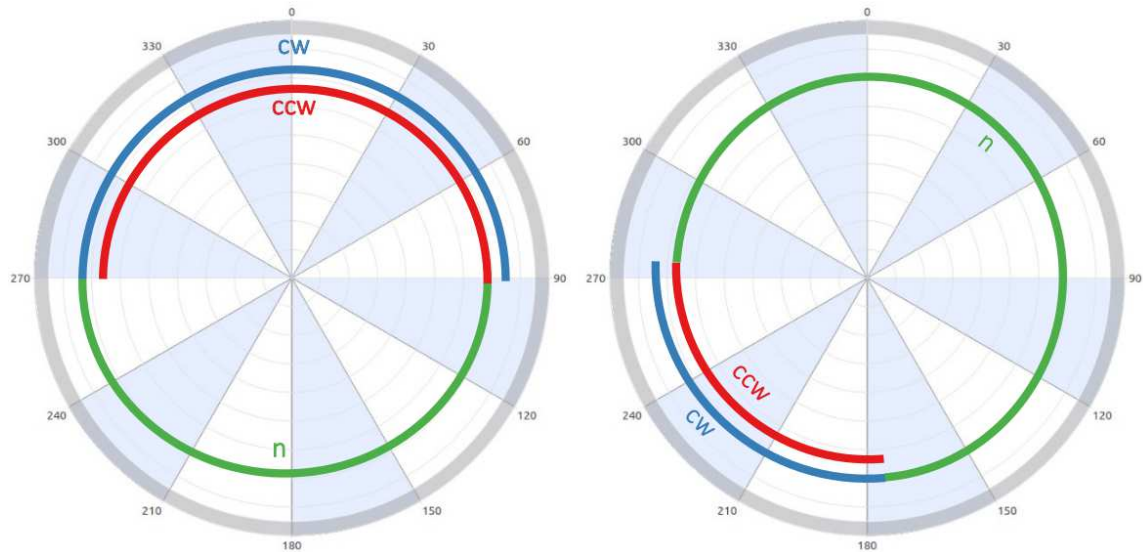


Figure 6: Visualization of the cable wrap for two different stations. The left plot visualizes the cable wrap for WETTZ13N while the right plot visualizes the cable wrap for HART15M. Different cable wrap sections are color-coded.

At the lower limit of the cable wrap, the counter-clockwise cable wrap (ccw) section starts. The ccw section covers the overlapping azimuth range of the cable wrap. After the ccw section, the neutral cable wrap (n) section starts and continues until the overlapping azimuth starts again. In this azimuth range, the cable wrap can be resolved unambiguously.

Afterwards, the clockwise cable wrap (cw) section starts until the upper limit is reached. If the antenna is observing sources in the overlapping areas it is of critical importance to know in which cable wrap section the antenna is located to properly calculate the slew times of the antennas and thus the possible start of the scan.

The cable wrap limits of each station are listed in the sked antenna catalog (see section 3.3.1). Typically, a small error margin is added to the cable wrap limits by the scheduling software to avoid tracking of sources near the limit.

Since the antenna cannot slew unrestricted it is possible that the slew distance between relatively close sources is very big. Considering a situation for WETTZ13N (Figure 6 left) where one source is observed at an azimuth of 280 degrees and the next source should be observed at an azimuth of 260 degrees. Depending on the cable wrap section the antenna is located, the slew distance differs greatly. If the antenna is at the cw section, the slew distance would only be 20 degrees, since the antenna can slew counter-clockwise. However, if the antenna is at the ccw section, it is not possible to slew in the counter-clockwise direction. Instead, the antenna has to slew 340 degrees in the clockwise direction resulting in a way longer slew time.

3.4.2 Slew time

The slew time between two subsequent scans is determined by the angular distance of the sources, the current cable wrap position, the required cable wrap position and the slew rates around the two rotation axis. Depending on the antennas, the slew times can vary greatly as indicated in Figure 7.

Figure 7 depicts the slew time models² for all azimuth elevation antennas included in the 2019 master schedule (see section 3.1). Some commonly used stations are highlighted for the sake of comparison. The slew time model consists of a constant offset c and a fixed slew rate r , usually defined in degrees per minute, resulting in a linear model. The model parameters are stored in the sked antenna catalog (see section 3.3.1).

Equation (3) can be used to calculate the required slew duration dur in seconds for a given angular distance d in degrees.

$$dur = c + \frac{d}{r} \cdot 60 \quad (3)$$

²according to sked antenna.cat version 2018Apr27_iGSFC

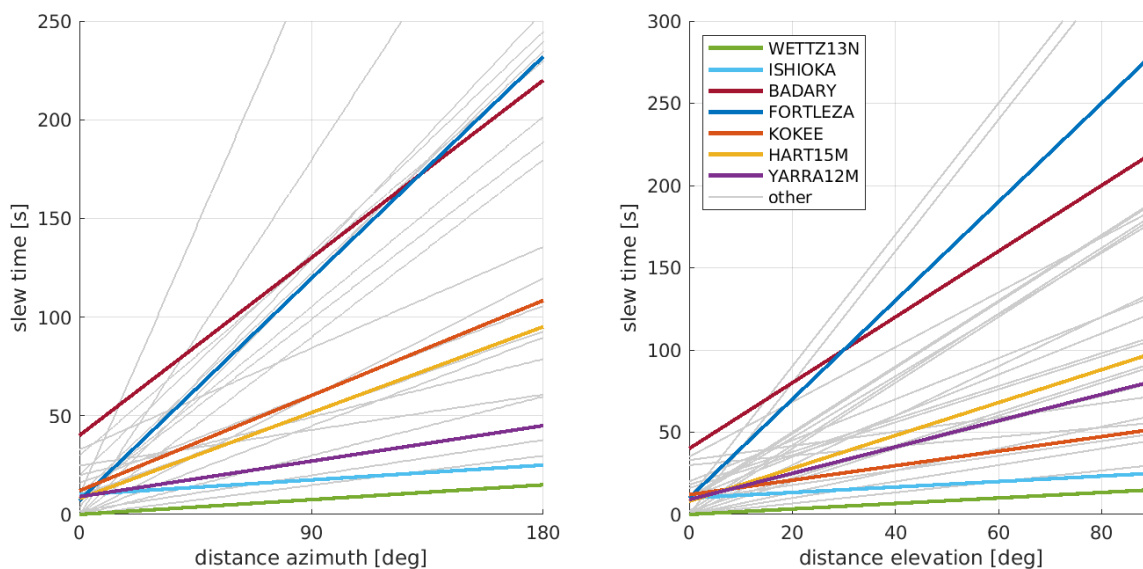


Figure 7: Slew time models for individual azimuth elevation antennas. The left plot displays the required slew time around the azimuthal axis up to 180 degrees angular distance. The right plot displays the same for the elevation axis up to 90 degrees angular distance.

The required slew time is calculated for both axis individually and the total slew time is the maximum of those two slew times.

While newer VGOS stations like WETTZ13N or ISHIOKA are especially built to provide fast slew time (Petrachenko et al., 2009; Petrachenko et al., 2012), other stations like FORTLEZA need significantly more time for slewing longer distances. Additionally, some stations like BADARY have a high constant offset c leading to high slew times for short distances as well.

3.4.3 Horizon mask

VLBI observes electromagnetic waves at radio frequencies which do not penetrate solid material very well. Therefore, it is not possible to observe sources at negative elevations, since the Earth is in between the source and the antenna. At some stations it is not possible to observe sources at certain areas above the horizon due to nearby mountains or obstacles like buildings or other antennas.

The information about visible areas from a station is stored in a so-called horizon mask, defined in the sked mask catalog (see section 3.3.1). Figure 8 visualizes two of those horizon

masks for station HART15M and KOKEE12M³.

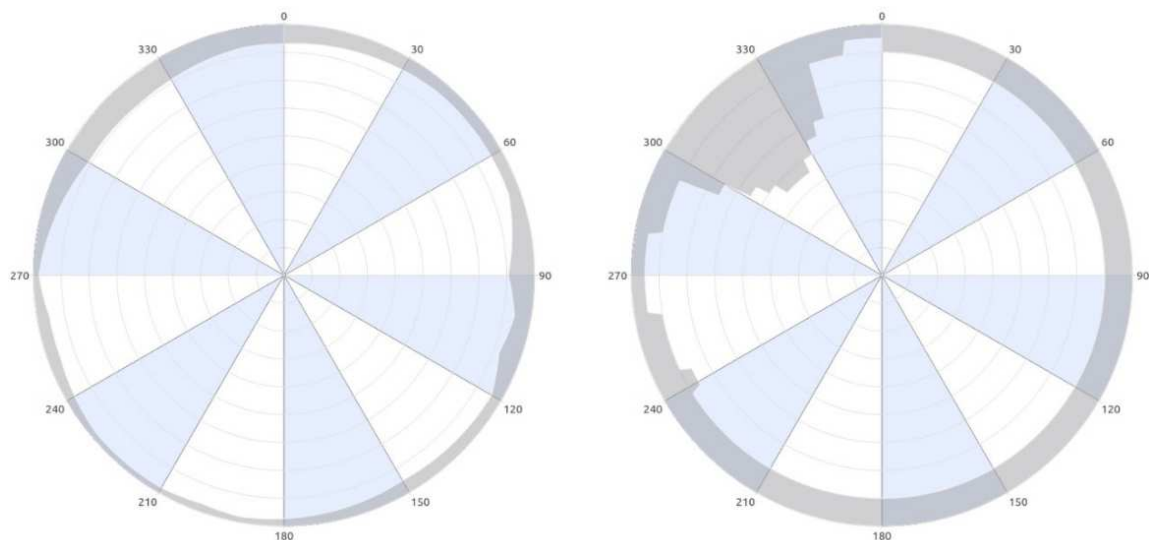


Figure 8: Horizon mask for station HART15M (left) and KOKEE12M (right). While the horizon mask on the left is defined via line segments, the mask on the right is defined through a step function.

Two different formats exist for horizon masks in the sked mask catalog (Gipson, 2016; Sun, 2013). The first is defined by azimuth elevation points which are connected through line elements as can be seen in Figure 8 left. The second is defined as a step function, providing azimuth ranges with a fixed elevation as can be seen in Figure 8 right.

Since not all stations have a defined horizon mask it is possible to set a minimum elevation of scans in the scheduling software which typically lies at 5 degrees elevation. While this is a fixed parameter in case of sked and VieVS_Sched, the minimum elevation can be set individually for each antenna and source in VieSched++, see section 5.8.2 and 5.8.3.

3.4.4 Antenna sensitivity

The sensitivity of an antenna is defined through its SEFD parameter:

$$SEFD = \frac{2kT_S}{A_e} \cdot 10^{26} = \frac{2kT_S}{\eta_A A_g} \cdot 10^{26} = \frac{8kT_S}{\eta_A \pi D^2} \cdot 10^{26}, \quad (4)$$

³according to sked antenna.cat version 2018Feb01.iGSFC

3. VLBI SCHEDULING

where k is the Boltzmann constant, A_e is the effective aperture, A_g is the effective aperture with the aperture efficiency factor η_A . For a circular aperture antenna, A_g can be calculated from the antenna diameter D as shown in the last term of equation (4). The unit of the SEFD parameter is Jansky (Jy) being:

$$1 \text{ Jy} = 1 \times 10^{-26} \frac{\text{W}}{\text{Hz m}^2} \quad (5)$$

A smaller SEFD parameter indicates a better system performance of the antenna. Thus, all things being equal, antennas with a larger dish have a better sensitivity and therefore shorter observing times until the required SNR is reached (see section 3.6).

Figure 9 depicts the distribution of antenna sensitivities for all antennas listed in the 2019 IVS schedule master. The SEFD parameter is stored per band in the sked equip catalog 3.3.1. The high number of stations with SEFD around 500 Jy for X-band and 400 Jy around S-band is due to the ten identical antennas forming the VLBA. The histogram in Figure 9 only shows SEFD values up to 7000 Jy for better visualization although five stations have significantly higher SEFD values like AGGO with 20 000 Jy in X-band and 15 000 Jy in S-band or OHIGGINS with 10 000 Jy in X-band and 18 000 Jy in S-band⁴.

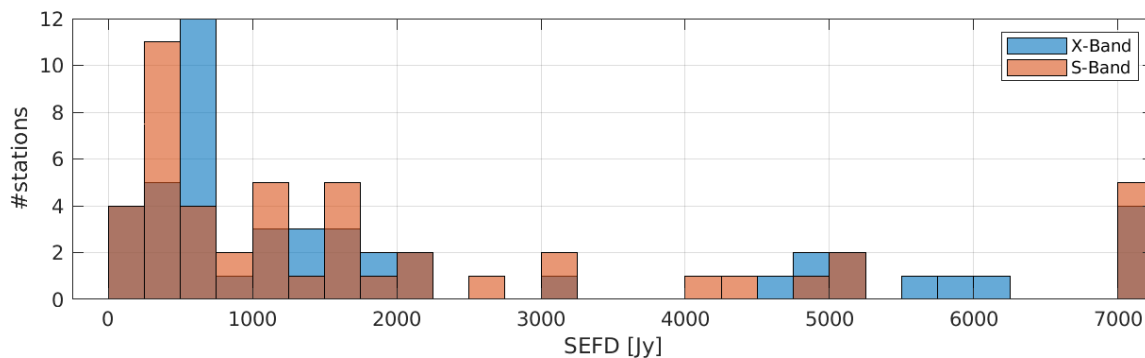


Figure 9: Histogram of the SEFD values of all antennas listed in the 2019 IVS schedule master.

Due to the atmospheric contribution to the system temperature and the changes in the amount of ground pickup caused by feed spillover, elevation depending SEFD values are calculated for some stations. Out of all stations included in the IVS master schedule elevation depending SEFD models are provided for 16 antennas. The SEFD parameter at

⁴according to sked equip.cat version 2018Oct09_IGSFC

3. VLBI SCHEDULING

a certain elevation el is calculated by multiplying the SEFD parameter in zenith direction with a elevation depending function.

$$SEFD(el) = SEFD_{zenith} \cdot f(el) \quad (6)$$

The scaling factor function $f(el)$ is given in equation (7).

$$f(el) = \sum_{i=0}^n \frac{c_i}{(\sin el)^i} \quad (7)$$

The elevation depending SEFD parameters are listed in the sked equip catalog (see section 3.3.1). Since this catalog only lists the parameters y , c_0 and c_1 (Vandenberg, 1999), equation (7) simplifies to equation (8).

$$f(el) = c_0 + \frac{c_1}{\sin el^y} \quad (8)$$

Figure 10 displays the elevation depending scale factor $f(el)$ model, see equation (8) for some stations⁵.

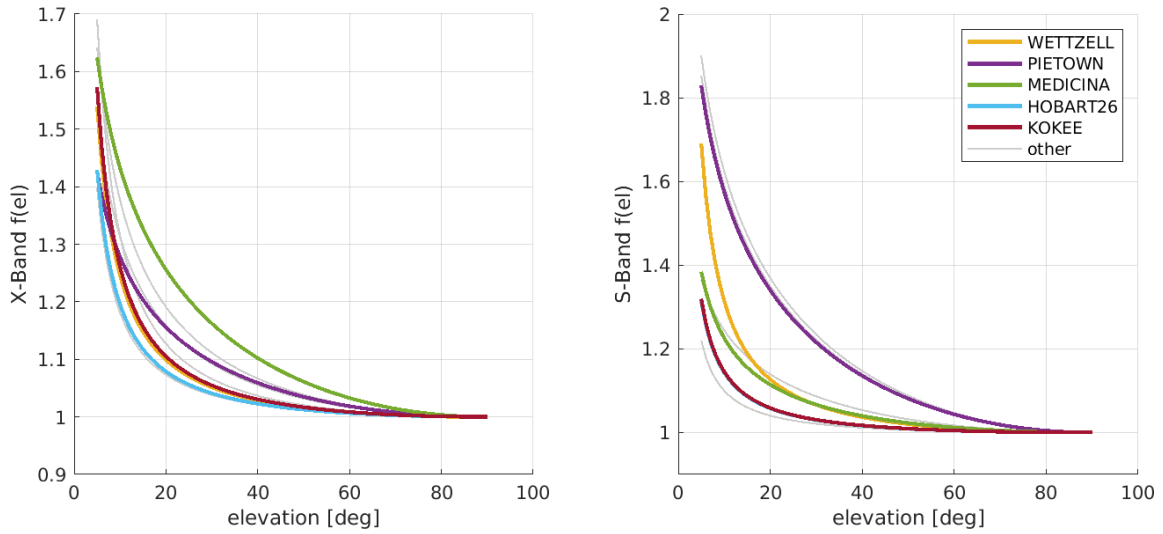


Figure 10: Elevation depending SEFD factors $f(el)$ for all antennas included in the IVS master schedule.

Typically, the elevation depending scale factor $f(el)$ is greater than 1. It increases with

⁵according to sked equip.cat version 2018Oct09_IGSFC

3. VLBI SCHEDULING

lower elevations resulting in higher SEFD values and thus longer integration times to reach the required SNR, see section 3.6. The elevation depending SEFD model is provided per band. While for some stations, only very low elevations are effected, the SEFD of stations like PIETOWN in S-band already increases for high elevations.

3.5 Flux models

Besides the position of the source, which defines the slew time between scans, their brightness is an important quantity defining the required integration time to reach a certain SNR (see section 3.6). The flux information is stored in the sked flux catalog (see section 3.3.2). This catalog is regularly updated due to changes in the flux density of sources over time. Figure 11 depicts the changes in the flux density of the often observed source 0059+581. Source 0059+581 is one of the brightest and thus most observed sources. It is one of the ICRF3 defining sources with over 400 000 observations from over 2600 sessions. The flux density displayed in Figure 11 is taken from the sked flux catalog (see section 3.3.2). Some values, which were only calculated based on one session were removed from the visualization. It can be seen that the brightness is not stable over time and varies over short time frames. Therefore, it is always necessary to use the latest version of the catalog files including the newest source flux information to properly calculate the required observing time and create a correct schedule.

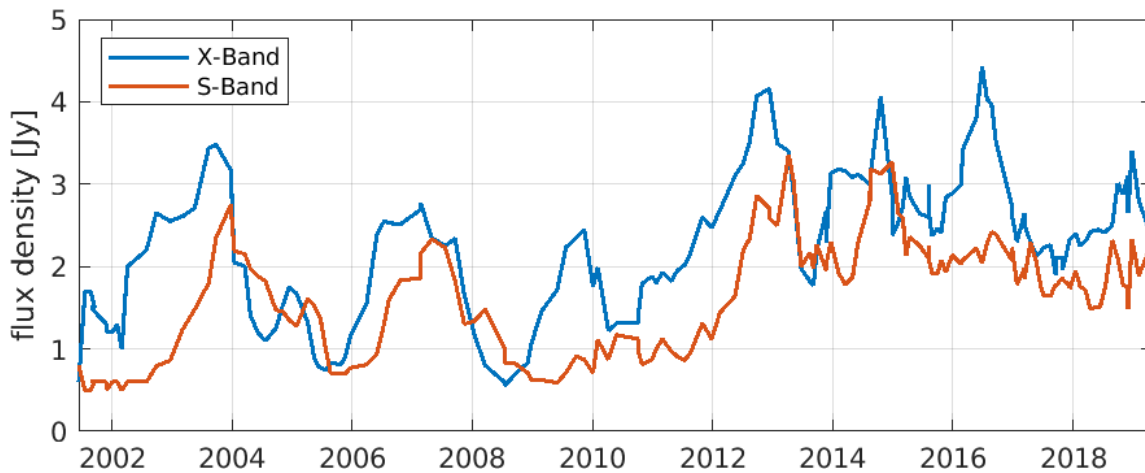


Figure 11: Evolution of flux density of source 0059+581 over time.

There are two different models available for defining the flux density, based on the

3. VLBI SCHEDULING

projected baseline length or provided via elliptical Gaussian models. Figure 12 depicts the expected flux density for source 3C274, also known as 1228+126⁶. It is a well-observed source in VLBI and part of the ICRF3 with over 70 000 observations from over 1900 sessions.

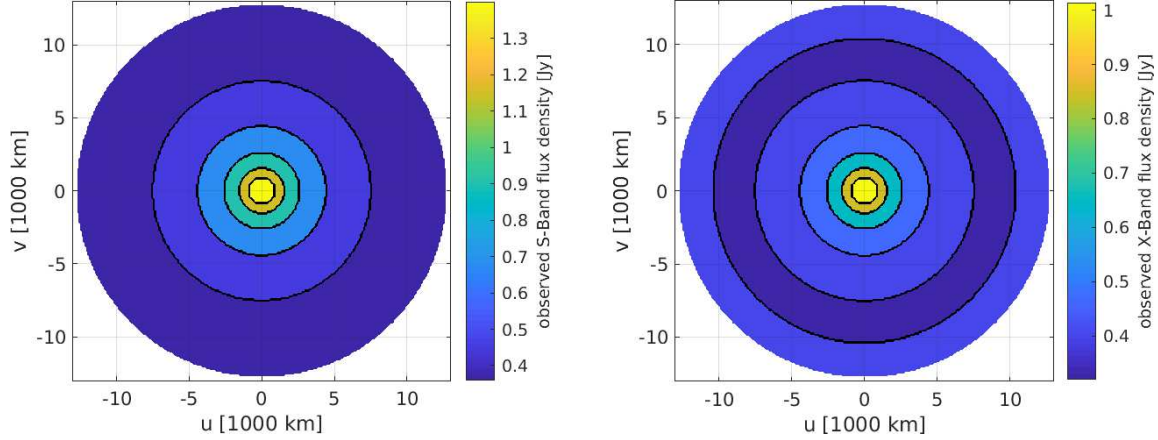


Figure 12: Expected flux density of source 3C274 derived from a baseline length based model on the uv-plane. Left for S-band and right for X-band.

The expected source flux of this source is provided per projected baseline length in the uv-plane:

$$ha = gmst - ra \quad (9)$$

$$u = b_x \cdot \sin ha + b_y \cdot \cos ha \quad (10)$$

$$v = b_z \cdot \cos \delta + \sin \delta \cdot (-b_x \cdot \cos ha + b_y \cdot \sin ha) \quad (11)$$

where b_x , b_y and b_z are the x , y and z components of the baseline vector, δ is the declination and ra is the right ascension of the source and $gmst$ is the Greenwich mean sidereal time.

The projected baseline length b_{proj} is given by:

$$b_{proj} = \sqrt{u^2 + v^2} \quad (12)$$

As it can be seen in Figure 12, the expected flux density model is defined by concentric circles in the uv-plane. Typically, sources with an extended structure are partially resolved on long baselines, thus reducing the observed flux.

⁶according to sked flux.cat version 2019APR04_iGSFC

3. VLBI SCHEDULING

Figure 13 visualizes the expected flux density for source 0458-020 provided by an elliptical Gaussian model⁷. This source is an ICRF3 defining source with more than 80 000 observations from over 2700 sessions.

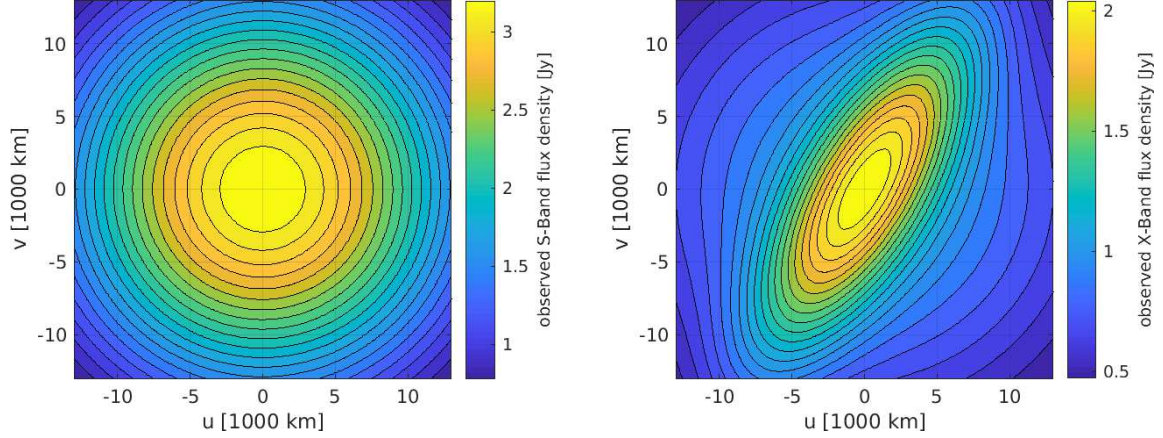


Figure 13: Expected flux density of source 0458-020 derived from an elliptical Gaussian model on the uv-plane. Left for S-band and right for X-band. The X-band model consists of two components, see Figure 14.

The model is defined as the sum of Gaussian components. Each component is defined by four parameters, the strength of the component F , typically in unit Jansky, see equation (5), the size of the component's major axis Θ , the axial ratio of the component R and the position angle of the major axis pa . The expected flux density F_{obs} can be calculated using the following equations for an observed wavelength of λ :

$$u_\lambda = \frac{u}{\lambda} \quad (13)$$

$$v_\lambda = \frac{v}{\lambda} \quad (14)$$

$$l = \sqrt{(v_\lambda \cos pa + u_\lambda \sin pa)^2 + R^2 (u_\lambda \cos pa - v_\lambda \sin pa)^2} \quad (15)$$

$$F_{obs} = F \cdot \exp \frac{-(\pi \Theta l)^2}{4 \ln 2} \quad (16)$$

The total X-band flux density model of source 0458-020 displayed in Figure 13, is defined through the sum of two components, displayed in Figure 14. While one of the two components is radially symmetric, the other one has an axial ratio of 0.3.

⁷according to sked flux.cat version 2019APR04_iGSFC

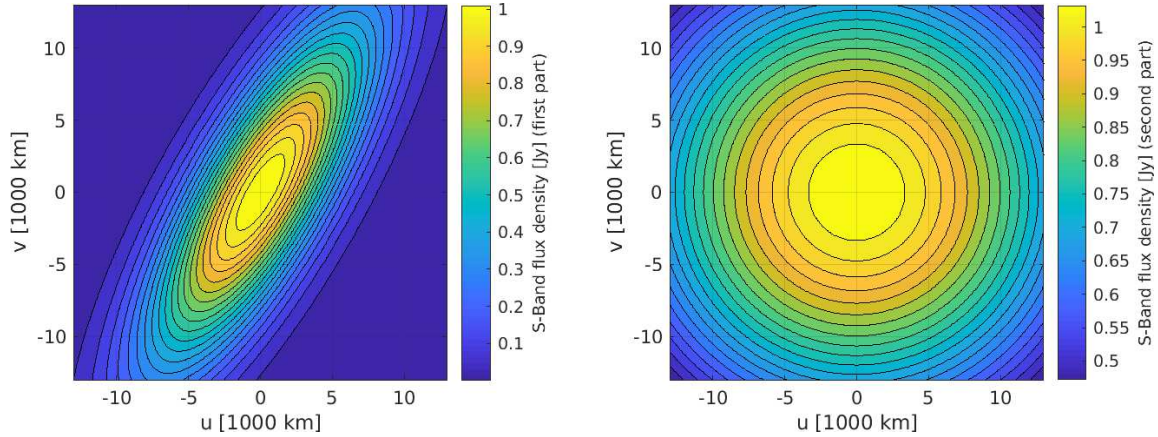


Figure 14: Two components of the elliptical Gaussian flux model of source 0458-020 in X-band. While the first component has a axial ratio R of 0.3, the second component is radial symmetric.

Although there is the possibility to create the flux model as a sum of multiple elliptical Gaussian components in the sked flux catalog, almost all models consist of only one component.

3.6 Required scan length

The required scan length is calculated per baseline between participating stations. It is determined by the desired SNR, the source strength F , the antenna SEFD and the recording rate rec .

The recording rate is the total number of recorded bits per second. It can be calculated using the sample rate per channel, which is usually two times the channel bandwidth, the number of channels $\#ch$ and the number of recorded bits per sample $\#bits$.

$$rec = sample_rate \cdot \#ch \cdot \#bits \quad (17)$$

The expected SNR is defined via

$$SNR = \eta \frac{F}{\sqrt{SEFD_1 \cdot SEFD_2}} \sqrt{rec \cdot sec} \quad (18)$$

3. VLBI SCHEDULING

which can be inverted to calculate the required scan length T in seconds per baseline

$$T = \left(\frac{SNR}{\eta F} \right)^2 \cdot \left(\frac{SEFD_1 \cdot SEFD_2}{rec} \right) \quad (19)$$

The variable η in equation (18) and (19) is the so-called efficiency factor, which depends on the bit efficiency, which is the degradation in SNR due to digital sampling and varies depending on how many bits are recorded per sample, and the correlator efficiency depending on the correlation software.

Figure 15 visualizes the required scan length depending on antenna SEFD and source strength.

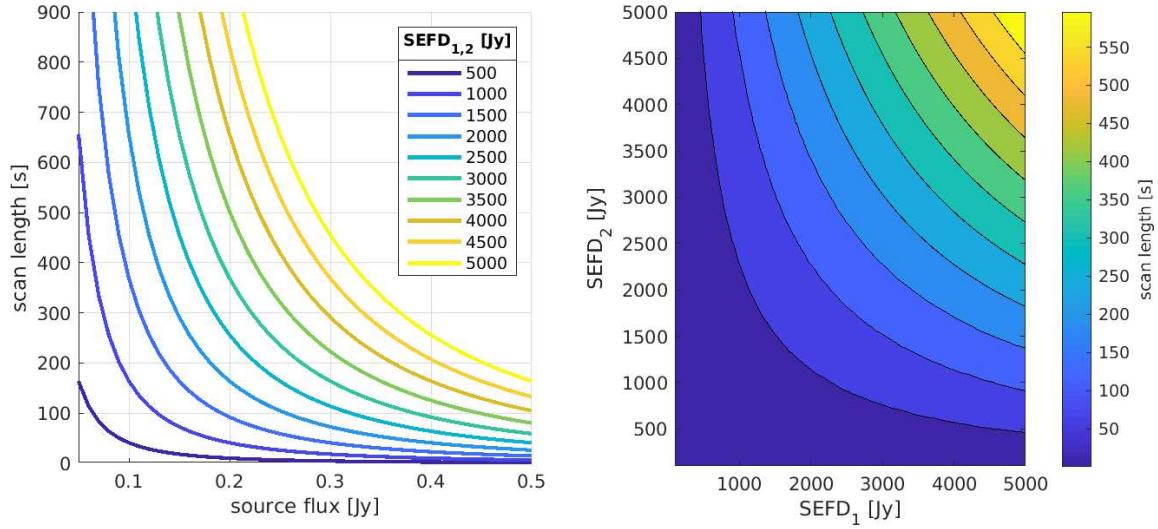


Figure 15: Required scan length necessary for reaching a SNR of 20. The left plot displays the required scan length depending on the source flux density assuming two antennas with the same SEFD. The right plot displays the required scan length for a fixed source flux of 0.25 Jansky but with varying SEFD parameters for both antennas. Both figures assume an observing mode with 2-bit sampling, a sample rate of 32 MHz and 10 recorded channels as well as an efficiency factor η of 0.6175.

Equation (19) shows that the required scan duration is calculated per band and baseline since the SEFD parameters differ between stations and between bands as well as the source flux density and the recording rate. The required scan duration per station is the maximum of the required scan duration per band and baseline containing this station. The right plot in Figure 15 indicates, that if one station has low sensitivity, meaning it has a high SEFD

it is still possible to achieve a relatively low required scan duration if the second station forming the baseline is very sensitive with a low SEFD. This makes it possible to include low sensitive antennas in scans with other highly sensitive antennas.

Since the antenna performance varies from time to time and the slew models 3.4.2 might not be 100% accurate, typically, a minimum scan time is set in the scheduling software, to avoid scan time below a certain threshold. Similar a maximum allowed scan time can be set, to avoid very long scans, which are inefficient and may suffer from unresolved changes in the troposphere during the scan time. Additionally, a few extra seconds are usually added to the required scan time for the correlator synch up, changing equation (19) to (20).

$$T = \left(\frac{SNR}{\eta F} \right)^2 \cdot \left(\frac{SEFD_1 \cdot SEFD_2}{rec} \right) + corsynch \quad (20)$$

3.7 Special scheduling algorithms

3.7.1 Subnetting

Subnetting is a technique used in global geodetic VLBI. The idea is to split the network into two parts, so-called subnets, and observe two sources simultaneously as indicated in Figure 16 (Gipson, 2016). The idea behind this approach is that it is not possible that all stations observe the same source simultaneously in a global antenna network, simply because the source is not visible from all parts of the Earth at the same time. The trade-off for subnetting is, that the number of observations gets reduced. The number of observations in a scan grows by $\frac{n(n-1)}{2}$ with the number of participating stations. Since during subnetting the network is divided into two subnetworks, the total number of observations from those two scans is smaller than it would be from one scan with the maximum number of observations. However, if this is not done, the scheduling software would likely focus always mainly on a subset of stations which are near to each other, especially, in case of an asymmetric station distribution, which is quite common due to the lack of southern stations as indicated in Figure 3. Thus, by using subnetting, the overall sky-coverage increases since the stations are way more flexible with what they observe.

Subnetting is a necessary tool in scheduling geodetic VLBI sessions. Although it drastically increases the complexity of the scheduling process, it also increases the overall quality of the generated schedule. By using subnetting it is way better for the scheduling software to compare different scan situations and select the best one. When subnetting is used, the

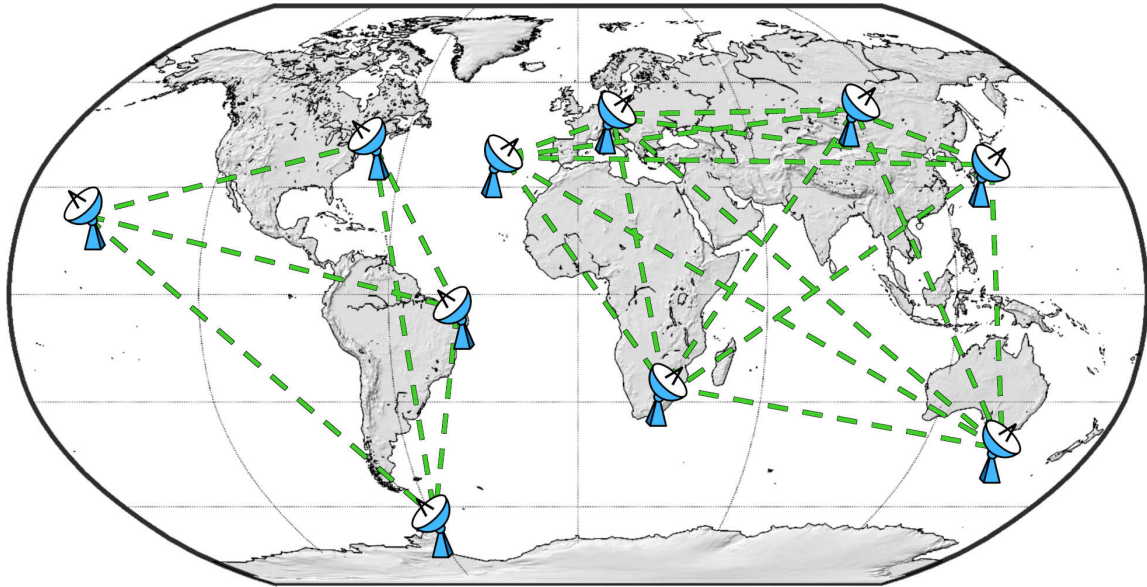


Figure 16: Schematic representation of subnetting. The network is split into two subnets which observe two sources simultaneously.

score of both considered subnetting scans is combined in the comparison process and this overall score is compared against other situations. Without subnetting some stations are idling during the scan comparison process due to the lack of common visibility, which the scheduling software usually tries to avoid. Idling stations do not contribute to the score of a scan thus making the scan comparison unfair and resulting in a scan selection mostly based on the number of participating stations. By using subnetting, scans including all stations can be evaluated and the comparison process works a lot better.

However, the optimization criteria used by the scheduling software have to be designed to work in the case of subnetting and without subnetting and they need to be able to compare those two situations with each other, making the definition of optimization criteria a lot harder. This means that the scheduling software has to be able to switch subnetting on and off, depending on what is best at this time.

It has to be noted that it is possible and in fact often the case that two or even more sources are observed simultaneously without the use of subnetting. Stations which are considered as idling during a scan or which have finished their observation earlier due to higher sensitivity can form another scan in the next scheduling step or can form a scan during the

fillin-mode process described in section 3.7.2, which overlaps with already existing scans. Subnetting only effects the decision, which scans should be selected by providing a lot more possibilities. The difference is, that by using subnetting the comparison of scans during the scheduling process works a lot better since the scheduling software already knows what all stations are doing. Without the use of subnetting the software only knows what stations participating in the investigated scan are doing, since the scheduling of the next scan or a fillin-mode scan is done in a further step. Additionally, by using subnetting the schedule can and often will contain situations where three or more sources are simultaneously observed for the same reasons although only two sources are evaluated simultaneously.

Section 5.3.5 describes in detail how subnetting is considered by VieSched++.

3.7.2 Fillin-mode

Fillin-mode is a method of reducing station idle time (Gipson, 2016). The possible start point of a scan and the observing duration can vary greatly between stations for multiple reasons.

Figure 7 visualizes that the slew speed of individual antennas can be very different. Additionally, it is possible that stations start slewing from different sources leading to different slew distances and thus slew times. In general, the slew distances are different for each station, since most antennas are azimuth and elevation antennas and the sources are on different positions on the local sky at different places on the Earth. The higher the elevation of a source the longer the azimuth slew distance becomes for Alt-Azimuth antennas. Since by definition of the .skd format a scan always starts at the same time for each station it is possible that fast slewing stations wait for slow slewing stations until they reach their final destination.

Furthermore, the required integration time of a scan is also different for different stations. Figure 9 depicts that the sensitivity of the antennas is very variable between antennas, leading to a different required scan duration according to equation (20) per antenna. Since the scan start time is fixed for all stations it can happen that some stations finish a scan earlier than others.

Both of these two factors introduce idle time to a schedule. Additionally, although subnetting is used, it is sometimes possible that one antenna is not part of any scan at a certain time resulting in this antenna idling as well.

The idea of a fillin-mode is to use this occurring idle time productively and schedule

3. VLBI SCHEDULING

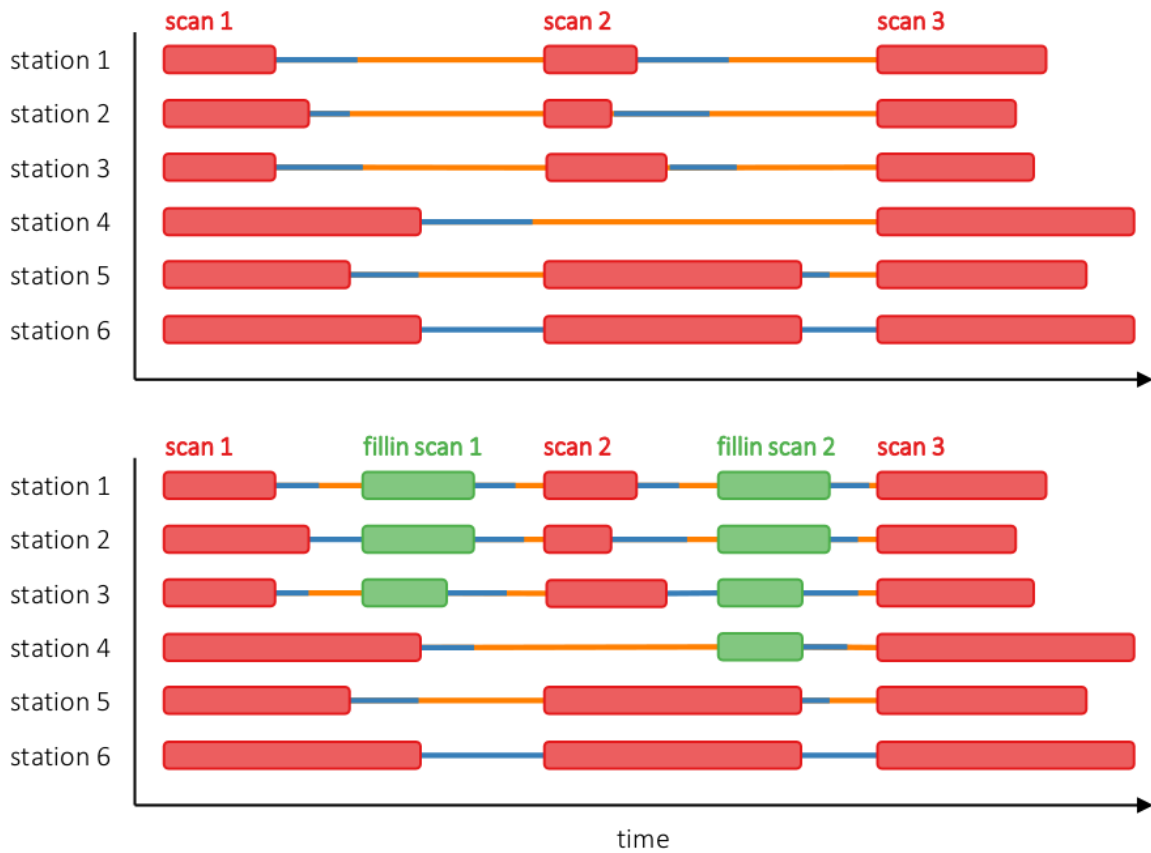


Figure 17: Visualization of fillin-mode. The top figure displays a situation without fillin-mode, the bottom figure displays the same situation with fillin-mode active. Red blocks are observing times during a scan. Blue lines represent required slew time. Orange lines represent the occurring idle time. Green blocks represent fillin-mode scans scheduled during the idle time between scans.

additional scans with a reduced number of otherwise idling stations as indicated in Figure 17. The observing duration of scan 1 in Figure 17, represented as a red bar, is different for each station and longest for station 4 and 6. The required slew time is drawn as a blue line. The observation of scan 2 starts as soon as all participating stations have finished their previous observation and finished slewing to source 2 observed in scan 2. In this example, the last station arriving at source 2 is station number 6. As soon as station 6 arrives on source 2 scan 2 can start. This leads to a lot of idle time for most other stations represented as an orange line. Station number 4 is not participating in scan 2 so it is idling as well.

3. VLBI SCHEDULING

After scan 2 is observed all stations are slewing to source 3 observed in scan 3. Again, every station has to wait until the latest station finishes slewing to source 3, which is in this example station 6 again. The bottom plot in Figure 17 visualizes how the occurring idle time can be used by scheduling fillin-mode scans. In this example, it is possible for station 1, 2 and 3 to observe another source during the idle time between scan 1 and 2. Similarly, it is possible for station 1, 2, 3 and 4 to observe a fillin-mode scan during the idle time between scan 2 and scan 3.

While both `sked` and `Vie.Sched` implement fillin-mode scans as part of an own scheduling mode by alternating between the standard scan selection and the fillin-mode described by [Gipson \(2016\)](#) and [Sun \(2013\)](#), `VieSched++` schedules fillin-mode scans during the recursive scan selection described in section 5.5 by using its main algorithm. Another main difference between the implementation in `VieSched++` in contrast to `sked` or `Vie.Sched` is that `VieSched++` schedules the fillin-mode scans between two already scheduled scans and thus taking advantage of the full available idle time (mainly due to different slew times and different observing times) while `sked` and `Vie.Sched` only add fillin-mode scans at the end of an already fixed scan ([Gipson, 2010](#)) and, thus, only minimizing idle time due to different observing times of antennas and not due to different slew times. More information about the `sked` fillin-mode including a visual example can be found in ([Gipson, 2010](#)).

Figure 18 depicts an example of different fillin-mode approaches. The top figure displays the initial situation without the use of fillin-mode. Scan 1 is scheduled with different observing times and different slew times. Scan 2 is scheduled with different slew times. The middle figure displays a fillin-mode solution where only different observing times are considered, such as it is the case of `sked` and `Vie.Sched`, where the order of scheduled scans would be: scan 1, fillin-scan 1, scan 2, scan 3. In this case, the algorithm is only able to schedule a short fillin-mode scan between scan 1 and scan 2. The bottom figure displays a fillin-mode solution where both, different observing times and different slew times are taken into account. In this case, the algorithm is able to schedule two fillin-mode scans. This situation reflects the case of `VieSched++` where the scans are scheduled recursively (see section 5.5), leading to the following scan schedule order: scan 1, scan 2, fillin scan 1, scan 3, fillin scan 2.

3. VLBI SCHEDULING

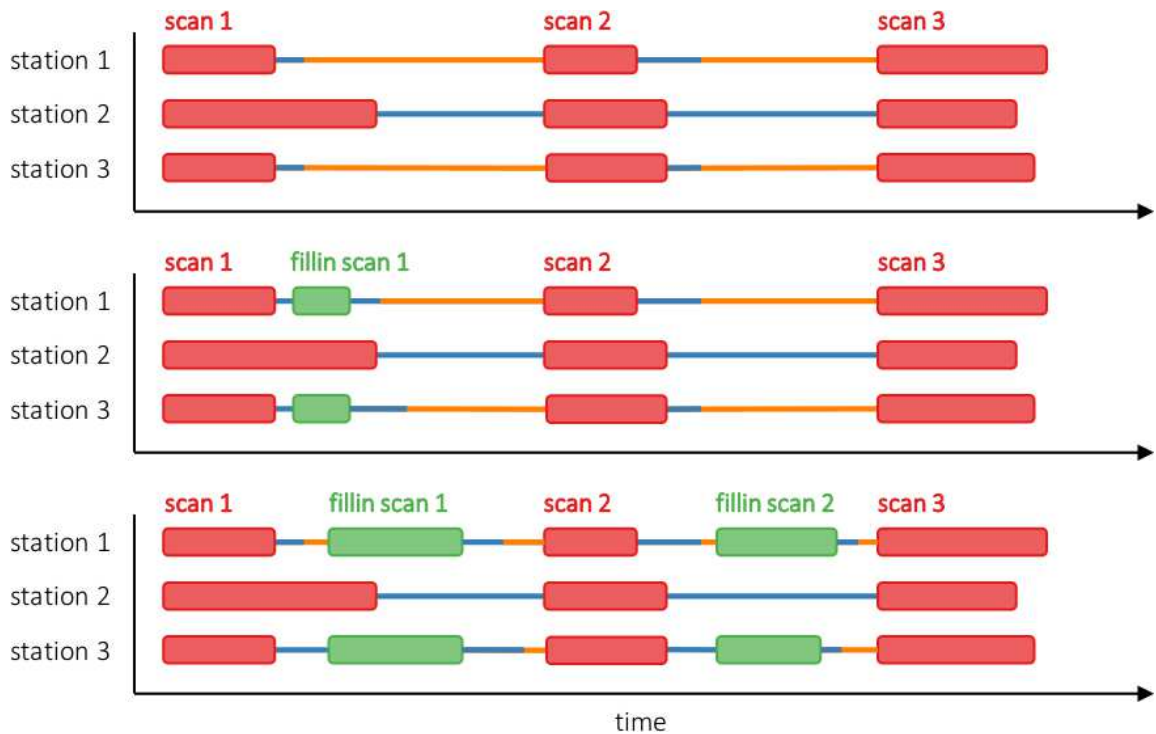


Figure 18: Comparison of different fillin-mode approaches. The top figure displays a situation without fillin-mode. The middle figure displays the same situation with a fillin mode considering different observing times. The bottom figure displays the same situation with a fillin-mode considering both, different observing times and different slew times. Red blocks are observing times during a scan. Blue lines represent required slew time. Orange lines represent the occurring idle time. Green blocks represent fillin-mode scans scheduled during the idle time between scans.

3.7.3 Tagalong-mode

Sometimes it is not sure if a station will participate in a session or if the recorded data of a station can be used for correlation. This is often the case for new stations or stations that might be on maintenance. If this is the case, it is often advantageous to add these stations as so-called tagalong stations.

The idea behind the tagalong-mode is, that the schedule is first created without considering the tagalong station and, in a further step, the tagalong station is added to the schedule trying to additionally observe as many of the already scheduled scans as possible. This makes sure that the schedule is still intact in case the tagalong station drops out of

3. VLBI SCHEDULING

the session.



Figure 19: Visualization of tagalong-mode. Red blocks are observing times during a scan. Green blocks are observing times added during tagalong-mode. First the schedule is created without the tagalong stations as displayed in the top figure and later the tagalong station is added in a further step as displayed in the bottom figure.

Figure 19 visualizes the concept of the tagalong-mode. The top figure displays the first step of this process, where the schedule is created without considering the tagalong station. If the schedule is finished the second step starts, visualized in the bottom figure, where the tagalong station is added to the already fixed scans.

3.7.4 Extending observing time

Another possibility to reduce station idle time is to extend the observing duration of a scan in case of available idle time. Typically, the station observing time is exactly as long as required until the target SNR can be reached on all scheduled baselines with this station, see section 3.6. If the idle time is not long enough to squeeze in another scan via the

3. VLBI SCHEDULING

fillin-mode the occurring idle time can be decreased by increasing the observation duration of already scheduled scans. The algorithm does not add any additional observations to the schedule, it just increases the SNR of the observations by increasing its observing duration which in turn will increase the precision of the observations. The downside of this approach is that the amount of recorded data, which is often a bottleneck in VLBI, gets increased without increasing the number of observations.

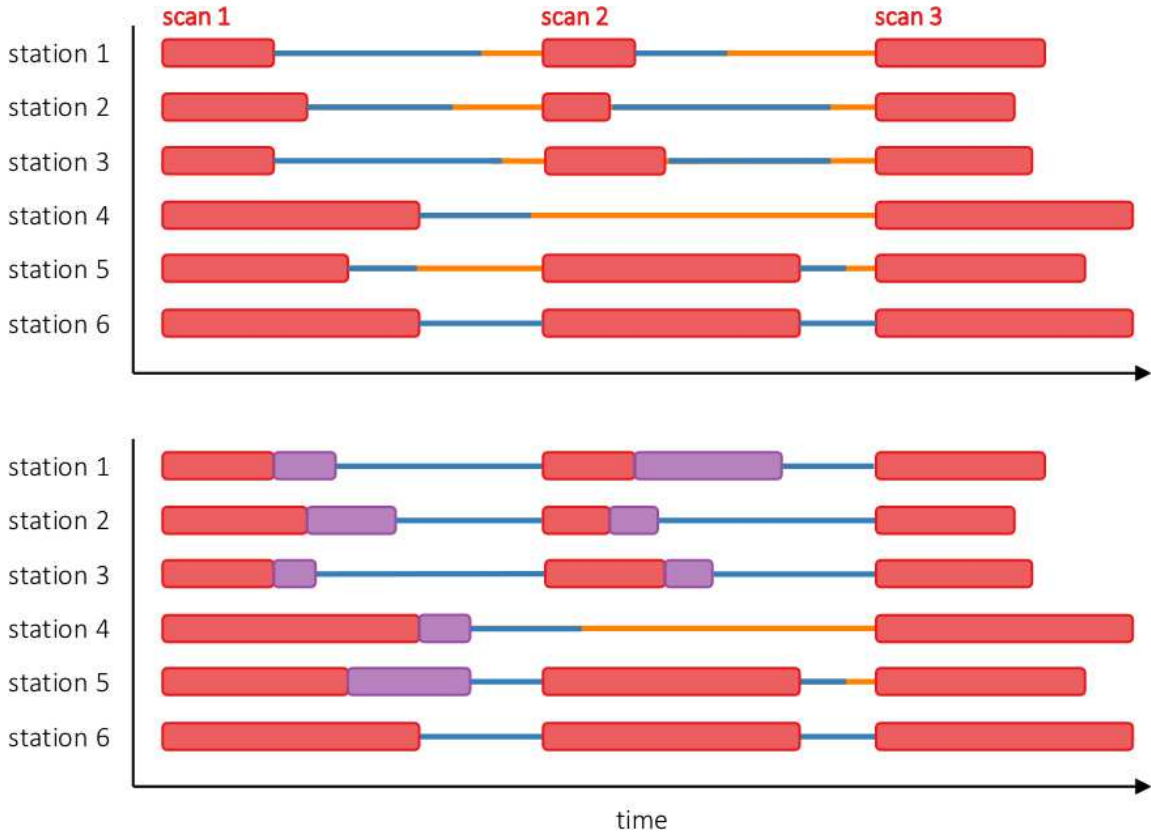


Figure 20: Visualization of how extending observing time works. The top figure displays a schedule without extending the observing time, the bottom figure displays the same situation with extended observing time. Red blocks are observing times during a scan. Blue lines represent required slow time. Orange line represent the occurring idle time. Purple blocks represent extended observing times.

Figure 20 visualizes this process. Red blocks represent observing times during a scan, blue lines the required slow time and orange line the occurring idle time. The purple blocks indicate extended observing times. In this example, the latest station which participates

3. VLBI SCHEDULING

in scan 2 and finishes slewing to the observed source is station number 6. The idle time of the other stations can be extended as far as there is still enough time slewing between the sources of scan 1 and scan 2. Note that in this example the total scan duration is increasing, since station 4 and 5 can both extend their observing time. Between scan 2 and 3 it is possible for stations 1, 2 and 3 to extend their observing time. It is not possible for station 5 since at least two stations have to observe simultaneously.

Both sked and VieSched++ have implemented an algorithm to extend the observing times in case of available idle time but it is missing in Vie_Sched. Since VieSched++ has the option to not only align scans at the scan start time but also at the end time or individually as described in section 5.11 it offers the possibility to extend the observing times at the end of a scan, at the beginning of a scan or both. Furthermore, VieSched++ recalculates the required slew time between sources when extending the observing time since the antenna is moving while tracking a source, thus, leading to different slew distances and slew times.

4 Simulations and Analysis

The following section gives a brief overview about VLBI simulations and the analysis of VLBI sessions. It covers topics which are necessary to understand the content of the upcoming sections, especially for the results, see section 6. Throughout this work, the VieVS package is used to generate simulations and analyze VLBI sessions.

4.1 Vienna VLBI and Satellite Software (VieVS)

The Vienna VLBI and Satellite Software (VieVS) is a scientific software package which is used for research and teaching space geodetic techniques (Böhm et al., 2012; Böhm et al., 2018). It is mostly known for its state-of-the-art VLBI analysis tools for geodesy and astrometry. VieVS is developed at TU Wien, Department of Geodesy and Geoinformation, since 2008 with contributions from multiple international colleagues. The software is written in MATLAB, which makes it easy to develop and test new approaches. The downside of MATLAB is, that it is an expensive commercial software.

The main purpose of the VieVS VLBI module is the analysis of VLBI sessions. Therefore, a least-squares adjustment is used. The theoretical delay for each observation is calculated according to the IERS conventions (Petit and Luzum, 2010) and their newest updates. Within the least-squares adjustments, most parameters are estimated by using Piece-Wise Linear Offsets (PWLO), see Schuh and Böhm (2013) and Teke (2011) for further information.

Besides analyzing individual VLBI sessions, it is possible to combine the results of single solutions to a so-called global solution by stacking the normal equation matrices. This opens up the chance to combine the whole history of VLBI sessions to estimate parameters with the highest precision. This is commonly used for the estimation of a new TRF or CRF as described in Krásná et al. (2014) and Mayer (2018).

Additionally, VieVS includes a tool to simulate artificial VLBI observations (Pany et al., 2011). The simulated observations can be analyzed similarly to a real VLBI experiment. Based on Monte-Carlo simulations (Metropolis and Ulam, 1949), statistical information like the repeatability of the estimated parameters can be calculated and investigated.

Finally, VieVS already includes a VLBI scheduling software called Vie_Sched (Sun, 2013; Sun et al., 2014). In the past, Vie_Sched was used to schedule the AUSTRAL VLBI sessions (Plank et al., 2017) and test new scheduling approaches like the star scheduling mode (McCallum et al., 2017). Additionally, this scheduling software includes the ca-

pabilities to schedule satellite observations with VLBI, see [Hellerschmied et al. \(2016\)](#), [Hellerschmied et al. \(2017\)](#), and [Hellerschmied \(2018\)](#)

More information about VieVS can be found at viewswiki.geo.tuwien.ac.at.

4.1.1 Simulation setup

Throughout this work, simulations include three of the main VLBI error sources, namely the tropospheric wet delay, station clock drifts and measurement errors in form of white noise ([Pany et al., 2011](#)). Another major error factor, especially for VGOS, are source structure effects ([Anderson and Xu, 2018](#)). Time delays due to source structure effects are not simulated in this work due to limitations in the software and limitations in available models.

If not explicitly stated otherwise, the following parameters are used to generate simulations in this work:

The tropospheric wet delay is simulated following an approach suggested by [Nilsson et al. \(2007\)](#). This approach is based on a turbulence model by [Treuhaft and Lanyi \(1987\)](#) which is using the Kolmogorov turbulence theory. All stations are simulated using a refractive index structure constant C_n of $1.8 \times 10^{-7} \text{ m}^{-1/3}$, with an effective height of 2 km and a constant wind velocity of 8 m/s towards east.

Stochastic errors of the station clock are simulated as the sum of random walk and integrated random walk ([Herring et al., 1990](#)). All stations are simulated assuming a clock accuracy with an Allan Standard Deviation (ASD) of 1×10^{-14} s after 50 minutes.

Additionally, 20 picoseconds of white noise are added to the observations to account for measurement errors.

4.1.2 Analysis setup

Within this work, standard 24-hour sessions are analyzed using the following setup:

The tropospheric zenith wet delay is estimated every 30 minutes using PWLO per station and loose relative constraints of 1.5 centimeters after 60 minutes are applied. The tropospheric north and east gradients are estimated as PWLO every three hours. Additionally, relative constraints of 0.05 centimeters after six hours and absolute constraints of 0.1 centimeters are applied.

4. SIMULATIONS AND ANALYSIS

The clock is estimated using PWLO every 60 minutes, as well as one rate and one quadratic term per clock. This is done for all stations, except for the station providing the reference clock. Relative constraints between the PWLOs are introduced with 1.3 centimeters after 60 minutes.

The EOP parameters are estimated using daily PWLO at 00:00 UTC. Very tight relative constraints of 1×10^{-4} microarcseconds are introduced between the PWLO. Effectively, this results in the estimation of the EOP parameters as one offset per session.

The station coordinates are estimated as one offset per session by introducing No Net Translation (NNT) and No Net Rotation (NNR) condition equations.

No source coordinates are estimated in case simulations are analyzed.

The least-squares method implemented in VieVS is following a two-step approach: First, a so-called first-solution is performed estimating a reduced set of parameters, followed by the main solution. The reason for the first solution is to provide good a priori values for the parameters. Most importantly, the clocks are only estimated as one offset, one rate and one quadratic. Then during the main solution, these a priori values are then used and all requested parameters are estimated as listed above.

In the case a real session is analyzed, an outlier test is applied and the outliers are removed from the analysis.

5 VieSched++

5.1 Software design

VieSched++ (Schartner and Böhm, 2019c) is developed at the Department of Geodesy and Geoinformation at Technische Universität Wien (TU Wien) under the umbrella of VieVS. It is written in modern C++ using an object-oriented software design. The software is distributed in two parts: the scheduler and a Graphical User Interface (GUI). The source code of both parts is hosted on GitHub under <https://github.com/TUW-VieVS>. The GUI is based on the Qt5 libraries and aims to be very intuitive and highly interactive. It provides a built-in help and multiple interactive schedule analysis and comparison features. The main function of the GUI is to create an Extensible Markup Language (XML) file with the scheduling setup. This XML file serves as input for the scheduler. To be consistent with today's schedules created with sked (Vandenberg, 1999; Gipson, 2010), the sked catalogs (Vandenberg, 1997) can be used in VieSched++.

5.2 Installation

VieSched++ provides an installer for Windows 10 and Ubuntu 18.04. The installer includes the scheduler as well as the GUI and additionally a recent version of the sked catalogs. Therefore, it is not necessary to manually build the software on these operating systems, which can be quite challenging and time consuming by itself, especially for scientific software.

In case the software has to be built manually, VieSched++ tries to simplify the process as much as possible by reducing the number of third-party libraries to a minimum as well as providing *cmake* and *qmake* script files. For the scheduler, the only dependency is the Standards of Fundamental Astronomy (SOFA) library (SOFA, 2019). Apart of that, a header-only version of the C++ boost libraries (Ling, 2011) is sufficient to compile the scheduler, although some features like improved log files are only available if a build version of the C++ boost libraries is available. The scheduler can be built easily using a provided *cmake* script file, which is a cross-platform tool to build software independent of the compiler.

For building the GUI, additionally, the Qt5 libraries are required. The build process can be automated by using a *qmake* script file, which is similar to *cmake* but specially designed to support the Qt libraries.

VieSched++ is a multi-platform application and is successfully tested on Linux and Windows using different compilers.

5.3 General scheduling concept

Figure 21 visualizes the work flow of the scheduling process in VieSched++. There are two input sources for VieSched++. An XML file which is typically called “VieSchedpp.xml” and is typically created by using the GUI and the sked catalog files. The XML file contains the full scheduling setup, containing the list of participating stations, the observing mode and most important the scheduling logic which should be used to generate the schedule. Additionally, it points to the catalog files (see section 3.3) where the information of the antennas, sources, and hardware is stored.

Using these input files, VieSched++ starts with the so-called initialization phase. During this phase the content of the input files is parsed, all necessary objects are constructed and the scheduling logic is set up. Furthermore, multiple look-up tables are generated to speed up the scheduling process. These look-up tables include astronomical parameters such as the IAU 2006 precession-nutation model (Petit and Luzum, 2010; Capitaine et al., 2009), Earth velocity and Sun positions but also fast look-up tables for trigonometric functions and the angular distance between two points on a sphere. Additionally, azimuth elevation values are provided per station for each source every minute which is further used for interpolation.

After the initialization process finishes the scheduling phase starts. During this phase, the schedule is generated scan after scan as indicated in Figure 2. The main algorithm used during the scheduling phase is the recursive scan selection, further explained in section 5.5 as well as in Schartner and Böhm (2019b) and Schartner and Böhm (2019c).

Optionally, it is possible to fix some scans a priori before the main recursive scheduling algorithm starts to make sure that these scans are always scheduled. This can be used to fix scans to sources near the corners of the commonly visible sky for intensive sessions, which are assumed to be the most important scans (Uunila et al., 2012). After the main recursive scheduling algorithm the fillin-mode a posteriori can be used to try to schedule additional scans. The concept of fillin-mode is discussed in detail in section 3.7.2 and further explanations are available in Gipson (2010). Additionally, VieSched++ provides a fillin-mode a posteriori which can be used optionally. While the basic fillin-mode is already handled by the main recursive scheduling algorithm, this mode is especially designed in

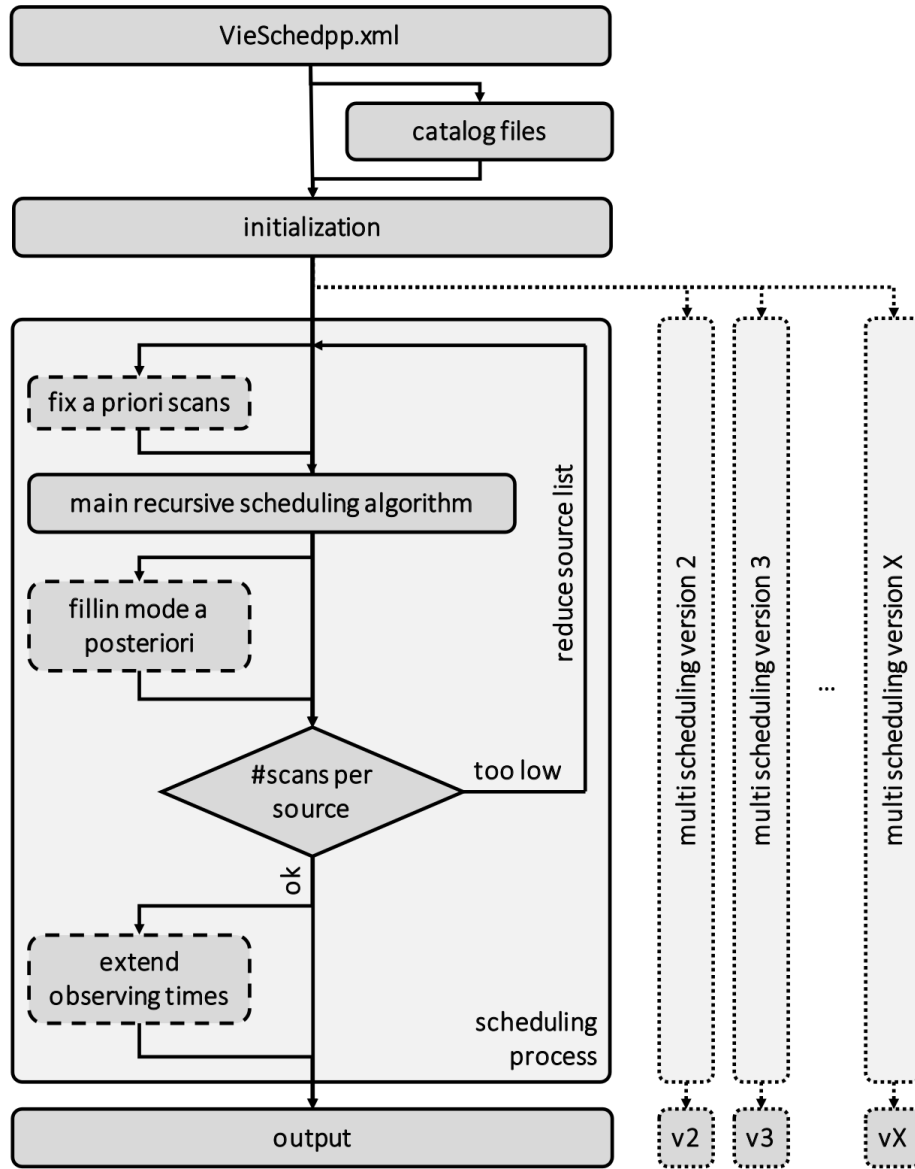


Figure 21: Flowchart of VieSched++ concept.

case multiple tagalong stations (see section 3.7.3) are used, like it was the case at the beginning of the VGOS era (Schartner and Böhm, 2019b).

At this stage, all scans and observations are fixed. VieSched++ is then evaluating if all required conditions, like the minimum number of scans per source, are fulfilled. If this is

not the case, the schedule is recreated using a reduced source list, as described in detail in section 5.7.

If all conditions are fulfilled it is possible to extend the observing times of all observations, similar as described in section 3.7.4, and finally, the output files are written.

VieSched++ supports a feature called multi-scheduling, see section 5.6 (Schartner et al., 2017; Schartner and Böhm, 2019b,c). By using this tool multiple schedules are generated simultaneously using varying parameters, as illustrated in Figure 21 with dotted lines. Since scheduling is a complex task and it is not possible to generate all possible schedules for a given session, the goal is mainly to generate a schedule which is considered “reasonably good”, although it is unlikely that it is the “best” one. By generating multiple schedules and using a huge variety of scheduling parameters, the likelihood increases that one of these schedules is good enough. The VieSched++ multi-scheduling feature supports the automatic variation of over 40 parameters and can generate hundreds of schedules in a reasonable short time. Since the antenna network, the source list, and the setup stays the same, the initialization phase has to be done only once. VieSched++ supports multi-threading for the multi-scheduling feature and thus benefits greatly in case multiple Central Processing Units (CPUs) are available.

5.3.1 Implementations of a scan

To understand the following sections and upcoming algorithm better, this section gives an insight into the implementation of a scan in VieSched++.

A scan consists of three major parts as illustrated in Figure 22, namely antenna pointing vectors at the observing start and end time, a list of all scheduled observations between the antennas and a time management system.

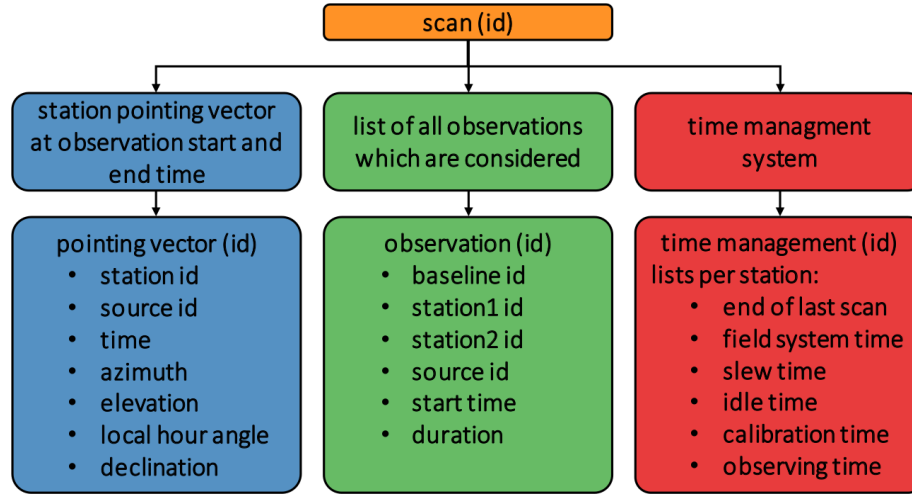


Figure 22: Main components of a scan in VieSched++.

A pointing vector describes the expected orientation of the antenna at a certain reference time. It stores the (unwrapped) azimuth and elevation information between an antenna and a source as well as the local hour angle and the declination. Pointing vectors are stored per station for the observation start and end time. Therefore, the number of pointing vectors per scan n_{pv} is two times the number of participating stations n_{sta} .

$$n_{pv} = 2 \cdot n_{sta} \quad (21)$$

Additionally, a scan contains a list of all observations which are assumed to be observed. Although the maximum possible number of observations per scan is given by (32), VieSched++ can decide to ignore certain observations. This is done in case the required observing time would be too long. Additionally, it is possible to define generally or for each source if observations at certain baselines should be ignored to be able to imitate the Star Scheduling Mode developed by [McCallum et al. \(2017\)](#). This can also be used to avoid the scheduling of single baseline scans between twin telescopes.

Therefore, the number of observation objects per scan n_{obs} is equal or less than the possible number of observations.

$$n_{obs} \leq \frac{n_{sta} \cdot (n_{sta} - 1)}{2} \quad (22)$$

In VieSched++ an observation object stores the information about which two antennas are

forming the baseline between which the delay will be observed, as well as which source should be observed. Additionally, the observation objects store its start time and the necessary duration of the observation needed to reach the desired SNR on all observed bands.

Finally, a time management system is included in each scan for performance reasons. The purpose of the time management system is to store information about the necessary slew time, idle time, calibration time, overhead time due to the execution of field system commands, as well as the observing start time and duration per station. During the computationally expensive scan selection process it is inapplicable to store the information about the observing start time and duration only in the antenna pointing vectors and observation objects. Many steps during scheduling require an iterative adjustment of the observation start and thus end time, see section 5.3.3, but their changes are mostly in the order of a few seconds. Since the information within a pointing vector or observation object should be consistent, a change of the reference time from one of these objects would require a recalculation of all other content with very little change. For this reason, the time management system is used. During the computationally expensive scan selection, the timing information is only updated in the time management system and is therefore allowed to differ from the reference times defined in the pointing vector and observation objects. As a first approximation during the iterative adjustment of the times, resulting changes in azimuth and elevation, and thus slew time and observing start and end time are often ignored, since they would not vary too much. Only if a scan is finally selected and is about to be scheduled this information is brought into consistency again, as described in section 5.3.7.

The important takeaway message of this section is, that in VieSched++ the smallest quantity is not a scan but an observation and individual antenna pointings. The following sub-chapters describe how VieSched++ calculates and handles scans.

5.3.2 Scan generation

For the selection of a scan during the generation of the schedule, VieSched++ investigates all available scans at the current schedule time. Therefore, the visibility of every source is evaluated from every station. Since this is done individually for each station, the real possible observing start time and thus the correct reference time is unknown since it is based on the availability of other antennas as well as the necessary slew times which are

not available at this point. As a first step, VieSched++ evaluates the visibility for a time calculated by using the end time of the last observation from this station plus the constant overhead and calibration times which are defined in the scheduling setup.

If a source is visible by more than the minimum number of required stations, it is further considered and slew times to this source are calculated using the models described in section 3.4.2.

Since VieSched++ is using a recursive scan selection it is possible that scans are already scheduled after the investigated scan. Therefore, VieSched++ checks, if this already scheduled scan can be reached after scheduling the tested scan, assuming an additional five second long slew time to reach the upcoming scan and an observing time equal to the minimum allowed observing time defined in the scheduling setup. This is done to reduce the number of scans which are further investigated for performance reasons. By assuming only five extra seconds for slewing and a minimum observing time, the possibility that a valid scan gets falsely removed is minimized.

5.3.3 Possible scan start

At this time, it is known which stations can participate in a scan and an initial slew time to reach the source is calculated. However, the antenna pointing reference time and thus the azimuth and elevation information used to calculate the slew time is still based on the end time of the previous observation of this station plus the constant overhead and calibration times, as described in section 5.3.2. Since the observation duration is defined through antenna sensitivity and source flux density and is calculated per baseline (see section 5.3.4), the observing time differs between stations leading to different observation end times per station. Additionally, antenna slew rates are very different, as already discussed in section 3.4.2, and the slew distances vary based on the position of the source at the sky, the antenna mount, and cable wrap limitation, see section 3.4.1. All these factors lead to a possible scan start time which is different for each station and the reference time has to be adjusted. In geodetic VLBI, per definition, every station starts its observation at the same time and thus the slowest antenna defines when the observation starts introducing idle time at all other antennas.

At this point, the antenna pointing vectors and the necessary slew times are recalculated using the real observation start time as the reference time. The real observation start time can differ multiple seconds up to some minutes from the earliest possible observing start

time per station which was earlier used as a reference time. Therefore, it can introduce changes in slew time, since the Earth keeps rotating during the occurring idle, changing the source position on the sky.

Most of the time, those changes in slew time are negligible but since VieSched++ often evaluates hundreds of millions of scans during a multi-scheduling approach, rare scenarios arise where e.g. the cable wrap changes or the cable wrap limit is reached which in turn is changing the slew direction and is changing the slew time significantly.

For providing a rigorous solution, the scan start time and the necessary slew time has to be iteratively calculated as done during the rigorous scan check, see section 5.3.7.

5.3.4 Scan observing duration

The required observation duration is calculated per observed baseline and per observed frequency band according to equation (20) in section 3.6. The maximum of the required observing time per band is used as the required time of this observation.

If the required observing time is longer than the maximum allowed observing time for this baseline the observation is not scheduled, meaning it is not included in the list of observations for this scan as described in section 5.3.1. In case the observation duration is shorter than a user-defined minimum observing time the minimum observing time is used instead. If it turns out that there are no valid observations with an antenna, the antenna is removed from the scans.

After all possible observations are generated and the necessary recording times per observation are known, the required recording time per antenna can be calculated. The required recording time per antenna covers the time span between the earliest observation start time of this antenna until the latest observation stop time of this antenna. It is further compared with the maximum allowed observing time per antenna. If the required observing time is longer than the allowed observing time per antenna, stations are iteratively removed from the scan until the required observing times are within the allowed duration. VieSched++ starts by removing the stations with the highest number of observations with a duration greater than the allowed duration per antenna. If multiple stations have the same number of observations with greater duration, the station with the highest SEFD parameter is removed. In case the SEFD parameter is equal for multiple stations the antenna with the lowest slew time is removed. In the rare scenario where all of these quantities are equal, a random antenna is chosen and removed from the scan.

If the required observing time is shorter than a minimum required observing time, the required observing time is extended to meet this requirement.

If there is already a scan scheduled after the investigated scan through the recursive scan selection, VieSched++ checks if the already scheduled scan can be reached after the tested scan within the available time. This is done multiple times during the calculation of the observing duration per observation and antenna to minimize the computation load and improve the performance.

5.3.5 Subnetting

As already discussed in section 3.7.1, subnetting is a good way to increase the quality of schedules, especially in case global networks are used, by considering not only one scan at a time but two parallel scans simultaneously during the scheduling process. Since for a global network, no source can be seen from every antenna simultaneously, the consideration of a second scan opens the possibility to consider and evaluate all antennas at the same time which works a lot better for the scan selection algorithm. As a side effect, it helps to provide a better sky-coverage, since it becomes more likely that sources at the edges of common visibility areas are selected if two of these scans are investigated simultaneously due to the combination of the individual scores per scan during the scan selection, see section 5.3.6.

Subnetting drastically increases the pool of possible scans to choose from. If the number of sources is denoted by n_{src} without subnetting there are only $n_{scans} \leq n_{src}$ possible scans which can be observed and thus have to be considered during the scan selection. By using subnetting the number of possible scan constellations increases to $n_{scans} \leq \frac{n_{src} \cdot (n_{src} - 1)}{2}$. In numbers, this means by using a list of 100 sources the number of possible subnetting scan combinations becomes ≈ 5000 , in case of a list of 300 sources, as it is the case in the commonly used geodetic good sources catalog, the number of possible subnetting scan combinations increases to $\approx 45\,000$.

Due to performance reasons, it is clear that the number of actually considered subnetting scan combinations per scan selection step has to be drastically lower. Therefore, several parameters can be used in VieSched++.

Since one benefit of subnetting is to be able to schedule all antennas of a global network in one step, it only makes sense to consider subnetting scan constellations to sources which are far apart on the sky to make sure that at least one source is visible for every antenna.

During the initialization phase of VieSched++, pairs of possible subnetting sources are calculated based on the angular distance between the sources and an user-defined minimum distance. Only subnetting scan constellations between these pairs of subnetting sources are further considered by the software. Additionally, subnetting scan constellations which include only a fraction of all available antennas are ignored as well since they mitigate the benefit of subnetting.

As an example: a standard ten station R4 network is scheduled in VieSched++ by evaluating $\approx 400\,000$ scans in total if subnetting is allowed between sources with an angular distance of 150° and the minimum number of participating antennas during subnetting is nine. The number of scans increases to $\approx 3\,500\,000$ if the angular distance between subnetting scans is lowered to 120° and scan constellations with up to seven antennas are considered. Therefore, minimizing the number of evaluated subnetting constellations and a fast implementation of these algorithms is the key for increased software performance. However, limiting these quantities too much can mitigate the benefit of subnetting, since possible good subnetting constellations are not considered.

VieSched++ is considering all possibilities for subnetting. For example, a situation as visualized in Figure 23 where two sources are visible from multiple antennas would lead to an investigation of multiple possible scan combinations as listed in Table 2. In this example, there is a total of ten antennas and both sources are visible from seven antennas each. For three of these antennas, only source one is visible, while for three other antennas only source two is visible. For the remaining four antennas both sources are visible simultaneously. This would result in 18 different scan constellations containing these two sources which are investigated, as listed in Table 2. In the case of version one and two, only one scan to one source is scheduled without the use of subnetting. All other versions are defined through different subnetting situations.

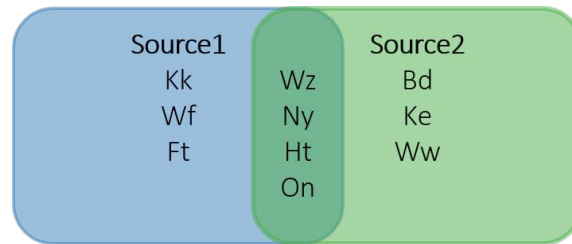


Figure 23: Example of a subnetting situation.

5. VIESCHED++

Table 2: List of all possible scans which are evaluated from a situation displayed in Figure 16 by using subnetting.

version	scan of source 1	scan of source 2
1	Ft Kk Wf Ht Ny On Wz	
2		Bd Ke Ww Ht Ny On Wz
3	Ft Kk Wf Ht Ny On Wz	Bd Ke Ww
4	Ft Kk Wf Ht Ny On	Bd Ke Ww Wz
5	Ft Kk Wf Ht Ny Wz	Bd Ke Ww On
6	Ft Kk Wf Ht On Wz	Bd Ke Ww Ny
7	Ft Kk Wf Ny On Wz	Bd Ke Ww Ht
8	Ft Kk Wf Ht Ny	Bd Ke Ww On Wz
9	Ft Kk Wf Ht On	Bd Ke Ww Ny Wz
10	Ft Kk Wf Ht Wz	Bd Ke Ww Ny On
11	Ft Kk Wf Ny On	Bd Ke Ww Ht Wz
12	Ft Kk Wf Ny Wz	Bd Ke Ww Ht On
13	Ft Kk Wf On Wz	Bd Ke Ww Ht Ny
14	Ft Kk Wf Ht	Bd Ke Ww Ny On Wz
15	Ft Kk Wf Ny	Bd Ke Ww Ht On Wz
16	Ft Kk Wf On	Bd Ke Ww Ht Ny Wz
17	Ft Kk Wf Wz	Bd Ke Ww Ht Ny On
18	Ft Kk Wf	Bd Ke Ww Ht Ny On Wz

5.3.6 Scan selection

As described in earlier sections, a schedule is typically generated scan after scan, as indicated in Figure 2. Each scan is selected from a pool of all possible scans, which can be hundreds or even thousands. VieSched++ is using optimization criteria for evaluating which scans should be scheduled. This process is discussed in detail in section 5.4. In short, the software calculates multiple scores based on several optimization criteria. A weighted sum of these individual scores is used to calculate the total score of a scan. This is done for every possible scan. In case of using subnetting the score is calculated for every scan constellation by adding the scores of the two individual scans forming the subnetting constellation. The scan or scan constellation with the highest score is then selected and added to the final schedule.

5.3.7 Rigorous scan check

After a scan or subnetting scan constellation is selected from the pool of possible scans by having the highest total score, rigorous checks are run to verify that everything is calculated correctly. For the sake of simplicity, only the case of a single scan is further discussed. In case a subnetting scan constellation is selected, the following steps are done for each subnetting scan individually.

First, the slew times are rigorously and iteratively recalculated. An iterative calculation is necessary, since the slew time depends on the source position, while the source position depends on the slew time due to Earth rotation. Afterward, the observing start and stop times are calculated again by rigorously calculating the observing duration per baseline followed by the observing duration per station as already described in section 5.3.4. Finally, it is investigated if the source is visible throughout the full scan. Therefore, the visibility is checked at the start of the observation and the end of the observation, as well as every 30 seconds in between. After these calculations, the reference times from the pointing vectors and the time management system are consistent and the score of the scan is recalculated. If the scan is still the highest-scoring scan it is finally selected and scheduled. Otherwise, these steps are repeated with the now highest-scoring scan until the rigorously updated scan is the highest scoring scan.

Based on these algorithms and ideas the full schedule is generated in VieSched++.

5.4 Optimization criteria and weight factors

The optimization criteria definitions and equations are discussed in [Schartner and Böhm \(2019c\)](#).

As discussed in section 3, a schedule is typically created scan after scan. Similar to sked and Vie_Sched, VieSched++ uses a brute force approach to select and schedule scans by generating and evaluating all possible scans and subnetting scan combinations ([Gipson, 2010](#); [Sun, 2013](#)). To select the best scan out of the pool of all possibilities, multiple optimization criteria are used. Every possible scan gains a score based on these optimization criteria $score_{opt}$. The total score $score_{scan}$ is the weighted sum of the scores per optimization criterion. Weight factors $weight_{opt}$ are used to combine multiple criteria

similar to “minor options” in sked, see [Gipson and Baver \(2016\)](#) or [Gipson \(2010\)](#).

$$score_{scan} = \sum_{i_{opt}=0}^{n_{opt}} weight_{i_{opt}} \cdot score_{i_{opt}} \quad (23)$$

Weight factors are scalar values which can be varied in VieSched++. The higher the value of a weight factor $weight_{opt}$ is, the more the score of this optimization criterion $score_{opt}$ contributes to the total score of a scan $score_{scan}$. For example, if only two optimization criteria, namely the number of observations per scan and the sky-coverage improvement should be used to generate a schedule, all weight factors except these two should get a value of zero. If the weight factor for improving the sky-coverage (see section 5.4.2) is given a value of 1 and the weight factor for the number of observations per scan (see section 5.4.3) is given a value of 0.1, the software will focus on optimizing the sky-coverage for all stations rather than try to schedule scans with a high number of observations. Instead, if the weight factor for improving the sky-coverage is given a value of 0.1 and the weight factor for the number of observations per scan is given a value of 1, the software tries to focus more on scheduling scans providing many observations.

Based on equation (23) it can be seen that only the relative ratio between the individual weight factors is of importance. Using only two weight factors with the values 1 and 0.1 will lead to the same schedule as if the same weight factors are used with values 10 and 1 or 100 and 10.

In the case of subnetting scan combinations, the score is calculated for each scan individually and summed up.

$$score_{subnetting} = score_{scan_1} + score_{scan_2} \quad (24)$$

The scan or subnetting combination of two scans with the highest score is selected and scheduled.

Currently VieSched++ supports nine optimization criteria:

- duration
- sky-coverage
- number of observations
- idle time
- average observations per stations

- average observations per sources
- average observations per baselines
- low elevation
- low declination

Choosing a good set of optimization criteria and weight factors are the key to create an optimized schedule (Schartner et al., 2017).

For developing a VLBI scheduling software like VieSched++, defining sophisticated optimization criteria is tricky because the criteria should be generally valid for all combinations of different antennas, sources and observing modes. Since by considering subnetting the score of two scans is added together, see equation (24), it is necessary to scale the weight factors carefully to allow a fair comparison between single-source scans and subnetting scan combinations objectively. Since the optimization criteria directly determine which scans are scheduled, they are the most critical part of the scheduling software. Thus, there are regular changes and improvements to these algorithms aiming to improve the quality of the schedule.

5.4.1 Duration

The optimization criterion for the duration of a scan is one of the trickiest to define while being one of the most important for the generation of a good schedule (Schartner and Böhm, 2019c). The difficulty arises due to the big variety of different antenna slew speeds (see section 3.4.2) and differences in recording modes. For fast slewing VGOS antennas recording with high sampling rates of several Gbit/s, observing a scan takes far less time than for slow slewing antennas with sampling rates of some hundred Mbit/s. The same is true for fillin-mode scans which include a reduced number of stations and are typically faster to perform. However, it is necessary to define an optimization criterion for the duration of a scan which is generally valid in all cases.

The idea behind this optimization criterion is that, all things being equal, a schedule with a high total number of observations leads to better results than a schedule with a lower total number of observations. The number of observations per schedule is determined by two factors: the number of scans and the number of observations per scan. The duration optimization criterion tries to maximize the number of scans, while the number of observations criterion (see section 5.4.3) tries to maximize the number of observations per scan. Together, they are used to influence the total number of observations in the schedule

which has to be balanced with the antenna sky-coverage.

The duration dur which is used as a metric to compare scans in this optimization criterion includes everything between the end of the previous scan until the end of the tested scan. This includes overhead time for field system commands, slew time, idle time, calibration time and observing time. In this context, the “end of the previous scan” is defined as the earliest time an in this scan participating antenna stops recording its previous scan. The score $score_{dur}$ (25) is based on the minimum dur_{min} and maximum time dur_{max} for all scans forming the pool of possible scans as well as on the duration dur of the tested scans (Schartner and Böhm, 2019c). Finally, a scale factor is applied based on the number of participating stations n_{sta} which is necessary to compare single source scans and subnetting scan combinations. Assuming scans containing all antennas, the scan with the shortest duration gains a score of 1 while the scan with the longest duration gets a score of 0 and linear interpolation is used in between.

$$score_{dur} = 1 - \frac{dur - dur_{min}}{dur_{max} - dur_{min}} \cdot \frac{n_{sta}}{n_{sta_{max}}} \quad (25)$$

Initial tests reveal that this weight factor is one of the most important for generating a good schedule (Schartner et al., 2017). It indirectly improved the sky-coverage as well, due to the inclusion of more scans.

5.4.2 Sky-coverage

An evenly distributed sky-coverage helps to estimate tropospheric time delays which are considered one of the major error sources in VLBI (Böhm et al., 2006). Therefore, a schedule should be optimized by planning observations at different azimuth and elevation angles over short periods. The idea of this score is to use the angular distance between the azimuth and elevation of previously scheduled observations and the azimuth and elevation of possible next observations together with the time difference between these observations to decide which scans would improve the sky-coverage at the stations best, see Figure 25 for some examples.

However, a proper definition of the sky-coverage is not trivial. Therefore, VieSched++ uses several parameters which define the sky-coverage:

- an angular distance transfer function $dist_{fun}$,
- an influence distance $dist_{inf}$,

- a time transfer function $time_{fun}$ and
- an influence time $time_{inf}$.

First, VieSched++ calculates the saturation of the sky-coverage based on the angular distance between each previously scheduled observation and the tested one, see equation (26a) and (27a). Additionally, VieSched++ calculates the saturation based on the time difference between each previously scheduled observation and the tested one, see equation (26b) and (27b). Finally, these two individual saturation values are combined to calculate the total impact of the tested observation for the sky-coverage based on each previously scheduled observation, see equation (28).

Currently, there are three possible angular distance and time transfer functions implemented, called: *cosine*, *linear* and *constant*. The variety of different parameters are necessary for providing a generally valid and usable sky-coverage optimization criterion.

The basic concept behind this optimization criterion is that the antenna pointings of each station are compared to all already scheduled antenna pointings of previous scans i_{prev_scan} (Schartner and Böhm, 2019c). Depending on the time difference $\Delta time$ and angular distance $\Delta dist$ a score per antenna pointing $sat_{dist_{i_{prev_scan}}}$ and $sat_{time_{i_{prev_scan}}}$ is calculated as shown in equation (26a) and (26b). Equation (27a) and (27b) list the possible functions used to describe the dependency of the angular distance and the time difference while Figure 24 displays the corresponding functions.

$$sat_{dist_{i_{prev_scan}}} = \begin{cases} 0 & \Delta dist > dist_{inf} \\ dist_{fun}(\Delta dist) & \Delta dist < dist_{inf} \end{cases} \quad (26a)$$

$$sat_{time_{i_{prev_scan}}} = \begin{cases} 0 & \Delta time > time_{inf} \\ time_{fun}(\Delta time) & \Delta time < time_{inf} \end{cases} \quad (26b)$$

with

$$dist_{fun}(\Delta dist) = \begin{cases} 1 & dist_{fun} = constant \\ 1 - \frac{\Delta dist}{dist_{inf}} & dist_{fun} = linear \\ \frac{1}{2} + \frac{1}{2} \cdot \cos\left(\frac{\Delta dist \cdot \pi}{dist_{inf}}\right) & dist_{fun} = cosine \end{cases} \quad (27a)$$

$$time_{fun}(\Delta time) = \begin{cases} 1 & time_{fun} = constant \\ 1 - \frac{\Delta time}{time_{inf}} & time_{fun} = linear \\ \frac{1}{2} + \frac{1}{2} \cdot \cos\left(\frac{\Delta time \cdot \pi}{time_{inf}}\right) & time_{fun} = cosine \end{cases} \quad (27b)$$

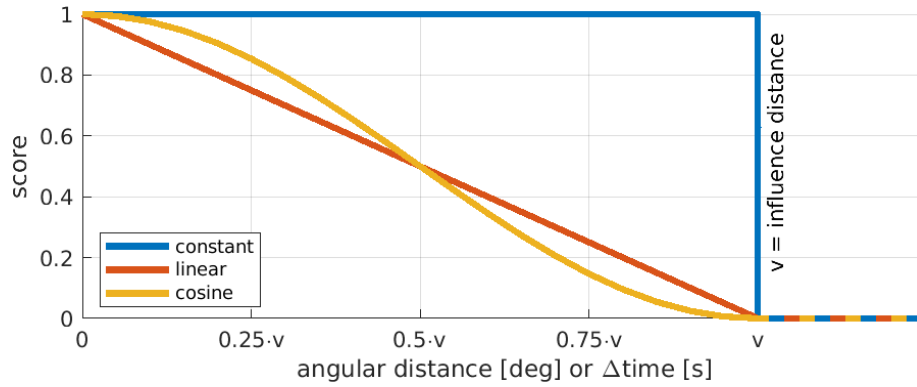


Figure 24: Available functions for calculation of sky-coverage saturation based on angular distance and time between two observations.

Based on the saturation due to the angular distance (26a) and the time difference (26b) to one previously scheduled scan the score based on the previously scheduled scan $score_{i_{prev_scan}}$ can be calculated according to (28).

$$score_{i_{prev_scan}} = 1 - \left(sat_{dist_{i_{prev_scan}}} \cdot sat_{time_{i_{prev_scan}}} \right) \quad (28)$$

The total score per sky-coverage $score_{i_{sky}}$ is defined as the minimum score from each previously scheduled scan $score_{i_{prev_scan}}$.

$$score_{i_{sky}} = \min_{prev_scan} (sat_{i_{prev_scan}}) \quad (29)$$

Therefore, the maximum achievable score per sky-coverage is one.

Finally, the total score for the sky-coverage optimization criterion is calculated based on the sum of the improvements for each sky-coverage i_{sky} divided by the total number of sky-coverages in this session n_{sky} . The normalization ensures that the maximum achievable score for this criterion is one.

$$score_{sky} = \sum_{i=0}^{n_{sky}} score_{i_{sky}} \cdot \frac{1}{n_{sky}} \quad (30)$$

If all stations are participating in a scan and all antennas point to a direction in the sky where no other observations were scheduled for a certain amount of time, this scan would get the highest possible score of 1 (Schartner and Böhm, 2019c). Figure 25 illustrates different sky-coverage scores based on a combination of different transfer functions.

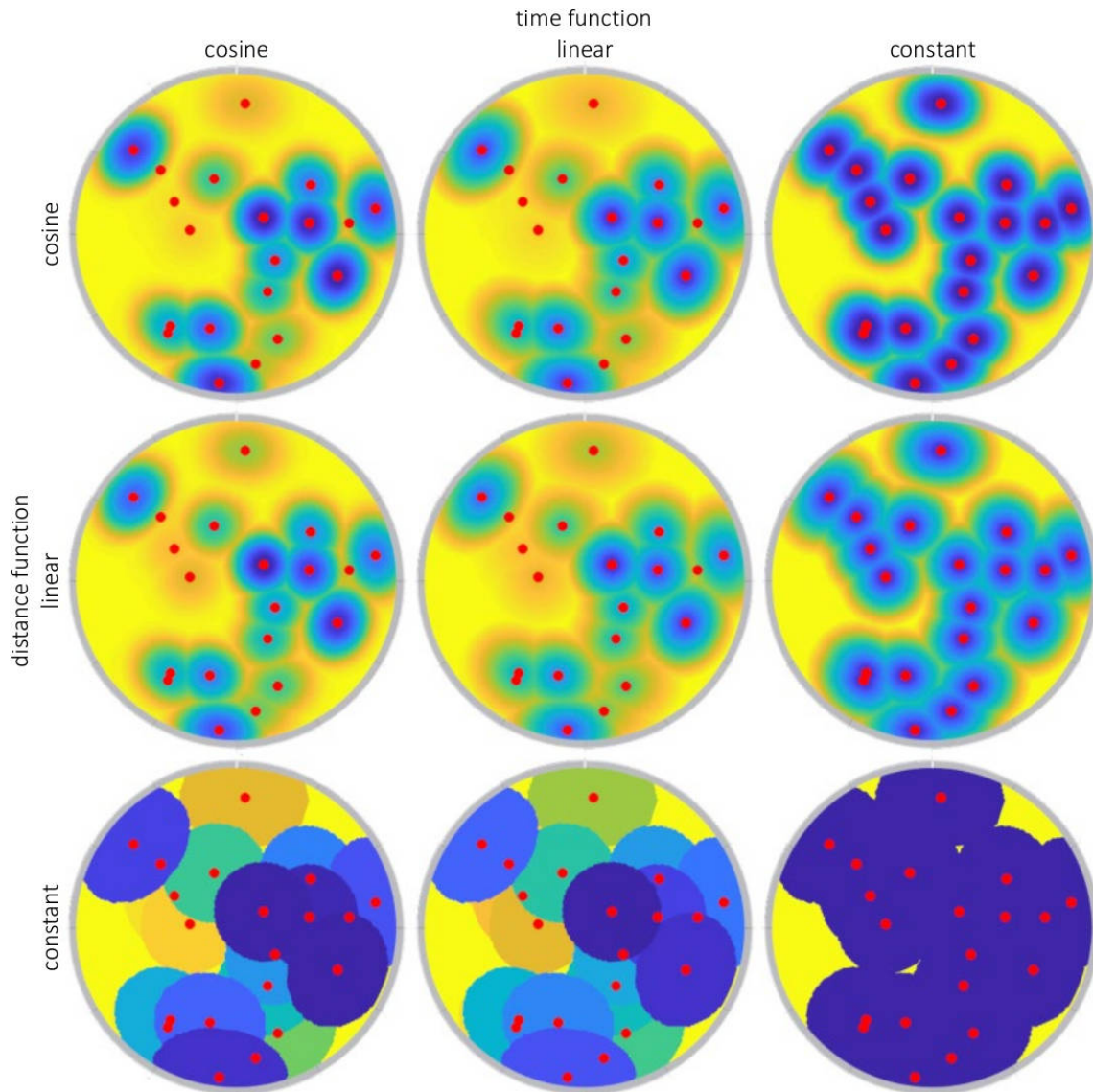


Figure 25: Example of sky-coverage score $score_{sky}$ from equation (30) based on a combination of different transfer functions. Observations in areas which are marked blue gain a low score, while observations in areas which are marked yellow gain a high score. Previous observations are marked with red circles.

VieSched++ supports the use of twin telescopes and more general multiple telescopes per observing site. In case of multiple telescopes per observing site all of these stations share the sky-coverage information. Therefore, the number of sky-coverages n_{sky} is always

less or equal to the number of stations participating in the session n_{sta} .

$$n_{sky} \leq n_{sta} \quad (31)$$

5.4.3 Number of observations per scan

A rule of thumb for evaluating a good schedule suggests that the higher the number of observations, the better the schedule (Gipson, 2010). Therefore, the number of observations per scan optimization criterion helps to generate a schedule with a high total number of observations. Since a schedule is generated scan after scan (see section 3), this can only optimize the number of observations per scan, not the total number of observations in the schedule. The total number of observations in the schedule is also determined by the number of scans per schedule, determined through the duration optimization criterion (see section 5.4.1).

The score for the number of observations $score_{n_{obs}}$ per scan optimization criterion is defined through the total number of observations n_{obs} scheduled in this scan and the maximum theoretically possible number of observations $n_{obs_{max}}$ assuming a scan with all stations $n_{sta_{max}}$ (Schartner and Böhm, 2019c). While the number of possible observations is defined by equation (32) the scheduled number of observations per scan can be lower in VieSched++ as explained in section 5.3.1 due to the way, how a scan is implemented in VieSched++ and how stations and observations are removed from scans.

$$n_{obs_{max}} = \frac{n_{sta_{max}} \cdot (n_{sta_{max}} - 1)}{2} \quad (32)$$

The score $score_{n_{obs}}$ is defined through the ratio of observations n_{obs} at this scan and the maximum possible observations $n_{obs_{max}}$ assuming a scan with all stations, see equation (32).

$$score_{n_{obs}} = \frac{n_{obs}}{n_{obs_{max}}} \quad (33)$$

5.4.4 Idle time

The score for the idle time optimization criterion $score_{idle}$ is calculated per station. The idea behind this optimization criterion is to give stations which have not been included in the schedule for the last couple of minutes a higher weight (Schartner and Böhm, 2019c). This helps to include geographically remote stations or stations with low sensitivity in the

schedule and makes sure that all antennas observe regularly.

Two parameters are used to calculate the idle time optimization criterion score, the so-called idle time interval *interval* and the actual idle time per station *idle* before this scan. The idle time before this scan *idle* is defined through equation (34), where *current_time* refers to the end time of the last observation scheduled for this station. From the scheduling software point of view, this is the current position and time of the antenna. The station idle time is divided by the *interval* time to get the idle time score per station $idle_{i_{sta}}$ as shown in equation (34).

$$idle_{i_{sta}} = \max(current_time) - current_time_{i_{sta}} \quad (34)$$

According to equation (34), stations which have not been observing for a duration of *interval* gain a score of one, while stations which have not been observing for a duration of $2 \cdot interval$ gain a score of two and so on.

The total score $score_{idle}$ is defined as the sum of the idle time scores per station $idle_{i_{sta}}$.

$$score_{idle} = \sum_{i_{sta}=0}^{n_{sta}} \frac{idle_{i_{sta}}}{interval} \quad (35)$$

Therefore, if a scan includes stations which previously have been idling for a long period of time, this scan gets a higher score and is more likely to get scheduled.

The idle time score is the only optimization criterion which is completely independent of the tested scan. This is necessary because otherwise, scans which would include long idle times would gain a higher score. This is unwanted because it is in direct contradiction to the score based on the duration, see section 5.4.1.

Additionally, the idle time score is the only score which can grow without bounds. All other scores are defined in a way, that the maximum achievable score is one for a scan or subnetting scan combination. The likelihood of selecting a scan with a station increases the longer this station is idling. Additionally, this means that scaling of the score by the total number of stations is not necessary for an objective comparison of single-source scans and subnetting scans as can be seen in equation (34).

5.4.5 Average observations per station

The idea behind the average observations per station optimization criterion is to increase the weight of stations with a lower number of scheduled observations compared to the average number of scheduled observations per station (Schartner and Böhm, 2019c). If the number of observations of a station $n_{obs_{i_{sta}}}$ is lower than the average number of observations per station $n_{obs_{mean}}$, it gets a score $score_{asta_{i_{sta}}}$ based on the difference, as defined in equation (36).

$$score_{asta_{i_{sta}}} = \begin{cases} 0 & n_{obs_{i_{sta}}} > n_{obs_{mean}} \\ \frac{n_{obs_{mean}} - n_{obs_{i_{sta}}}}{n_{obs_{mean}} - \min(n_{obs_{sta}})} & n_{obs_{i_{sta}}} < n_{obs_{mean}} \end{cases} \quad (36)$$

Therefore, the station with the lowest number of observations gets a score of one while a station with an average or higher number of scheduled observations get a score of zero. Linear interpolation is used in between.

The total score of the average observations per station criteria $score_{asta}$ is the sum of the station wise scores $score_{asta_{i_{sta}}}$ multiplied by a scale factor as defined in equation (37). The scale factor is the fraction between the number of observations with this station $n_{obs_{i_{sta}}}$ in the tested scan and the maximum number of theoretically possible observations per station, which is the number of stations in this session minus one. While the numerator of the scale factor is used to prefer scans with many observations with this station, the denominator is necessary to properly compare single source scans and subnetting scans.

$$score_{asta} = \sum_{i_{sta}=0}^{n_{sta}} \left(score_{asta_{i_{sta}}} \cdot \frac{n_{obs_{i_{sta}}}}{n_{sta_{max}} - 1} \right) \quad (37)$$

Together, this makes sure that scans with so far rarely scheduled stations would get an increased weight and the weight gets higher the more observations with these stations are scheduled in the scan.

5.4.6 Average observations per sources

Similar to the average observations per station optimization criterion (see section 5.4.5), the average observations per source criterion is using equation (36) to calculate the score for this source $score_{asrc_{i_{src}}}$ but with the number of observations per source $n_{obs_{i_{src}}}$ instead of the number of observations per station as can be seen in (38).

$$score_{asrc_{i_{src}}} = \begin{cases} 0 & n_{obs_{i_{src}}} > n_{obs_{mean}} \\ \frac{n_{obs_{mean}} - n_{obs_{i_{src}}}}{n_{obs_{mean}} - \min(n_{obs_{src}})} & n_{obs_{i_{src}}} < n_{obs_{mean}} \end{cases} \quad (38)$$

The total score per source is calculated using equation (39). Similar to most other score functions, a scale factor is necessary. The scale factor is defined as the fraction between the number of observations scheduled in this scan n_{obs} and the theoretically maximum number of observations possible, see equation (32).

$$score_{asrc} = score_{asrc_{i_{src}}} \cdot \frac{n_{obs}}{n_{obs_{max}}} \quad (39)$$

The scale factor satisfies two purposes: the numerator makes sure, that the scans with more observations get a higher weight while the denominator is necessary to properly compare subnetting scans with single-source scans.

However, this optimization criterion will only work if a small source list is used and all of those sources should be observed during the schedule. The official sked source lists contain 300 (*source.cat.geodetic.good*) or 700 sources (*source.cat*). In a typical 24-hour global session, only ≈ 80 different sources are scheduled. This leads to a lot of sources with zero observations and equation (38) might not work as intended due to the low average number of observations. Therefore, it is advisable to use the iterative source selection feature described in section 5.7 for geodetic purposes.

5.4.7 Average observations per baselines

The idea of this optimization condition is to increase the weight of certain baselines which have not been regularly scheduled so far to create scans with different subnetworks. The score per baseline is defined similar as (36) and (38) based on the number of observations per baseline $obs_{i_{bl}}$ instead of the number of observations per station or source to calculate the score per baseline $score_{abl_{i_{bl}}}$.

$$score_{abl_{i_{bl}}} = \begin{cases} 0 & n_{obs_{i_{bl}}} > n_{obs_{mean}} \\ \frac{n_{obs_{mean}} - n_{obs_{i_{bl}}}}{n_{obs_{mean}} - \min(n_{obs_{bl}})} & n_{obs_{i_{bl}}} < n_{obs_{mean}} \end{cases} \quad (40)$$

The final score $score_{abl}$ is the sum of the individual baseline scores $score_{abl_{i_{bl}}}$.

$$score_{abl} = \sum_{i_{bl}=0}^{n_{bl}} score_{abl_{i_{bl}}} \quad (41)$$

A scale factor is not necessary, since the number of observations per baseline during a scan is always one.

5.4.8 Low elevation

Tropospheric time delays are considered to be one of the biggest error sources in geodetic VLBI (Böhm et al., 2006; Petrachenko et al., 2012). The tropospheric time delays can be better estimated if observations are scheduled at low elevation angles (Schuh and Böhm, 2013). Therefore, the low elevation optimization criterion can be used to prefer scheduling scans with stations observing also at low elevations. The score $score_{el}$ is calculated per station $score_{el_{i_{sta}}}$ and is based on the elevation of the observation as well as on two elevation thresholds el_{begin} and el_{full} (Schartner and Böhm, 2019c). If the elevation is above the el_{begin} threshold the score is zero. If the elevation is lower than the el_{full} threshold the score is one. Linear interpolation is used in between.

$$score_{el_{i_{sta}}} = \begin{cases} 0 & el > el_{begin} \\ \frac{el_{begin} - el_{i_{sta}}}{el_{full} - el_{begin}} & el_{begin} > el_{i_{sta}} > el_{full} \\ 1 & el < el_{full} \end{cases} \quad (42)$$

A visualization of equation (42) is visualized in Figure 26.

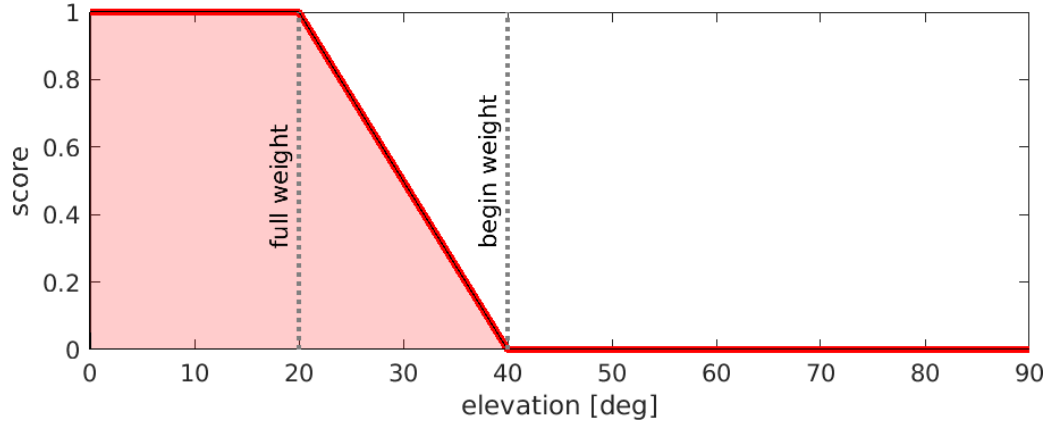


Figure 26: Low elevation score function.

The approach of using two thresholds and a linear interpolation in between is used for smoothing the score function. If a step function is desired, this can be achieved by giving the two parameters el_{begin} and el_{full} the same value.

The total score $score_{el}$ is calculated via the sum of the individual scores per station for all participating stations normalized by the total number of stations in this session $n_{sta_{max}}$. Due to the normalization, the maximum achievable score is one.

$$score_{el} = \sum_{i_{sta}=0}^{n_{sta}} score_{el_{i_{sta}}} \cdot \frac{1}{n_{sta_{max}}} \quad (43)$$

5.4.9 Low declination

Since most VLBI antennas are located in the northern hemisphere (see Figure 3) most scans are observing sources at high declination and between northern baselines (Plank et al., 2015). Therefore, the accuracy of sources at high declination is better than on low declination. To address this situation, special focus should be put on observing sources in the south (Fey et al., 2015).

The low declination optimization criterion helps to achieve this by increasing the score of scans to sources at lower declination. Similar to the low elevation criterion (see section 5.4.8) the low declination criterion is defined by two parameters, dec_{begin} and dec_{full} and by the declination of the source dec . Equation (44) shows the formula used to calculate

the low declination score per source $score_{dec_{src}}$ and Figure 27 visualizes the function.

$$score_{dec_{src}} = \begin{cases} 0 & dec > dec_{begin} \\ \frac{dec_{begin} - dec}{dec_{full} - dec_{begin}} & dec_{begin} > dec_{src} > dec_{full} \\ 1 & dec < dec_{full} \end{cases} \quad (44)$$

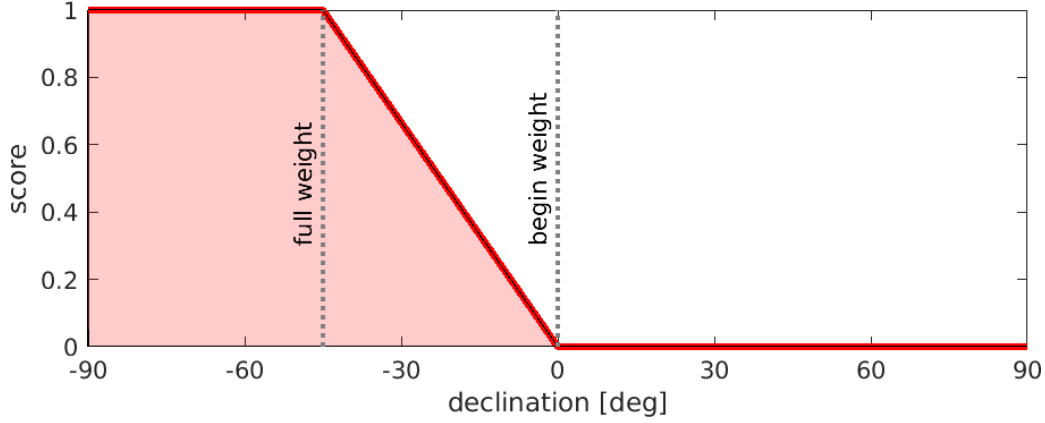


Figure 27: Low declination score function.

The total score $score_{dec}$ is the source based score $score_{dec_{src}}$ multiplied by a scale factor where n_{obs} is the number of observations in this scan and $n_{obs_{max}}$ is the maximum possible number of observations assuming a scan with all stations, see equation (32).

$$score_{dec} = score_{dec_{src}} \cdot \frac{n_{obs}}{n_{obs_{max}}} \quad (45)$$

Due to the scale factor scans with a higher number of observations at low declination get an increased score.

5.4.10 Other

Besides optimization criteria 5.4, other factors influence the calculated score (Schartner and Böhm, 2019c). All stations, sources and scheduled baselines can get an individual weight in the parameters, $weight_{sta}$, $weight_{src}$, and $weight_{bl}$, see section 5.8. As described in section 5.3.1 VieSched++ does not necessarily schedule all possible observations between all participating stations. Therefore, only the weights of baselines which are scheduled are

used. By default, all weights are set to one which means they have no influence on the total score $score_{scan}$. When using individual weight equation (23) expands to (46), where \prod is used to represent the product of the terms.

$$score_{scan} = \sum_{i_{opt}=0}^{n_{opt}} (weight_{i_{opt}} \cdot score_{i_{opt}}) \cdot \prod_{i_{sta}=0}^{n_{sta}} \cdot weight_{src}(weight_{i_{sta}}) \cdot \prod_{i_{bl}=0}^{n_{bl}} (weight_{i_{bl}}) \quad (46)$$

Besides this, there is another optional multiplicative factor of the score based on custom scan sequences, see section 5.10. When using this option scores from scans observing sources of the current target group are multiplied by a factor of 100 otherwise they are divided by a factor of 100.

5.5 Recursive scan selection

A scheduling software should aim to generate a schedule which is as good as possible. This means that the scan sequence should be carried out as efficiently as possible to meet all requirements and especially antenna idle time should be avoided as much as possible. There are three main reasons why antenna idle time can occur: First, an antenna cannot participate in any of the scheduled scans at that time. Second, the antenna has to wait for other antennas to finish slewing until the observations can start. Third, an antenna is more sensitive than the other, thus leading to shorter observing times since the observing time is based on the antenna sensitivity, the recording rate, the observed source flux density, and the SNR which should be achieved, see section 5.3.4. While the first cause can be avoided by scheduling scans that include all antennas, the second and third reason cannot be avoided easily. However, an antenna with a bigger dish size is more sensitive but is, in general, slower slewing. This means that a bigger antenna will finish its observation earlier and can use the extra time to earlier start slewing to the next source. Although this helps in theory, in practice the effects do not fully balance each other out and idle time still occurs in the schedule.

To minimize the idle time additional scans are inserted in case multiple antennas are idling for too long which is called a fillin-mode (Gipson, 2010). Previously developed scheduling software is checking if multiple stations finish a scan way earlier than other stations. If this is the case additional scans which only consider these early finishing antennas are evaluated and scheduled. While this works well in certain cases it has some

drawbacks: It only considers idle time at the end of a scan, which is mostly appearing due to different sensitivities and thus observing times. Idle time due to different slew times is not affected by this approach.

VieSched++ uses a different approach to minimize idle time. It is using a recursive scan selection (Schartner and Böhm, 2019b,c). After VieSched++ schedules a scan, it checks if it is possible to squeeze in another scan between the scheduled scan and previous scans and, if available, between the scheduled scan and next scans. Using this approach the idle time can be reduced significantly and idle times due to all causes like different slew times and observing times are considered. Moreover, the idle time due to different observing times from the previous scans and the idle time due to different slew times of the upcoming scan can be combined, and viewed as one larger idle time block, making it more likely that a fillin-mode scan can be scheduled successfully.

5.5.1 Concept

Figure 28 illustrates how the recursive scan selection algorithm works. At the beginning of the session, scan 1 is scheduled followed by scan 2. As soon as scan 2 is fixed the first recursion starts and the algorithm checks if there is time between scan 1 and scan 2 to schedule another scan. In this example, it is possible to schedule scan 3. As soon as scan 3 is scheduled the next recursion starts and checks if there is time between scan 1 and scan 3. If this is not the case this recursion stops and the time between scan 3 and scan 2 is investigated. Here, it is possible to schedule scan 4, leading to a new recursion checking the time between scan 3 and scan 4. In this example, it is possible to schedule scan 5, which starts a new recursion, testing the time between scan 3 and scan 5 followed by the time between scan 5 and scan 4. Since no additional scans can be scheduled in these two cases, the recursion stops and the time between scan 4 and scan 2 is tested. If all recursions stopped the time between scan 1 and scan 2 is fully optimized and the scheduler continues to schedule scan 6, starting the whole process again. These steps are repeated until the full schedule is generated.

After the schedule is finished, leftover idle time can be used to extend the observing time of the stations to increase the SNR as described in section 3.7.4.

Obviously Figure 28 is highly simplified. In reality, most stations have a different possible start and stop time which has to be monitored individually. If there are multiple antennas participating in a session, and their sensitivities and slew speed are very different,

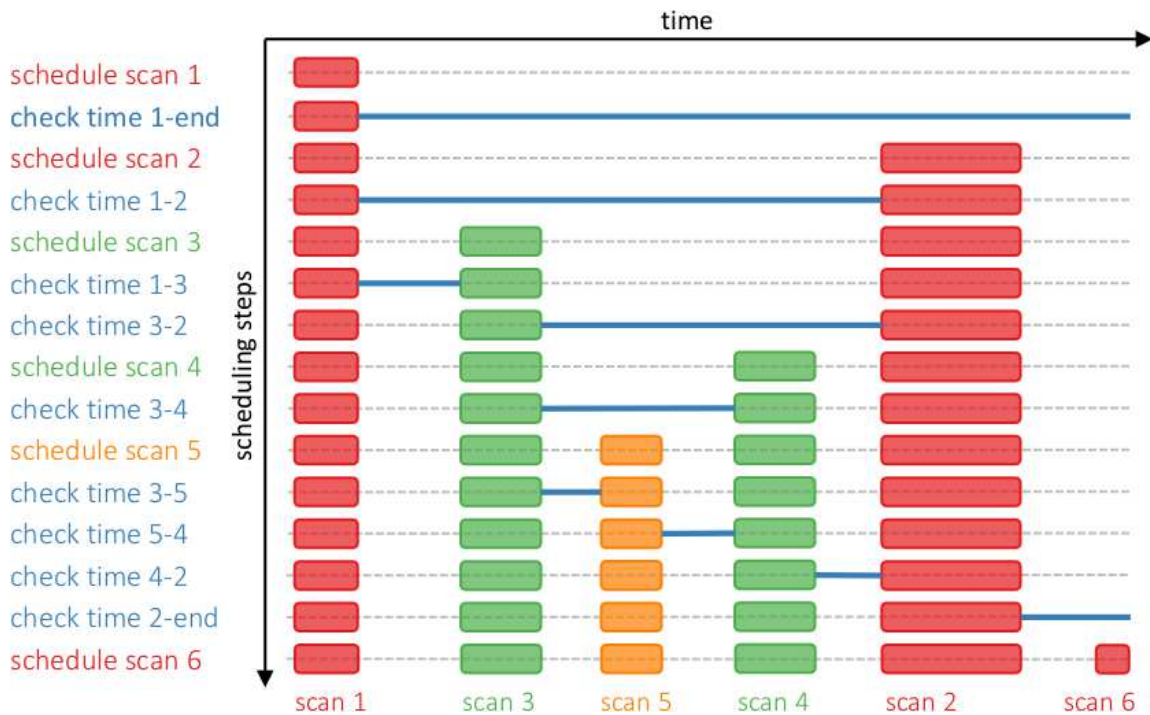


Figure 28: Concept of recursive scan selection.

it commonly happens that scans are scheduled which are three levels deep in the recursion, which is even one level deeper as illustrated in Figure 28.

Figure 29 visualizes the flowchart of how the recursive scheduling process is implemented in detail. It starts with the currently scheduled antenna pointing directions and times as well as optionally some required antenna pointing and times for already scheduled scans in the future. Based on the currently scheduled antenna pointing direction and time, all available sources are investigated based on the visibility of the stations, see section 5.3.2. If enough stations are available to form a valid scan to a source, the slew times from the antennas to this source are calculated, see section 5.3.3.

If the slew times of enough stations are valid based on the defined scheduling parameters, observations are formed between the participating stations and the minimum required observing duration is calculated, first per baseline and per band and later per antenna, see section 5.3.4.

After the necessary observing durations are fixed it is checked if a possible required antenna pointing can be reached within the available time or not. If this is not the case,

single stations are removed from the scan until this is the case for all stations. Finally, all subnetting scan combinations are formed as discussed in section 5.3.5 resulting in a pool of all available scans at this time.

Based on this pool of scans it is decided if the recursion continues. If there is at least one valid scan, the scores per scan based on the optimization criteria are calculated, see section 5.4. The scan, or subnetting scan combination, with the highest score is selected and checked with rigorous models as described in 5.3.7. If it passes all rigorous models it is saved and it is about to be added to the schedule.

This is when the first recursion starts, which checks the time between the previously scheduled scans and the scan which is selected and about to be scheduled. In this recursion, the required antenna pointings and times for the “next scan” are replaced by the antenna pointings at the start time of the selected schedule. However, the slew times and observing duration of all possible scans stay the same and the algorithm can start directly to check if the required antenna pointings and times for the next scan can be reached as visualized in Figure 29.

If the iteration stops, the previously selected scan which was about to be scheduled is finally added to the schedule and the second part of the recursion starts. In this recursion, the current antenna pointings and times are replaced based on the antenna pointings at the end time of the selected scan. This time, the recursion has to start from the beginning, since the progression in time changes the position of all sources in the sky.

5.5.2 Fix scans a priori

The recursive scan algorithm opens up the chance to create schedules which are not necessarily in sequential time order. As visualized in Figure 21, VieSched++ supports the creation of the schedule in different phases. During the first phase, it is possible to fix some scans in the schedule. This option can be used in case some scans are considered to be highly important for the success of the session. For example, in case the session is scheduled for a certain experiment like for close observations to the Sun (Titov et al., 2018) the necessary scans can be fixed a priori. Or in case of intensive sessions, scans which are close to the edges of the commonly visible sky can be fixed because it is assumed that those scans have the highest impact on the result (Uunila et al., 2012). In the future, it is also planned to use this feature to fix scans to satellites in the schedule.

After these scans are fixed the recursive scan selection algorithm is used to fill the gaps

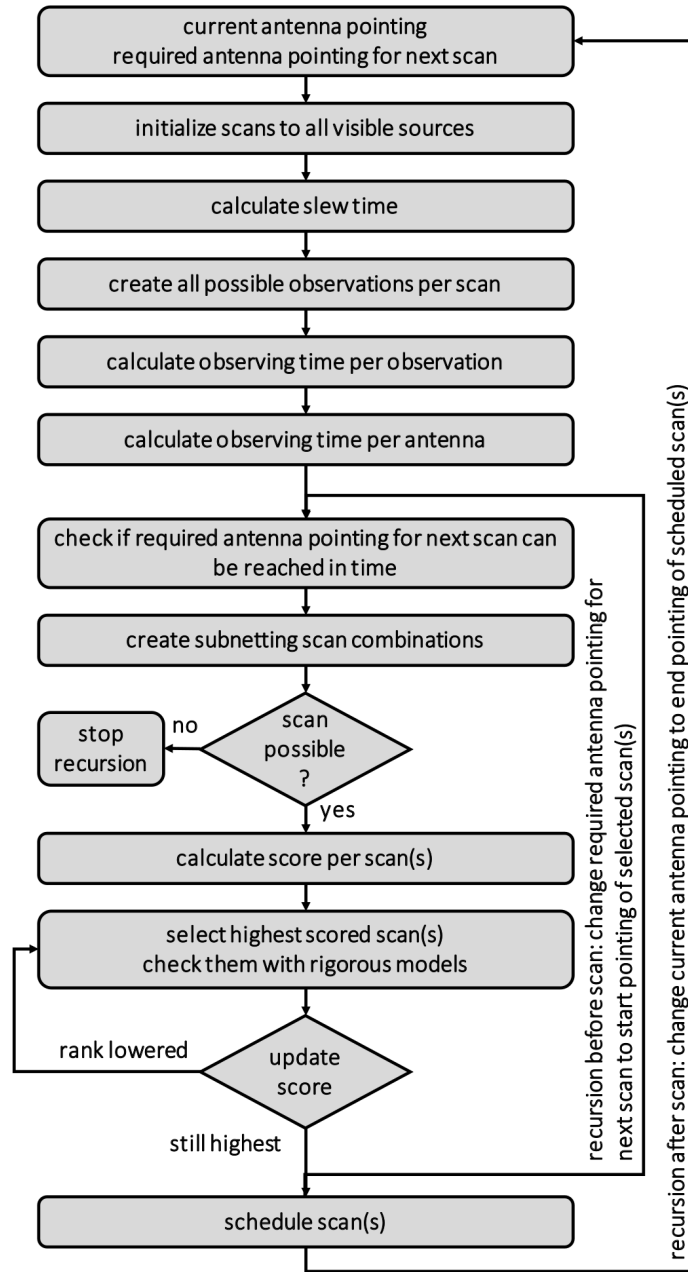


Figure 29: Recursive scan selection flowchart.

between the already scheduled scans. Although the option of fixing scans a priori is not regularly used during the scheduling of geodetic VLBI sessions, the algorithm works, and

VieSched++ supports this process.

5.5.3 Fillin-mode a posteriori

Another possible use case of the recursive scan selection which is already implemented in VieSched++ and regularly used is the so-called fillin-mode a posteriori. The fillin-mode a posteriori starts if the schedule is already generated after the main recursive scan selection. This algorithm checks the time between every scheduled scan and tries to squeeze in another scan in between to further minimize the idle time. In standard VLBI sessions this will not lead to huge improvements since the time between two scans is already investigated by the main recursive scheduling phase. However, it can help to reduce idle time in case some stations are scheduled in tagalong-mode, see section 3.7.3. Since tagalong stations are not considered during the main recursive scan selection phase and are instead added to already scheduled scans, these stations are not scheduled in an optimal way. This is intended since observations with tagalong stations will not necessarily be observed and correlated. Therefore, scheduling these stations like normal will affect the quality of the remaining schedule in case the tagalong station will drop out.

The fillin-mode a posteriori is perfectly capable to include the tagalong stations more into the existing schedule, without mitigating the result gained from the remaining stations.

5.6 Multi-Scheduling feature

VieSched++ comes with a feature called multi-scheduling which helps to optimize a schedule through finding a good set of scheduling parameters and weight factors (Schartner et al., 2017; Schartner and Böhm, 2019b,c). Instead of creating only one single schedule for a session, it is possible to create multiple schedules automatically, as already indicated in Figure 21.

The benefit of this approach is, that different sessions benefit greatly by using individually optimized scheduling parameters instead of using the same parameters for all sessions independent of the antenna network and scientific goal. In total, over 40 different parameters can be adjusted via the multi-scheduling feature. The parameters can be selected and different values of the parameters which should be tested can be defined. The multi-scheduling feature will then generate schedules with all combinations of different parameters.

For example, if the tested multi-scheduling parameters are:

- subnetting *subnet* (sec: 5.3.5): yes, no
- sky-coverage influence distance $dist_{inf}$ (sec: 5.4.2): 15, 30, 45 [deg]
- sky-coverage influence time $time_{inf}$ (sec: 5.4.2): 900, 1800, 3600 [s]

a total of 18 schedules ($2 \cdot 3 \cdot 3$) will be generated as shown in equation (47) and (48).

$$subnet := \begin{pmatrix} yes \\ no \end{pmatrix}, \quad dist_{inf} := \begin{pmatrix} 15 \\ 30 \\ 45 \end{pmatrix}, \quad time_{inf} := \begin{pmatrix} 900 \\ 1800 \\ 3600 \end{pmatrix} \quad (47)$$

$$\begin{pmatrix} subnet \\ dist_{inf} \\ time_{inf} \end{pmatrix} = \underbrace{\begin{pmatrix} yes \\ 15 \\ 900 \end{pmatrix}}_{v1}, \underbrace{\begin{pmatrix} yes \\ 15 \\ 1800 \end{pmatrix}}_{v2}, \underbrace{\begin{pmatrix} yes \\ 15 \\ 3600 \end{pmatrix}}_{v3}, \underbrace{\begin{pmatrix} yes \\ 30 \\ 900 \end{pmatrix}}_{v4}, \underbrace{\begin{pmatrix} yes \\ 30 \\ 1800 \end{pmatrix}}_{v5} \dots \underbrace{\begin{pmatrix} no \\ 45 \\ 3600 \end{pmatrix}}_{v18} \quad (48)$$

Since the number of possible schedules based on different parameters grows fast, it is possible to limit the number of generated schedules. Presently, a total maximum of 999 schedules can be generated at once. If the number of generated schedules is less than the total number of possible parameter combinations, the tested parameter combinations are randomly picked. However, it is possible to seed the random number generator to duplicate the result.

When optimizing schedules, the recommended option is to adjust the weight factors as they directly determine the scan selection and, therefore, have the most significant impact on the result. Since only the relative ratio between the individual weight factors is of importance, see equation (23), parameter combinations which will lead to the same schedule are not tested. Therefore, only solutions with linearly independent weight factors are generated.

If the tested multi-scheduling parameters are:

- duration weight factor (sec: 5.4.1): 0.25, 0.50, 0.75, 1.0
- sky-coverage weight factor (sec: 5.4.2): 0.25, 0.50, 0.75, 1.0
- number of observations weight factor (sec: 5.4.3): 0.25, 0.50, 0.75, 1.0

and this are the only weight factors $\neq 0$, a total of 55 schedules ($(4 \cdot 4 \cdot 4 - \text{number of linearly dependent combinations})$) will be generated.

The result of the VieSched++ multi-scheduling feature is the individual output files from every generated schedule, as well as a summary file in comma-separated values (csv) format called *statistics.csv*. This summary file contains all scheduling statistics, including

the number of scans and observations separated by stations, sources, baselines and in total, as well as the sky-coverage scores (see section 5.13, the multi-scheduling parameters used to derive this solution, the weight factors and statistics about how much time is spent per station for the individual tasks. The content of this summary file can be displayed in the VieSched++ multi-scheduling analyzer which is part of VieSched++.

5.6.1 Multi-core support

To keep processing time low the multi-scheduling feature uses multi-core support. Four different types of job scheduling approaches can be selected:

- **static:** the total number of schedules is divided by the total number of CPU threads to generate blocks of equal-sized chunks. Each of these chunks is assigned to one CPU thread. This option produces the least overhead, but in case some schedules take longer to finish than others, the total run time is limited by the slowest CPU thread. Especially if subnetting or weight factors are changed, the time it takes to generate a schedule and thus the CPU time which is needed can vary highly.
- **dynamic:** The total number of schedules is grouped in (smaller) individual blocks of equal size. Every CPU thread gets one of these groups to process. If a CPU thread finishes processing its block, it gets a new block. This is repeated until all blocks are processed. This approach produces more overhead since blocks have to be assigned to individual CPUs more often, but it also averages out the workload more evenly which can result in faster run times.
- **guided:** Similar to the dynamic job scheduling mode the total number of schedules is grouped in individual blocks. This time, the blocks are bigger at the beginning and become smaller at the end. Therefore, the CPU thread starts by processing a big group of schedules. When the scheduling process comes near to its end, the size of the block decreases to average out the CPU load. This approach produces less overhead than the dynamic job scheduling approach since fewer blocks exist while providing the benefit of averaging out the workload more evenly than in the static job scheduling approach.
- **auto:** If this option is used, the decision which job scheduling approach should be used is forwarded to VieSched++, or more precisely, to the C++ compiler which was used to build the application.

All of the listed job scheduling approaches have their benefits and drawbacks. The decision which approach should be used depends on the hardware and has to be tested on every computer individually. However, on standard computers and for generating normal schedules the differences should not be too big. The focus of this feature is to provide tools to increase the performance for large-scale studies running on server CPUs with many threads.

5.6.2 Interaction with VieVS

Since VieSched++ is part of VieVS, the interaction between the two software packages is straightforward. The result of VieSched++, especially the result of the multi-scheduling feature, can be used directly in VieVS to perform Monte-Carlo simulations. This opens up the chance to compare the generated schedules based on repeatability values or formal uncertainties of geodetic parameters instead of using abstract scheduling statistics like the number of observations or sky-coverage. The result of the Monte-Carlo simulations from VieVS can be written directly in the summary statistics csv file and can be displayed in the VieSched++ multi-scheduling analyzer.

5.7 Iterative source selection

A challenging problem for VLBI scheduling is the selection of appropriate sources. Typically, a geodetic source list contains several hundred sources. During a standard 24-hour session typically less than one hundred of those sources are observed. One requirement which is often used is that every source should be scheduled at least three times to properly be able to estimate the source position. This is a challenge for the scheduling software because the schedule is created scan after scan (as discussed in 3) and the software does not know in advance if a source will be scheduled again. Several studies have been made to manually preselect sources, especially for intensive sessions like [Baver et al. \(2012\)](#), [Baver and Gipson \(2013\)](#), and [Gipson and Baver \(2016\)](#). Sked has an algorithm which tries to preselect the “best” sources for the session and only creates a schedule using these sources. It creates a highly simplified test schedule using a series of pseudo-scans in a fixed interval of ten minutes. A score is given to each scheduled scan and the cumulative score for each source is calculated. Based on this score and the sky-coverage, the list of best sources is selected which can then be used to generate the final schedule. More information about the algorithm can be found in [Gipson \(2016\)](#) under the *bestsource* command.

However, there are two downsides in this approach: First, it is necessary to manually select the number of sources which shall be used. Second, the source selection does not rely on a real schedule but rather on a series of pseudo-scans with equal spacing of ten minutes. The first issue can be countered by using an experienced scheduler operating the scheduling software who knows the number of necessary sources to generate a good schedule. The second issue is more complicated since the number of scans per session varies greatly between the different observing programs. A fixed spacing of ten minutes is most likely not optimal in all cases. The frequency of scan occurrences during VGOS sessions is way higher than for T2 sessions, which include many slow slewing stations. Additionally, the generated schedule using pseudo-scans does not represent a real schedule. The “best” sources during the pseudo-scan schedule are not necessarily scheduled often enough during the real schedule.

VieSched++ solves this issues by using an iterative source selection algorithm which runs a posteriori, as indicated in Figure 21 and in more detail in Figure 30.

A desired number of required scans and observations can be defined for each source. The idea of this approach is, that the software starts by generating a schedule using all available sources. After the schedule is finished, the total number of scans and observations per source are compared with the number of required scans and observations for this source. If there are more scheduled scans and observations than required scans and observations the source is considered a good candidate for the session, otherwise it is considered a bad candidate for the session. If the number of sources which are scheduled but do not reach the required number of scans and observations is higher than a user defined threshold, a new schedule is generated automatically using the reduced source list. This process is repeated until all requirements are met, making sure that each source is scheduled often enough. Therefore, the source selection is based on a real schedule instead of a sequence of pseudo-scans. The iterative source selection approach is somehow similar to using sked’s “cull” command (Gipson, 2016).

There are multiple ways to fine-tune the removal of the sources between each iteration. Typically, the biggest difference is between the first and the second iteration. The first iteration starts by using all available sources form the source list, which can be several hundred. Based on the scheduling parameters it often happens that too many sources are used to generate the schedule and most of them are only scheduled in a few scans. Therefore, the number of removed sources between the first and second iteration is likely too high, resulting in too few sources to generate a good schedule. To counter this, a

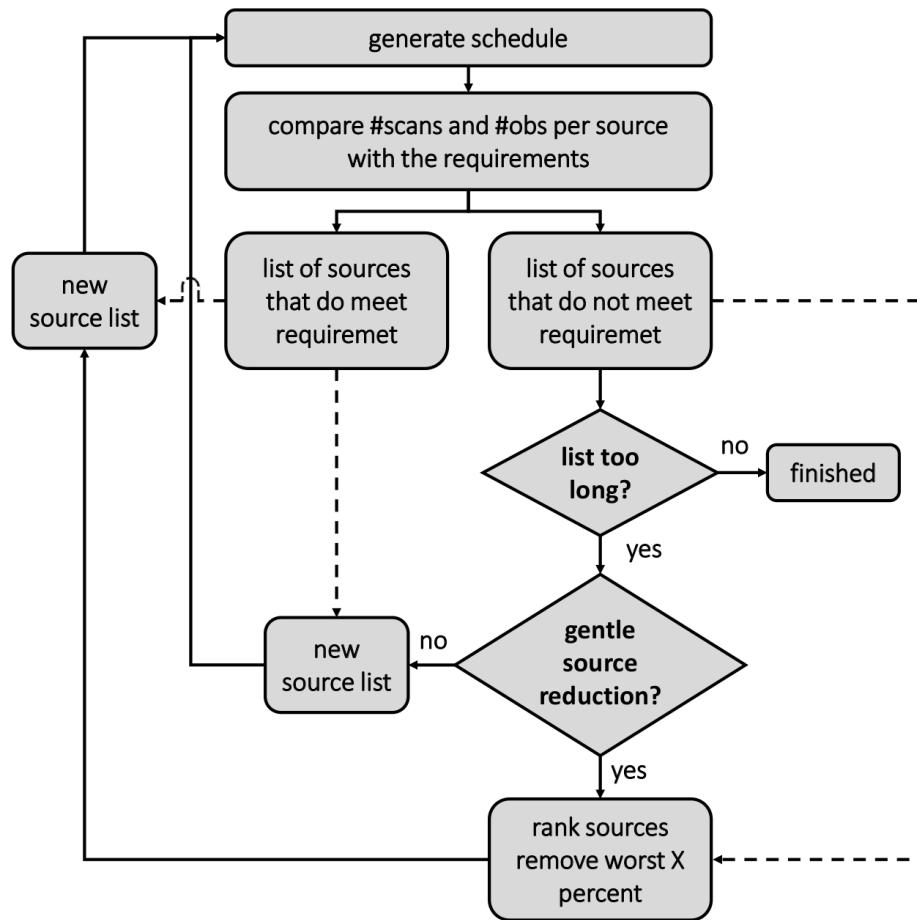


Figure 30: Iterative source selection flowchart.

so-called “gentle source reduction” can be used for the first couple of iterations. During this gentle source reduction, the removal of the sources is done differently. All sources are ranked based on the number of scheduled scans and only an user-defined percentage of sources is removed from the source list, starting with the lowest ranking sources as indicated in Figure 30. This makes sure, that there are enough sources left between the iterations and it will not happen that too many sources are removed at once.

The ranking does not include sources which have never been scheduled in the session, since these sources are assumed to either never be visible by enough antennas, or are bad in general. These sources are always removed.

5.8 Parameterization

VieSched++ aims to be as flexible as possible. Therefore, it is possible to change the parameters of every station, source, and baseline individually. Examples for these parameters are the minimum and maximum allowed observing time, the minimum time between two scans to the same source, or the minimum number of stations per scan. Additionally, these parameters can be changed over time. To simplify the scheduling setup as much as possible, multiple stations, sources or baselines can be organized in groups and the parameters can be set for each group as well. Furthermore, a tree-based parameter setup is used. This allows to efficiently generate schedules with individual parameters.

There are several use-cases where using individual parameters are advantageous:

If the goal for the sessions is astrometry, special sources are introduced for calibration purposes. These calibration sources should be scheduled differently than astrometric sources (Petrov et al., 2009). While the goal of calibration sources is to reach a high SNR, it might be necessary to optimize astrometric sources concerning the uv-plane for imaging. It is possible to generate two source groups, one for the calibrator sources and one for the target sources and adjust the scheduling parameters accordingly.

Another use-case is the distinction between VGOS and legacy antennas during geodetic sessions. While VGOS antennas are small and fast slewing antennas the legacy antennas are bigger and slower. Different parameters can help to optimize the given network (Schartner and Böhm, 2019b). For example, the slew distance of legacy antennas can be limited to increase the number of observations, while there is no restriction for the VGOS antennas.

Finally, one more use-case is if the session has a specific purpose and should highly focus on specific sources as described in Titov et al. (2018). Additionally, the session described in Titov et al. (2018) is a good example of when a change of parameters over time is useful since it is scheduled using three different phases: The session start with a standard geodetic block followed by a long period where the special sources which were needed for the experiment were observed very frequently followed by another block with standard geodetic scans.

The time-dependent change of parameters is most often used to add station downtime to schedules which might appear if there is an intensive schedule during a 24-hour session or satellite passes should be observed. During the downtime, the station can simply be set to “not available”. Moreover, it is also possible to schedule the stations in tagalong-mode during this time, which was done in the Continuous VLBI Campaign (CONT) 2014

(Behrend, 2015).

Since the optimal parameters depend on the network, the source list, and other factors, the multi-scheduling feature, described in section 5.6, is a handy tool to test and compare different approaches.

As noted in Table 3, 5 and 6, several parameters are defined multiple times in different places. If this is the case it is made sure, that each definition is fulfilled through the scheduling process. For example, the minimum required observing time can be set in the station based parameters, the source based parameters, and the baseline based parameters. If the minimum required observing time is set to 20 seconds for the station, 10 seconds for the source and 30 seconds for the baseline forming the observation, the actual scheduled minimum time is set to 30 seconds to fulfill all conditions. Similarly, if the maximum allowed observing time is set to 600 seconds for the station, 400 seconds for the source and 900 seconds for the baseline forming the observation, a value of 400 seconds is used.

5.8.1 Groups

As already mentioned it is possible to group certain elements, to speed up the parametrization of the schedule. A group does always contain only one type of elements: either stations, sources or baselines. Instead of changing the properties of each station, source or baseline individually, the parameters of a whole group can be changed instead. It simply serves as a quality of live improvement. The groups can further be used for defining custom scan sequences, see section 5.10, defining calibrator sources for calibration blocks, see section 5.9.2, defining minimum number of scans and observations per source, see section 5.7, and for multi-scheduling setups, see section 5.6.

5.8.2 Station based parameters

Table 3 lists the station based parameters which can be used to define the scheduling setup. Moreover, it lists the default values of these parameters and gives a short description of the idea of this parameter.

Table 3: List and description of station based parameters.

name [unit]	default	short description
available	yes	Defines if the antenna is available or not. This option can be used to define antenna downtime.
available for fillin-mode	yes	Defines if the antenna is available for fillin-mode scans during the recursive scan selection. Some stations have restrictions on how many scans they can participate per session. Since fillin-mode scans tend to have less impact on the solution due to the lower number of participating stations, stations can be defined to ignore those fillin-mode scans and instead focus purely on standard scans including many other stations.
tagalong	no	Used to put stations in tagalong mode, see section 3.7.3.
weight	1.00	Individual weight of the antenna, see equation (46).
max slew time [s]	600	Maximum allowed slew time of this station, see section 3.4.2. If the slew time to the source is longer than this value, the station is removed from the scan.
min slew distance [deg]	0.00	Minimum required slew distance of this station. If the slew distance to the source is shorter than this value, the station is removed from the scan.
max slew distance [deg]	175.00	Maximum allowed slew distance of this station. If the slew distance to the source is longer than this value, the station is removed from the scan.
max wait time [s]	600	Maximum allowed waiting time for slow stations. If the resulting idle time is longer than this value, the station is removed from the scan.
min elevation [deg]	5.00	Minimum elevation for observations to a source. If the elevation to the source is lower than this value, the station is removed from the scan. This parameter can also be set for sources individually.

(Continued on following page)

5. VIESCHED++

Table 3: List and description of station based parameters (continued).

name [unit]	default	short description
max number of scans	9999	Maximum number of scans for this station. If the maximum number of scans is reached, no more scans will be scheduled with this station.
min scan time [sec]	30	Minimum required observing time. If the estimated observing time is lower than this value, it is extended to this value, see section 5.3.4. This parameter can also be set for sources and baselines individually.
max scan time [sec]	600	Maximum allowed observing time. If the necessary observing time is higher than this value, the observation is removed from the scan, see section 5.3.4. This parameter can also be set for sources and baselines individually.
target SNR [Jy]	0.00	Target SNR per band. This parameter is also defined globally in the observing mode and can additionally be set for each source and baseline individually.
ignore sources	-	List of sources or source groups which should not be scheduled with this station.

Additionally the following parameters listed in Table 4 can be set per station as well but the values are fixed over the whole session duration:

Table 4: Constant station (overhead) times and cable wrap buffers.

name [unit]	default	short description
field system time [s]	6	Constant overhead time per scan for field system commands.
preob time [s]	10	calibration time per scan.
extra midob time [s]	3	Additional observing time added to estimated observing time, see equation (20).

(Continued on following page)

5. VIESCHED++

Table 4: Constant station (overhead) times and cable wrap buffers (continued).

name [unit]	default	short description
postob time [s]	0	Constant overhead time after scan finishes - currently not properly implemented!
axis limit buffer (1 low) [deg]	5.00	Cable wrap buffer for lower limit of first axis.
axis limit buffer (1 up) [deg]	5.00	Cable wrap buffer for upper limit of first axis.
axis limit buffer (2 low) [deg]	0.00	Cable wrap buffer for lower limit of second axis.
axis limit buffer (2 up) [deg]	0.00	Cable wrap buffer for upper limit of second axis.

5.8.3 Source based parameters

Table 5 lists the source based parameters which can be used to define the scheduling setup as well as the default values and a short description of the idea of this parameter.

Table 5: List and description of source based parameters.

name [unit]	default	short description
available	yes	Defines if the source should be scheduled or not.
available for fillin-mode	yes	Defines if the source should be scheduled during fillin-mode.
weight	1.00	Individual weight of the antenna, see equation (46).
min number of stations	2	Minimum number of stations required in a scan to this source.
min flux [Jy]	0.05	Minimum flux density required for scans to this source. If the flux density is lower, scans to this source are not scheduled. This option is used to reduce the number of possible sources and thus scans for performance reasons.
max number of scans	999	Maximum number of scans to this source. If the maximum number of scans is reached, no more scans will be scheduled to this source.

(Continued on following page)

5. VIESCHED++

Table 5: List and description of source based parameters (continued).

name [unit]	default	short description
min elevation [deg]	0.00	Minimum elevation for observations to this source. If the elevation to the source is lower than this value, the station is removed from the scan. This parameter can also be set for each station individually.
min sun distance [deg]	4.00	Minimum angular distance between the sun and the source. If the distance is lower, scans to this source are not scheduled.
variable scan duration: min scan time [s]	0	There are two options to define the scan duration, either by using a variable approach which calculates the required observing times as described in section 3.6 or by using a fixed time per scan. Minimum required observing time for the variable scan duration approach. If the estimated observing time is lower than this value, it is extended, see section 5.3.4. This parameter can also be set for stations and baselines individually.
variable scan duration: max scan time [s]	9999	Maximum allowed observing time. If the estimated observing time is higher than this value, the observation is removed from the scan, see section 5.3.4. This parameter can also be set for stations and baselines individually.
variable scan duration: target SNR [s]	0.00	Target SNR per band. This parameter is also defined globally in the observing mode and can additionally be set for each station and baseline individually.

(Continued on following page)

5. VIESCHED++

Table 5: List and description of source based parameters (continued).

name [unit]	default	short description
fixed scan duration [s]	300	All observations to this source are scheduled by using this observation duration, independent of the flux density of the source and the achieved SNR.
variable minimum time between scans: target number of scans	2	There are two options to define a minimum time between two scans to the same source, either by using a fixed value or by calculating the minimum time based on a target number of scans which should be scheduled and the visible time of this source. By using the variable minimum time option, the minimum time between two scans to the same source is calculated based on the visible time of this source and based on the target number of scans to this source $min_tim = \frac{visible_time}{target_#\#scans}$
variable minimum time between scans: duration [s]	1800	Backup minimum value for the minimum time between two scans in case it is calculated based on the visible time of the sources and the target number of scans. If the calculated time is lower than this value, this value is used instead.
fixed minimum time between scans [s]	1800	Minimum time between two scans of the same source. This value is independent of the visible time of the source in this session.
increase weight if observed once: weight factor	1.00	This option is used to increase the weight of observations to this source, as soon as it is scheduled once, making it more likely that this source is scheduled again in the future. The weight is increased by this value, based on the occurrence and the increase-type.

(Continued on following page)

Table 5: List and description of source based parameters (continued).

name [unit]	default	short description
increase weight if observed once: occurrence	once	Defines how often the weight of a scan to a source should be increased as soon as it is scheduled. Can either be <i>once</i> or <i>per scan</i> .
increase weight if observed once: type	multiplicative	Increasing type of the weight of a source as soon as it is scheduled once. Can either be <i>multiplicative</i> or <i>additive</i> . In the case of multiplicative, the score of the scan is multiplied by the previously defined increase weight if observed once weight factor. In case of additive, the defined increase weight if observed once weight factor value is added to the score of the scan
ignore stations	-	List of stations or station groups which should be ignored and thus never participate in scans to this source.
required stations	-	List of stations or station groups which are required to form a valid scan to this source.
ignore baselines	-	List of baselines or baseline groups which should be ignored and thus never be scheduled in scans to this source.

5.8.4 Baseline based parameters

Table 6 lists the baseline based parameters which can be used to define the scheduling setup as well as the default values and a short description of these parameters.

Table 6: List and description of baseline based parameters.

name [unit]	default	short description
ignore	no	Defines if observations on this baseline should be ignored or not. If it is ignored, it is never scheduled in a scan, see section 5.3.1
weight	1.00	Individual weight of the baseline, see equation (46).
min scan time [sec]	30	Minimum required observing time. If the estimated observing time is lower than this value, it is extended, see section 5.3.4. This parameter can also be set for station and source individually.
max scan time [sec]	600	Maximum allowed observing time. If the estimated observing time is higher than this value, the observation is removed from the scan, see section 5.3.4. This parameter can also be set for station and source individually.
target SNR [Jy]	0.00	Target SNR per band. This parameter is also defined globally in the observing mode and can additionally be set for each station and source individually.

5.9 Astrometric optimization

The main focus of VieSched++ is to generate high-quality geodetic VLBI schedules. Additionally, it supports the generation of astrometric schedules. Astrometric schedules typically contain two source lists, one for calibrator sources and one for astrometric sources (Petrov et al., 2009). In VieSched++, it is possible to distribute the source list in different groups, as described in section 5.8.1. This can be used to separate calibrator sources from target astrometric sources. Based on their role, the different groups can be assigned to different parameters, see section 5.8.

Astrometric target sources can be scheduled to optimize the uv-coverage of these sources. This helps with generating images. To achieve this, a target number of scans *target_scans* can be set, see Table 5. VieSched++ calculates how many minutes the source is visible *min_visible* based on the parameters. The fraction of the minimum visible time and the target number of scans is then set as the minimum time between two scans to the

same source.

$$\text{min_between}_{src} = \frac{\text{min_visible}_{src}}{\text{target_scans}_{src}} \quad (49)$$

In conjunction, it is possible to increase the weight of sources as soon as they are scheduled, see Table 5, which makes it more likely that scans to this source are scheduled again after it is selected once. By increasing the weight drastically, the chance increases that the source is scheduled every time the minimum time between two scans is reached, resulting in observations spanning the maximum of different hour angles and therefore optimizes the uv-coverage. This astrometric optimization approach can be mixed into standard geodetic sessions as well. It is possible to define only a small subset of sources during a geodetic schedule to be scheduled in a way that they are optimized for imaging. This might be useful for VGOS schedules where it is necessary to image the sources regularly for highest precision.

5.9.1 Source selection

In contrast to geodetic scheduling, where the source selection and distribution of scans over sources do not play a major role, the situation is very different in astrometry. Typically, a source has to be observed for a certain amount of times. Too many scans per source should be avoided since the time could be more efficiently used to schedule other sources. Therefore, source selection is very challenging. It has to be made sure, that each source is scheduled between a lower limit (e.g.: 6) and an upper limit (e.g.: 8). As already described in section 5.9.1, it is beneficial if the scans are spread out over the different hour angles, meaning, it should be scheduled at different times during the session. Since the schedule is generated scan after scan, it is unknown if the lower limit will be reached for a source at the time it is first scheduled. Moreover, the source list can be a lot longer than for geodetic sessions. For the official IVS CRF sessions, the source list includes several thousand sources.

The iterative source selection (see section 5.7) together with the weight increase after a source is scheduled once (see Table 5) can be used to reach the minimum number of scans. Defining a target number of scans, as listed in Table 5, helps to limit the number of scans per source to the upper bound and distributes the observations over the visible time.

By using the iterative source selection (see section 5.7), with many gentle source reductions that only reduce a low percentage of the sources (e.g.: 5%), the source list can iteratively be reduced step by step until every source meets the requirement. This often

takes over twenty iterations, depending on the source list and the minimum and maximum number of scans. However, this process is fully automated and very fast and efficient in VieSched++.

For adding calibrator scans to the schedule, either calibration blocks (see section 5.9.2), or a custom scan sequence (see section 5.10) can be used.

5.9.2 Calibration block

The idea of the calibrator block is to observe 3-5 tropospheric calibrators. Observations to tropospheric calibrators should occur at different elevations. The purpose of including calibrators is to estimate the tropospheric delay during analysis and to link the positions of rarely observed astrometric sources with those of frequently observed calibrators (Petrov et al., 2009). During the calibration block, the calculation of the score of a scan is not done by using the weight factors but instead a high elevation score and a low elevation score is used. The limits of the high and low elevation areas are user-defined as indicated in Figure 31.

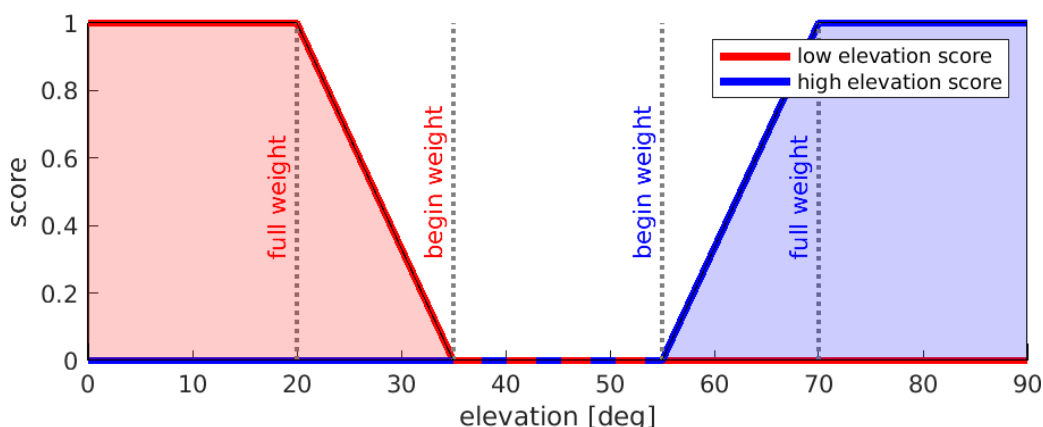


Figure 31: High and low elevation score functions during calibration blocks.

5.10 Custom Scan sequence

It is possible to define in which sequence sources or source groups should be observed. The sequence length can be set by the user. It is possible to assign a source or source group to every step of the sequence. Figure 32 depicts an example, with a sequence length of five. In the first three scans, a source from the source group named *target* will be observed, followed

by two sources from the source group named *calibrator*. Afterward, the whole process starts over again and three sources of the source group named *target* will be observed again.



Figure 32: Source sequence flowchart.

If no source of the defined group is available at this point in the schedule, any of the other sources will be scheduled instead.

Internally, VieSched++ will multiply the score of a scan with the factor of 100 if the scan observes a source which is contained in the assigned source group at this step of the sequence. Otherwise, the score will be multiplied by a factor of 0.01. This should make sure, that scans to sources of the assigned group will have the highest score and are therefore selected by the scheduling algorithm.

An user-defined custom scan sequence can serve multiple use-cases: It can be used to schedule calibrator scans in between other scans, as indicated in Figure 32. Other than that, it can be used to force scans to special sources as needed for the relativistic experiments described in Titov et al. (2018). In this example, two sources, namely *0229+131* and *0235+164* are passing the sun at a very small elongation. The goal of the experiment is to observe these two sources as much as possible. Therefore, the sequence length of four can be used, first a scan of source *0229+131* followed by a scan of *0235+164* and two scans to any other source. The two scans to any other source are necessary to provide good sky-coverage which is needed to estimate tropospheric time delays. During the times where source *0229+131* and *0235+164* are not available, any other source with the highest score will be scheduled instead.

5.11 Scan alignment

VieSched++ supports three ways to align the observing times of individual stations within a scan:

- start
- end
- individual

The default and typically used version is to align the start time of the observations. This

5. VIESCHED++

means every station starts recording at the same time. Stations which finish slewing earlier must wait for slower slewing stations. This is also the only option which is supported by the *skd* scheduling file format, the scheduling file format used within the IVS. An example of aligning the observing start time is visualized in Figure 33 in red color. The benefit of this approach is, that the scheduling process becomes easier when all stations start observing at the same time.

The other options of aligning the observation end time and the individual start and end times are only available by using the VLBI experiment definition (*vex*) scheduling file format. An example of aligning the observing end time is visualized in Figure 33 in green color. The benefit of this approach is, that all stations are at the same time available for evaluating the next scan and thus it is less likely that the network is falling apart. The third option of using individual start and stop times is visualized in blue in Figure 33. This is the most complex approach, since the individual start and stop times of the recording has to be monitored by each station individually and it must be made sure that the overlapping observing time between two stations is long enough to reach the target SNR of this observation. However, it also introduces the least idle time at the stations.

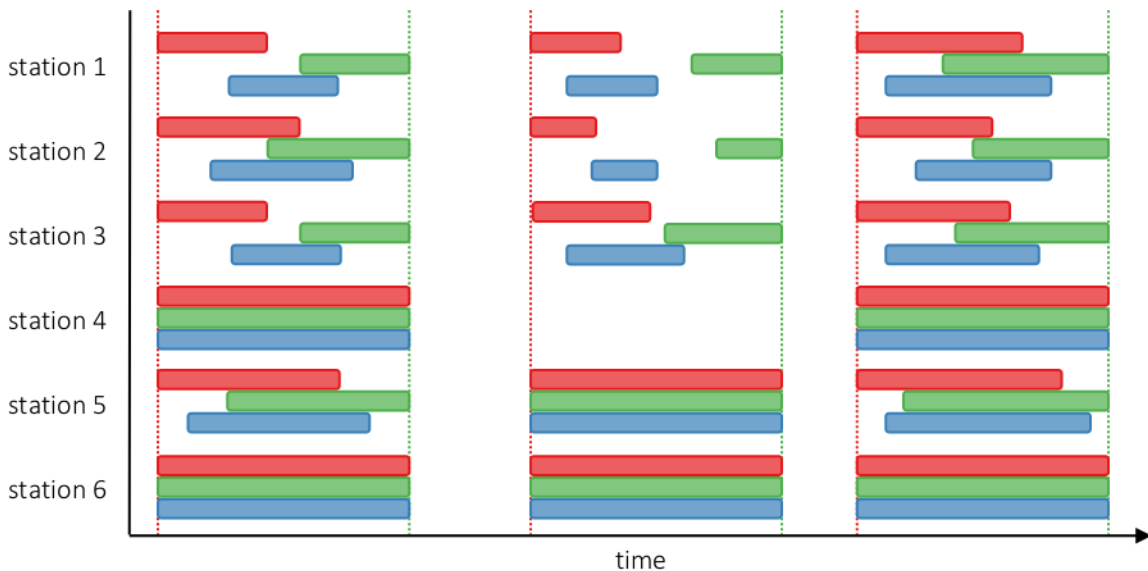


Figure 33: Comparison of different scan alignment approaches.

5.12 Manual and multiple observing modes

There are multiple ways to define an observing mode in VieSched++. The default option is to use a predefined observing mode provided in the sked catalogs, see section 3.3.3. These catalog files contain all necessary information to generate schedules in *skd* and *vex* format. However, not all stations are defined for every observing mode in the official sked catalogs. Adding new stations to existing observing modes can be challenging since the observing mode catalogs are heavily linked, see section 3.3.3 and Figure 4. Therefore, VieSched++ adds the possibility to manually define or update observing modes via a GUI.

5.12.1 Simple manual Observing mode

The simple manual observing mode is the easiest to define but is only useful if the schedules are made for simulations or if the observing mode blocks in the schedule files are copied and inserted manually from another already existing scheduling file.

It is defined through four parameters:

- the sample rate,
- the number of sampling bits,
- the sky frequency per band and
- the number of channels per band.

This is the minimum number of information needed to calculate the observing duration of a scan, see equation (20). As all other manual observing modes, this mode is not limited to two bands per schedule.

This option is very useful, if the effect of different observing modes and data rates should be investigated for a given network, or if a new antenna is added to the network which is not yet defined in the official sked catalogs. In both cases, it is not necessary to manually edit the sked catalogs which saves a lot of work and is a lot safer.

However, in the output files, the observing mode block remains empty when using this option, since not enough hardware information is available.

5.12.2 Advanced manual Observing mode

The advanced manual observing mode is a powerful tool to test new observing modes and setups. It is inspired by the *vex* observing mode blocks. By using this option, a new GUI appears, where all necessary information of the observing mode can be inserted. This includes the frequency setup, BBC, IF, and tracks information, or more generally,

everything observing mode related which is also listed in the vex output format. To simplify the process of defining a new observing mode per band, it is instead possible to start the definition based on an already existing official sked observing mode. The GUI guides the user and lists the appropriate keywords during the creation of the observing mode. Additionally, a summary of the defined observing mode can be displayed and missing connections between the individually defined parts of the observing mode are highlighted.

The advanced manual observing mode can also be used to define mixed-mode observations and to define multiple observing modes per session.

5.12.3 Mixed-mode observations

VieSched++ supports mixed-mode observations defined through an advanced manual observing mode. For mixed-mode observations, overlaps between the observed bands of two stations are calculated. Based on these overlaps, the effective observing rate per observation is calculated.

5.12.4 Multiple observing modes

In theory, VieSched++ supports the definition of multiple observing modes through an advanced manual observing mode. However, so far it cannot be defined which scan should be observed in which observing mode. The reason for this is, that it is still unclear how the change of the observing mode should be defined. Possible options are, to define an observing mode per source, or to define observing mode changes after a certain amount of time. It is planned to use this option in the future to include satellite schedules into the schedule.

5.13 Sky-coverage quantification

As already described in section 5.4.2, the sky-coverage during the scheduling process is defined through the angular distance and time between observations. Based on a combination of the distance and time and two transfer functions, the saturation of the sky-coverage at the observation point is calculated. While this is a very sophisticated approach, it is difficult to compare the sky-coverages between different stations and sessions based on this metric. For this reason, several sky-coverage quantifications are defined. The result of each sky-coverage quantification is a single number, ranging from zero to one, while one being a perfect sky-coverage based on this quantification.

5. VIESCHED++

The calculation of the sky-coverage quantification number is based on distributing the sky in different areas over short periods. So far, VieSched++ uses three different numbers of areas, namely 13, 25 and 37 (see Figure 35) and two different time duration, 30 and 60 minutes, to calculate a total of six different sky-coverage scores. Depending on the network, the average number of scans per hour and the purpose of the sessions, one score might be more appropriate than the others for this session. For example, in VGOS sessions, the average number of scans per hour is very high and the troposphere should be estimated in short time intervals. Therefore, the most appropriate sky-coverage score is the score based on 37 different areas with a 30 minutes time interval.

The sky-coverage quantification is defined through two parameters, the number of areas in which the sky is separated and the duration of one block. The algorithm used to calculate the score is visualized in Figure 34.

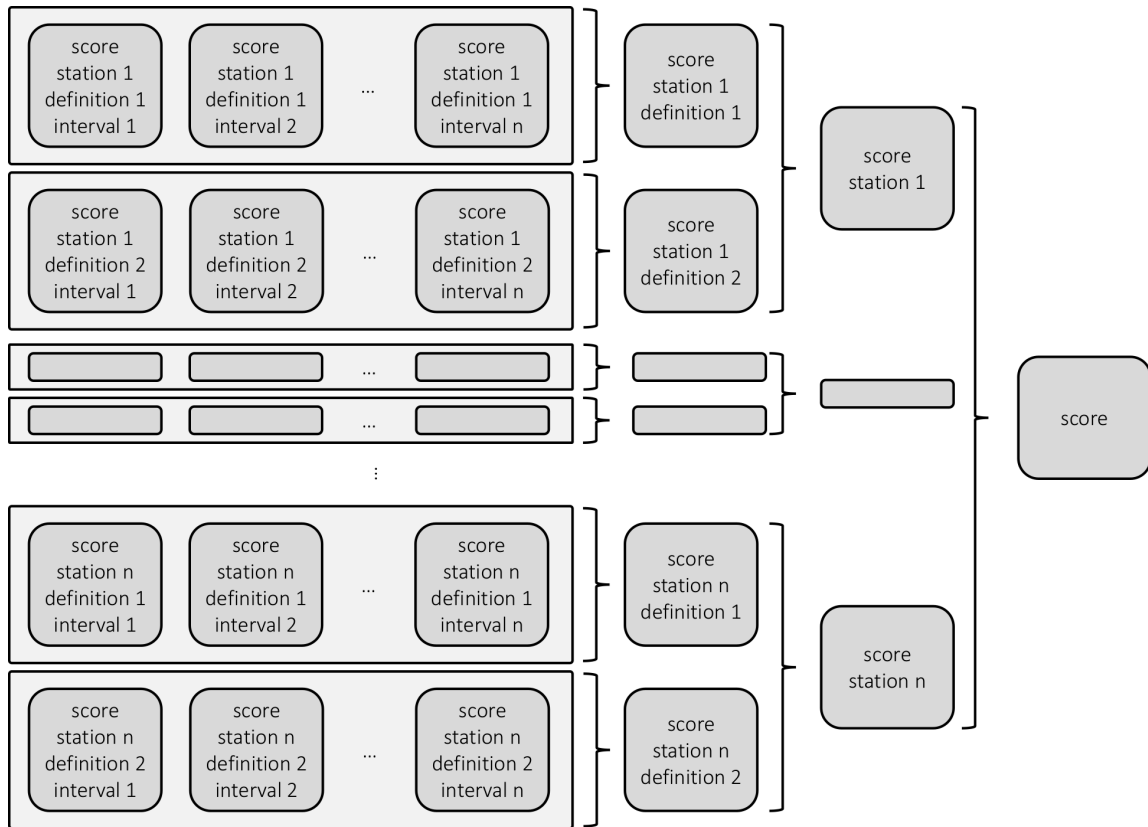


Figure 34: Sky-coverage score calculation flowchart.

As a first step, the sky above the station is divided into smaller areas with approximately equal size. This is done in two ways by using a different number of elevation levels. Figure 35 depicts the distribution of the different areas for both ways with 13, 25 and 37 areas. The two different definitions are necessary to avoid high scores in cases where the observations are clustered near the edges of the individual areas.

Within a given time interval, the azimuth and elevation of every scheduled scan are investigated. If the azimuth and elevation fall into one area, the area is marked as saturated. This is done for all scans within the time interval and for both area definitions. The score per station, area definition and time interval $score_{sta,def,int}$ is the number of saturated areas divided by the total number of areas.

$$score_{sta,def,int} = \frac{\text{saturated areas}}{\text{total number of areas}} \quad (50)$$

The intervals start at the session start time and have a duration of either 30 or 60 minutes. The next interval starts half of the duration later than the previous interval, meaning, half of the time is overlapped. This helps to smooth out effects which might otherwise occur at the end of the intervals. Therefore, a 24-hour long session with an interval duration of 60 minutes would result in 47 different time intervals: 00:00-01:00, 00:30-01:30, 01:00-02:00 ... 22:30-23:30, 23:00-24:00. The use of 30-minute intervals would result in 95 different intervals. Based on these scores, the total score per station and area definition $score_{sta,def}$ is calculated as the average over the scores of all intervals.

$$score_{sta,def} = \frac{1}{n_{int}} \cdot \sum_{i=1}^{n_{int}} score_{sta,def,int_i} \quad (51)$$

The total score per station $score_{sta}$ is defined through the average of the two scores with the different area definitions.

$$score_{sta} = \frac{score_{sta,def_1} + score_{sta,def_2}}{2} \quad (52)$$

Finally, the total score per session $score$ is defined through the average of all station dependent scores.

$$score = \frac{1}{n_{sta}} \cdot \sum_{i=0}^{n_{sta}} score_{sta_i} \quad (53)$$

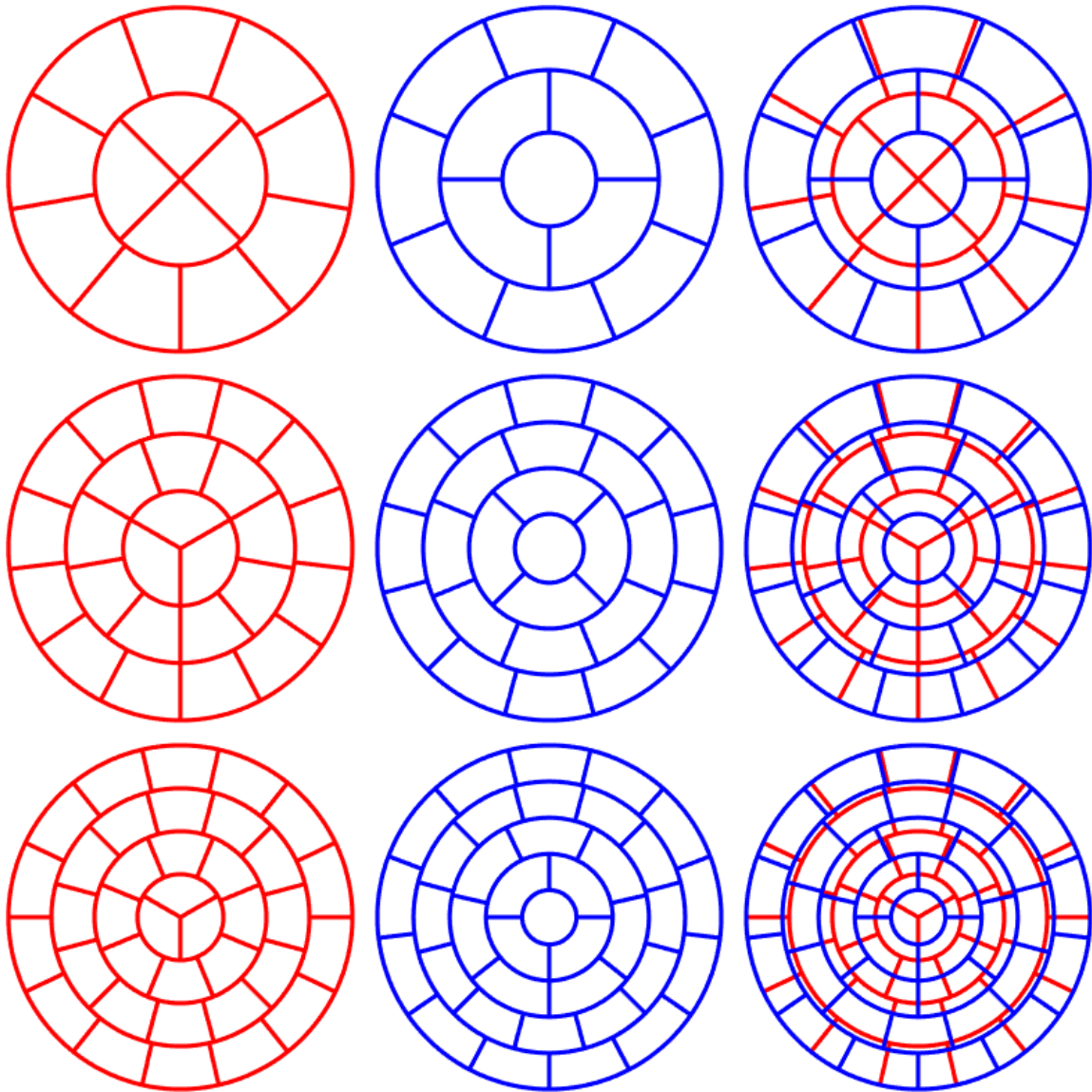


Figure 35: Distribution of sky-coverage areas based on 13 (top), 25 (middle) and 37 (bottom) areas. The first two columns display the two different distributions while the third column displays them on top of each other.

5.14 Output

VieSched++ supports a variety of different output formats. The scheduling files are available in both, *skd* and *vex* format. Preparations are already made to support *vex2* if the definition

5. VIESCHED++

of the file format is finally released. Additionally, VieSched++ generates an operation notes file, which includes useful information and many statistics about the schedule as well as the whole scheduling setup. For simulations and the interaction with VieVS, *ngs* files can be written.

Furthermore, VieSched++ will generate useful log files monitoring the scheduling process.

It is also possible to generate SNR tables, which is a list of all observations at all bands including the information of the antenna SEFDs, source flux density, observing duration, theoretical SNR and more.

If needed, source group based statistics files can be generated as well. This is useful for astrometric sessions since these files include information about all sources, including their visible times, scheduled observations and their parameters.

6 Results

In the following sections, results from sessions scheduled with VieSched++ are summarized and comparisons with previous sessions are made.

All schedules which are generated with VieSched++ and are created with the multi-scheduling feature 5.6 in conjunction with large-scale Monte-Carlo simulations as described in section 4.1.1. The analysis of the simulated and real sessions is done as described in section 4.1.2.

6.1 T2

The T2 observing program aims to provide high-quality station coordinates for the realization of a TRF. Sessions of the T2 observing program use the biggest station network of all official IVS programs observing with a low recording rate of only 128 Mbit/s. One challenging aspect of the T2 sessions is, that the antennas are very different in terms of sensitivity and slew speed. In the years 2018 and 2019, the scheduled network contained between 15 and 22 antennas, see Table 1 and 7. Figure 36 visualizes the position of all antennas scheduled in recent T2 sessions.

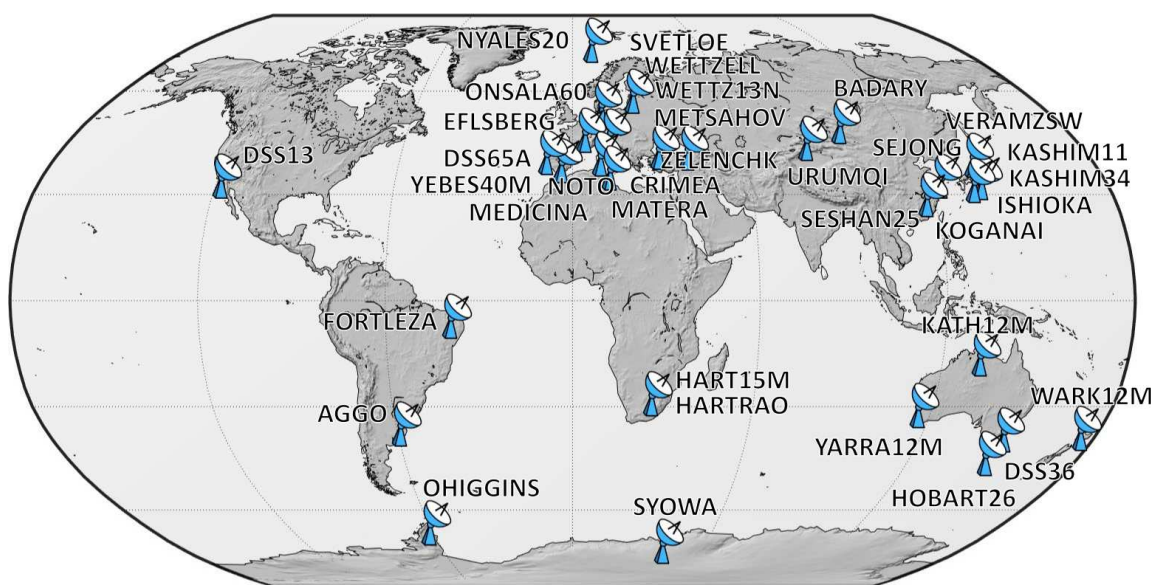


Figure 36: Antennas participating in recent T2 sessions.

Another challenge in scheduling T2 sessions is the asymmetry of the antenna network.

6. RESULTS

Most of the antennas are located in the northern hemisphere. This leads to problems when trying to properly include the antennas located in the southern hemisphere into the schedule. For example, session T2129 was scheduled using a network of 15 antennas. Of these 15 antennas, only two were located in the southern hemisphere, namely HART15M in South Africa and OHIGGINS in Antarctica.

As already noted, one difficulty in scheduling these sessions is the big difference in antenna sensitivity compared with the low recording rate of only 128 Mbit/s. Some stations have very high SEFD values, such as AGGO (X-band: 20 000 Jy, S-band: 15 000 Jy), SYOWA (X-band: 11 230 Jy, S-band: 7500 Jy), KASHIM11 (X-band: 11 000 Jy, S-band: 3000 Jy), OHIGGINS (X-band: 10 000 Jy, S-band: 18 000 Jy) and METSAHOV (X-band: 6000 Jy, S-band: 8000 Jy)⁸.

While the overall goal of the T2 sessions is to provide high-quality coordinates for all participating antennas, special focus is laid on the proper involvement of OHIGGINS into the schedule, since it is especially difficult to include OHIGGINS in a schedule due to its remote location and its low sensitivity.

Table 7 lists some general scheduling statistics for the T2 sessions scheduled in 2018 and 2019. Starting with T2129, VieSched++ is used to generate the schedules. It is difficult

Table 7: Scheduling statistics for all T2 sessions from the year 2018 and 2019. Sessions highlighted in blue were scheduled using VieSched++.

	#sta	#scans	#obs	%idle	%obs	#obs Oh
T2124	17	733	7175	28.10	44.54	22
T2125	17	1064	5528	22.94	53.70	48
T2126	17	1075	6081	24.55	49.66	98
T2127	19	627	6304	34.30	45.22	73
T2128	18	803	5983	26.24	44.90	97
average	17.6	860	6214	27.23	47.60	77
T2129	15	526	12713	8.20	66.90	400
T2130	22	626	16730	10.45	69.24	451
T2131	19	771	15714	4.33	73.68	267
T2132	18	631	10219	6.04	73.37	406
T2133	19	732	12978	10.07	65.90	285
average	18.6	657	13671	7.82	69.82	362

⁸according to sked equip.cat version 2018Oct09_IGSFC

to directly compare the individual sessions since the antenna network changes between sessions. However, it can be seen that the schedules generated with VieSched++ are superior in terms of raw scheduling statistics. The number of observations has increased by at least a factor of two and the average observing time per antenna has increased from $\approx 50\%$ to $\approx 70\%$, while the average idle time per antenna has decreased from $\approx 27\%$ to $\approx 8\%$. Additionally, the inclusion of OHIGGINS into the schedule works a lot better as can be seen by looking at the number of observations with OHIGGINS (Oh) listed in Table 7.

It is important to note here that the big differences in terms of the number of observations as well as observing and idle time is not necessarily only explainable by the superior algorithm VieSched++ uses. More importantly, the multi-scheduling feature compared with the Monte-Carlo simulations are increasing the quality of the schedule by finding a set of good weight factors and good scheduling parameters. The key for generating a good schedule is to not simply use the same parameters for all sessions as it was done before VieSched++ but instead, optimize each schedule individually. Luckily, this process is fully automated in VieSched++ and VieVS.

6.1.1 Simulations

The VieSched++ schedules are generated using the multi-scheduling feature and Monte-Carlo simulations. Based on the repeatability of the station coordinates, the best schedule is selected and submitted to the participating stations.

Figure 37 visualizes the expected 3D-station coordinate accuracy defined through:

$$\sqrt{\delta x^2 + \delta y^2 + \delta z^2} \quad (54)$$

6. RESULTS

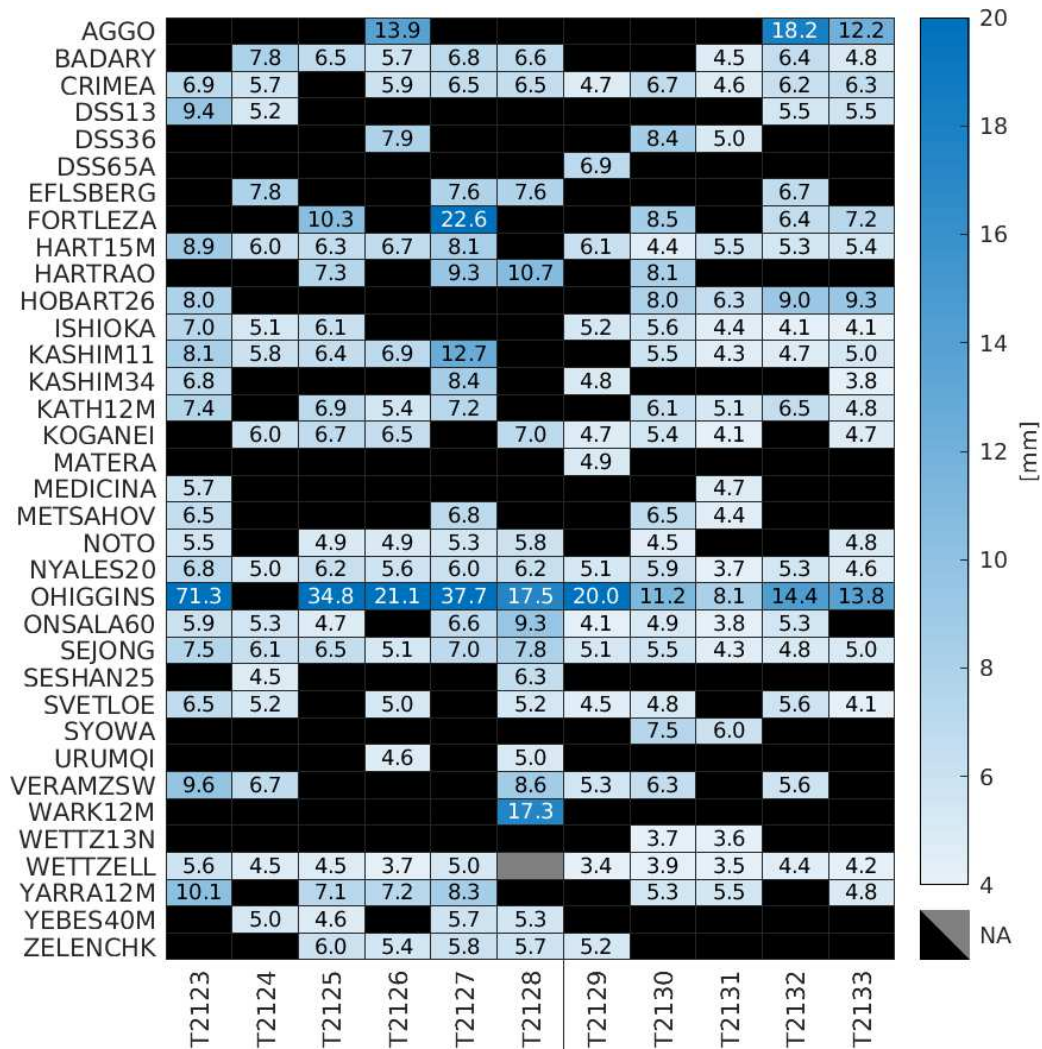


Figure 37: Simulated station coordinate repeatabilities of T2 sessions. A black box indicates that this station was not scheduled in this session. A gray box indicates that this station was not included in the official schedule but did participate.

Based on these simulations, the improvements in terms of station coordinate accuracy are only minor for most stations. By comparing the average of the expected station coordinate accuracy for all sessions before the use of VieSched++ and after the use of VieSched++, an average improvement of 35% can be seen. The highest improvement based on the simulations is achieved for OHIGGINS and FORTLEZA. Both stations are located in remote places as can be seen in Figure 36.

6. RESULTS

Figure 38 displays the expected EOP accuracy based on the repeatability estimates from Monte-Carlo simulations. It can be seen, that the expected EOP accuracy signifi-

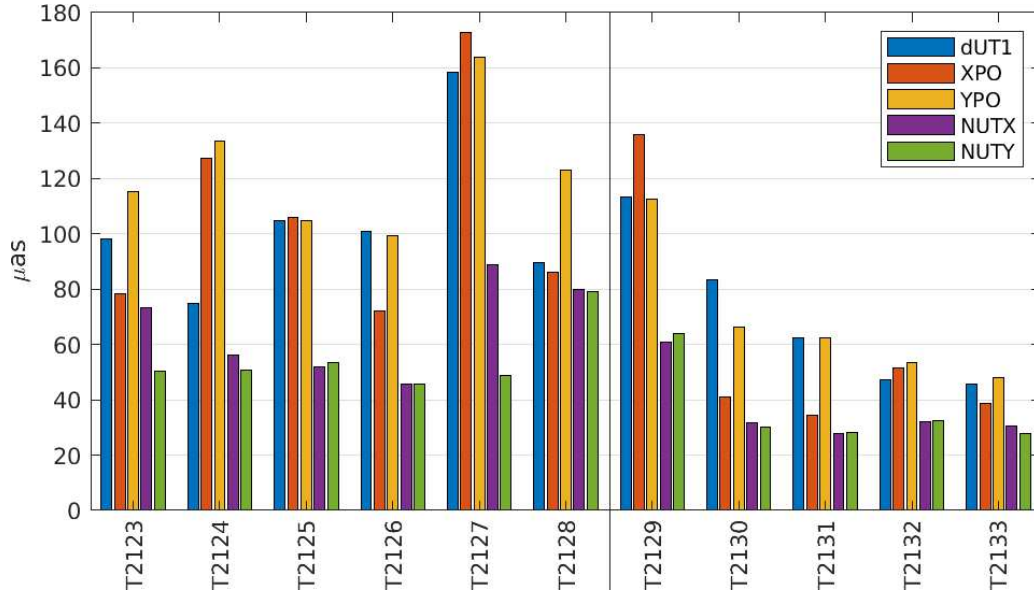


Figure 38: Simulated EOP repeatabilities of T2 sessions.

cantly increases for the sessions scheduled with VieSched++. The EOP accuracy of session T2129 is still on the same level as the accuracy of the sessions before VieSched++. Especially the low accuracy of the polar motion variables can be explained by the antenna network. Polar motion is most sensitive to north-south baselines and since there are only two stations in the southern hemisphere for T2129, the number of north-south baselines is very low in this session. Additionally, T2129 was the first big 24-hour session scheduled with VieSched++ and thus the experience in generating these sessions was very low. The session was also generated using an old version of VieSched++ and several improvements have been implemented in the meantime, which would increase the quality of the schedule now.

All other sessions scheduled with VieSched++ reveal a noticeable improvement in terms of expected EOP accuracy.

6.1.2 Real observations

Currently, two of the five scheduled sessions, namely T2129 and T2130, are correlated and VgosDB files are available and ready for analysis.

Unfortunately, the T2 sessions suffer a lot from antenna losses. Many of the participating stations are not built for geodetic VLBI and do not regularly observe geodetic sessions. Figure 39 visualizes the number of scheduled observations and compares them with the number of successfully correlated and recoverable observations and it lists the number of observations which were used for the analysis. The number of correlated, re-

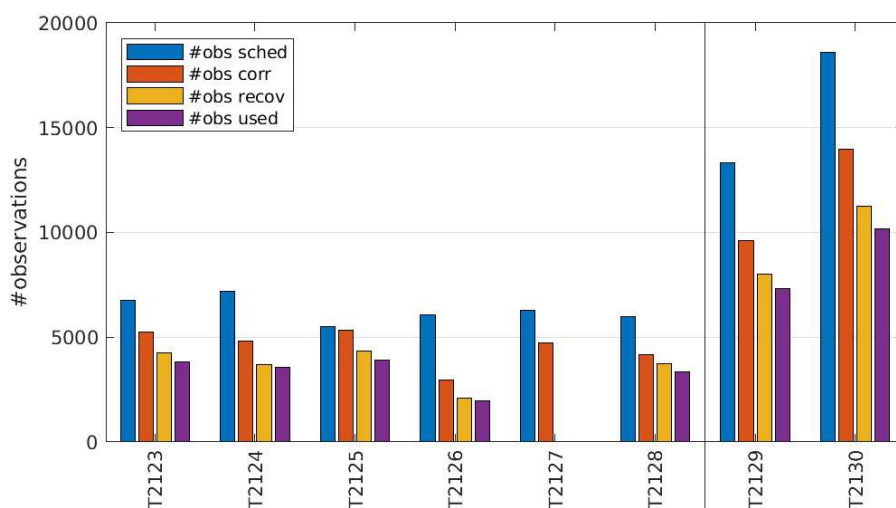


Figure 39: Number of observations scheduled, correlated, recoverable and used for the T2 sessions as listed in the official IVS analysis report.

coverable and used observations are taken from the official IVS analysis reports, while the number of scheduled observations is taken from the scheduling operator notes files. It can be seen that the number of available observations for the analysis significantly increases for the two schedules generated with VieSched++. The increase is a factor of two for T2129 and a factor of three for T2130, although these two sessions both lost five antennas due to technical, non-scheduling related problems. Most other sessions lost fewer antennas, as can be seen later in Figure 41.

There is no official IVS analysis report for session T2127. For session T2128, the number of scheduled observations does not include all observations with WETTZELL, since this station was only scheduled for 55 minutes in the official schedule due to human error

6. RESULTS

in defining the station downtime. Nevertheless, WETTZELL did participate in T2128 through an unofficial update of the schedule file (which is not publicly available) where the station was added in tagalong mode and thus the number of successfully correlated observations extends the number of scheduled observations for this station.

Figure 40 visualizes the EOP formal errors which are analyzed using VieVS as described in section 4.1.2. The dUT1 formal error is multiplied by a factor of 15, to convert it from μs to μas . Although the simulations predicted a different behavior, the formal errors for

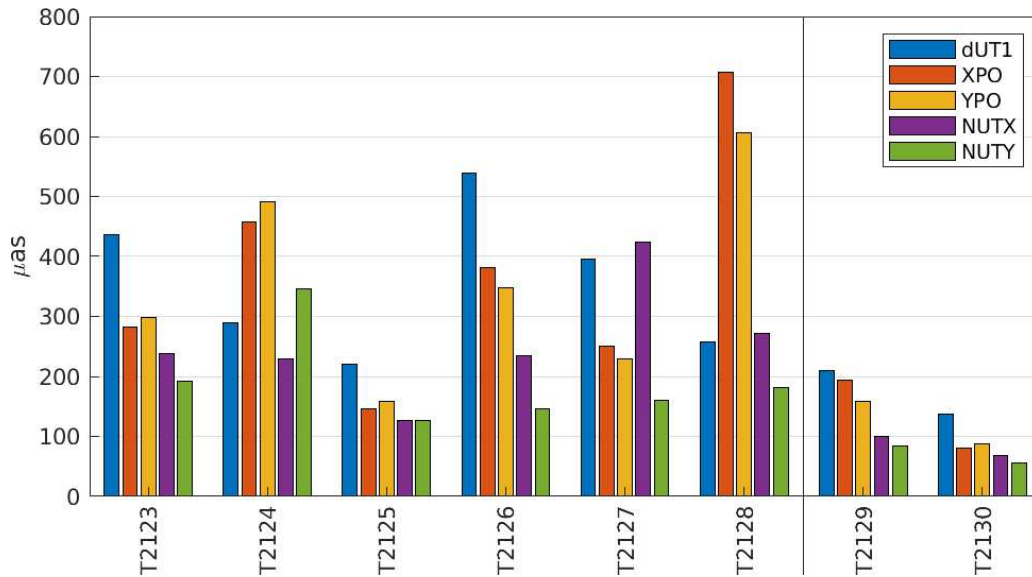


Figure 40: Formal errors of EOP estimates from T2 sessions.

the EOPs decreased drastically for both sessions scheduled with VieSched++. As expected, T2130 is superior to T2129.

Figure 41 depicts the average 3D-station coordinate formal errors as defined in equation (54). Although a fair comparison cannot be made due to the change in the antenna network, a clear positive trend can be seen. The coordinate accuracy of most stations has increased by at least a factor of two. Furthermore, a big improvement can be seen for OHIGGINS. Figure 41 also displays how many antennas did not make it to the analysis. Most of the antenna losses are due to hardware problems, but some are also removed during the analysis since their observations were too noisy.

6. RESULTS

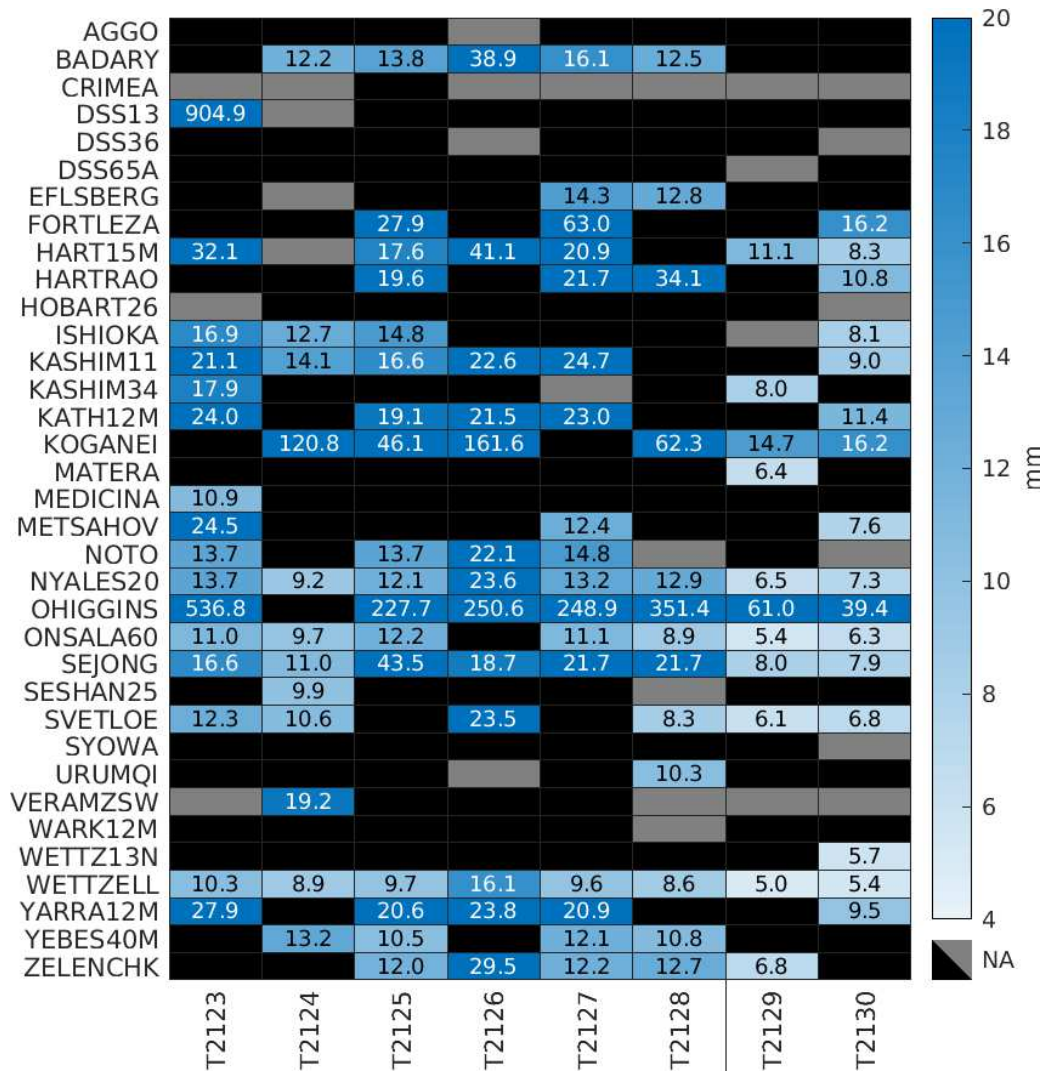


Figure 41: Formal errors of 3D-station coordinate estimates of T2 sessions. A black box indicates that this antenna was not scheduled in this session. A gray box indicates that this antenna was scheduled but was not available or usable in the analysis.

6.2 EURR&D

The goal of the EURR&D observing program is to provide high-quality station coordinates for the realization of a TRF. Thereby, the EURR&D antenna network mostly consists of European antennas with the addition of some Russian antennas as displayed in Figure 42. A 512 Mbit/s observing mode is used to record the observations.

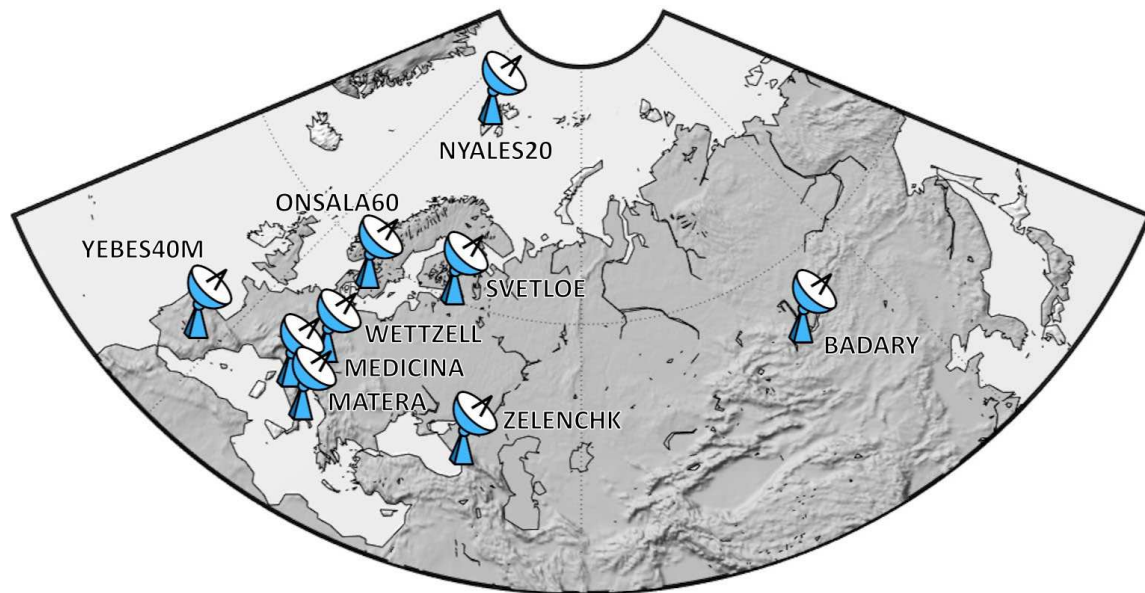


Figure 42: Antennas participating in recent EURR&D sessions.

Since this is a regional station network consisting of antennas which are well suited for geodesy and observing with a high recording rate, scheduling EURR&D sessions is easier compared to scheduling T2 sessions.

Table 8 lists some general scheduling statistics for the EURR&D sessions scheduled in 2018 and 2019. Compared with the results gained with the T2 sessions, the improvement in terms of the number of observations and additional observing time is not that impressive. The schedules generated with VieSched++ contain $\approx 30\%$ more observations. However, the average idle time decreases from $\approx 25\%$ down to $\approx 5\%$. Instead of idling, the antennas are slewing a lot more when using VieSched++, leading to a far better sky-coverage. The improvement in sky-coverage is listed in Table 8 in terms of the sky-coverage score by using 13 and 25 areas after 60 minutes, see section 5.13. The scores with more areas or a shorter time span are not listed since the average number of scans per station is around 15 before

6. RESULTS

Table 8: Scheduling statistics of all EURR&D sessions from the year 2018 and 2019. Sessions highlighted in blue were scheduled using VieSched++. The columns 13@30, 13@60 and 25@60 refer to the sky-coverage scores, calculated with 13/25 areas after 30/60 minutes (see section 5.13).

	#sta	#scans	#obs	%idle	%obs	13@30	13@60	25@60
EURD05	8	374	10134	25.00	39.97	0.44	0.59	0.42
EURD06	6	538	8061	21.63	30.87	0.51	0.64	0.49
EURD07	8	344	9437	36.42	29.40	0.39	0.56	0.40
EURD08	7	361	7215	25.78	33.08	0.46	0.56	0.40
average	7.3	404	8712	27.21	33.33	0.45	0.59	0.43
EURD09	8	665	11565	5.78	39.03	0.64	0.80	0.60
EURD10	8	669	13480	3.08	42.70	0.65	0.80	0.60
average	8	667	12523	4.43	40.87	0.65	0.80	0.60

the use of VieSched++ and around 22 when using VieSched++.

Figure 43 visualizes the sky-coverage of three selected stations for sessions scheduled before and after the use of VieSched++. These sky-coverage visualizations are representative of all antennas and all sessions. VieSched++ generates schedules with a far better sky-coverage. The reason for this is, again, the use of individually optimized weight factors but also the fact, that VieSched++ decides more often to use subnetting even for this regional network, to improve the sky-coverage. This is possible since the optimization conditions are specially designed to properly compare single source observations with subnetting scan combinations, see section 5.4. The fact that subnetting is often used can also be seen when looking at the number of scans listed in Table 8. The number of scans almost doubles when using VieSched++ compared to previously observed schedules.

To confirm this, Table 9 lists the number of stations per scan for all EURR&D sessions. When looking at Table 9, it is visible that before the use of VieSched++ the scheduling software was trying to generate scans containing all antennas. This is the reason, why the sky-coverage is that poor since the commonly visible part of the sky is very small. This also explains why it is not possible to increase the number of observations by a factor of two for these sessions as it is the case for T2. Since before the use of VieSched++ almost all scans include all antennas and since the observations focus on a small part of the sky with short slew distances, the total number of observations is already very high for these sessions.

6. RESULTS

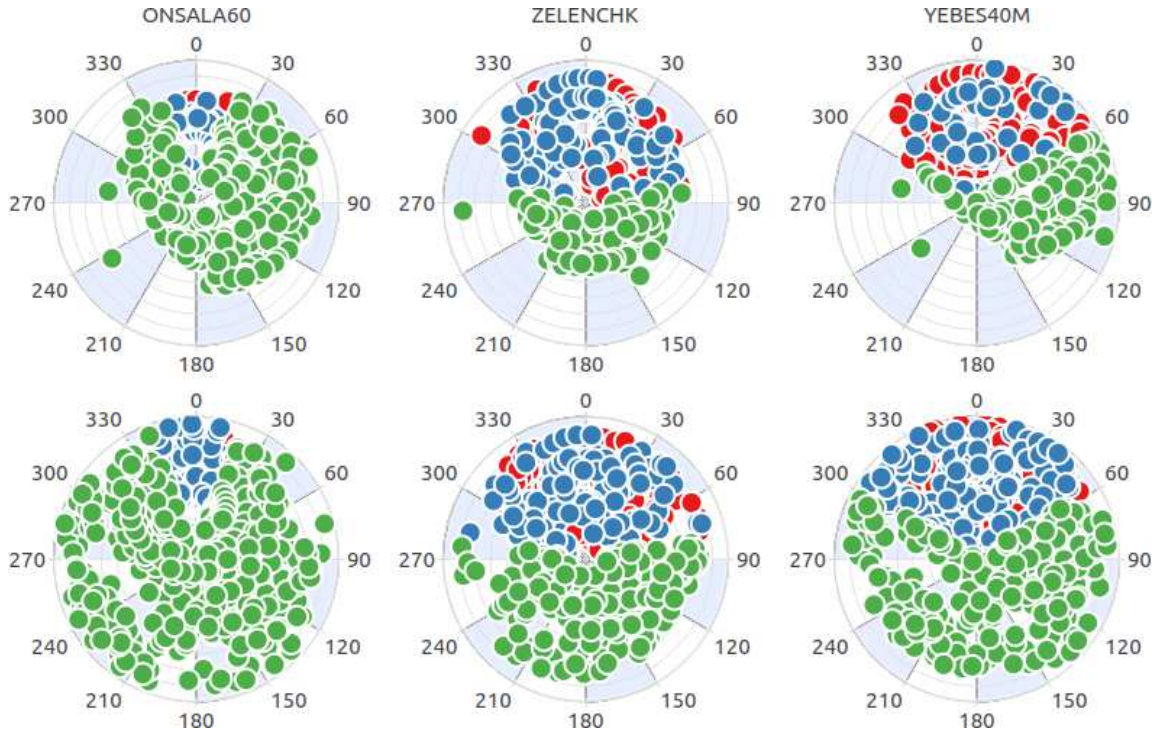


Figure 43: Sky-coverage of selected stations of EURR&D sessions. The first row visualizes the sky-coverage of a session before the use of VieSched++, while the second row visualizes it for a session scheduled with VieSched++. The cable wrap information is color-coded with green being neutral, blue being clockwise, and red being counter-clockwise cable wrap. The results look similar for all other stations and sessions.

Table 9: Number of stations per scan for EURR&D sessions. Sessions highlighted in blue were scheduled using VieSched++.

percentages [%]	EURD05	EURD06	EURD07	EURD08	EURD09	EURD10
2-station scans:	0.00	0.00	0.00	0.00	0.00	0.15
3-station scans:	0.00	0.00	0.00	0.00	17.59	15.25
4-station scans:	2.41	0.19	0.58	3.88	13.23	7.92
5-station scans:	0.00	0.00	0.29	0.00	3.61	9.12
6-station scans:	0.00	99.81	0.00	7.20	2.41	0.90
7-station scans:	5.35		5.52	88.92	33.23	7.03
8-station scans:	92.25		93.60		29.92	59.64

6. RESULTS

However, as already discussed in section 3, a high number of observations comes with the cost of poorer sky-coverage and one of the major challenges is to find a good compromise between these two factors.

The high occurrence of three and four station scans for the VieSched++ schedules EURD09 and EURD10 can be explained through subnetting and fillin-mode scans. For EURD09, 148 out of 665 scans are scheduled using subnetting and 63 scans are scheduled during the fillin-mode. For EURD10, 148 out of 669 scans are scheduled using subnetting and 73 scans are scheduled during the fillin-mode.

6.2.1 Simulations

Figure 44 visualizes the expected accuracy of the EOPs based on Monte-Carlo simulations as described in section 4.1.1. Since the network for EURD05, EURD07 is identical with EURD09 and EURD10 (see Figure 45), the results of these sessions can be directly compared. It can be seen that improvements for the accuracy of the EOP can be expected

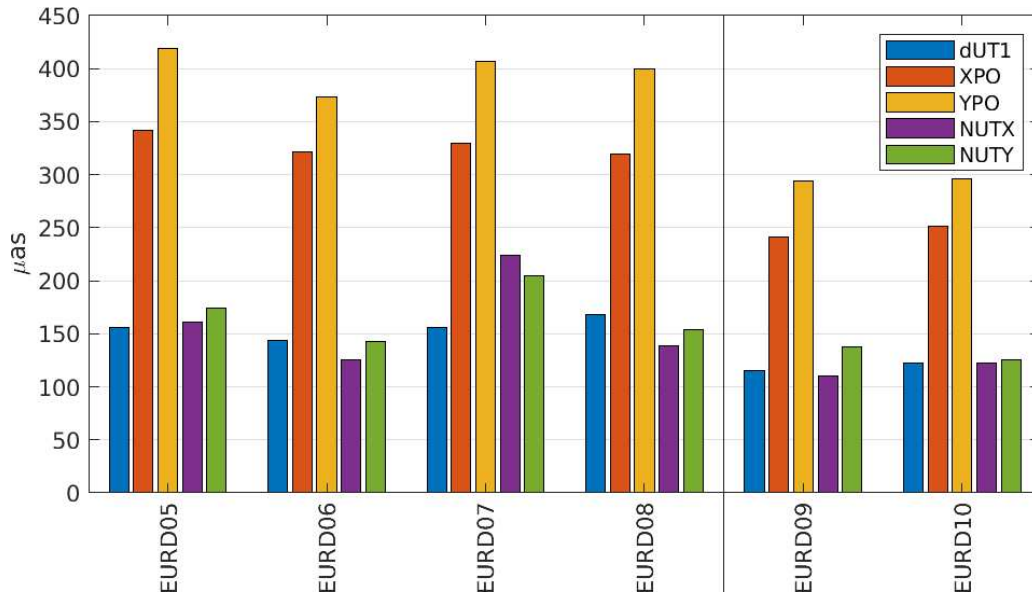


Figure 44: Simulated EOP repeatabilities from EURR&D sessions.

based on the simulations, especially for polar motion. However, since this is a regional network without good north-south baselines, the overall quality of the EOP accuracy is rather poor.

6. RESULTS

The dedicated goal of the EURR&D session are high-quality station coordinates. Therefore, Figure 45 visualizes the expected 3D-station coordinate accuracy. Especially by

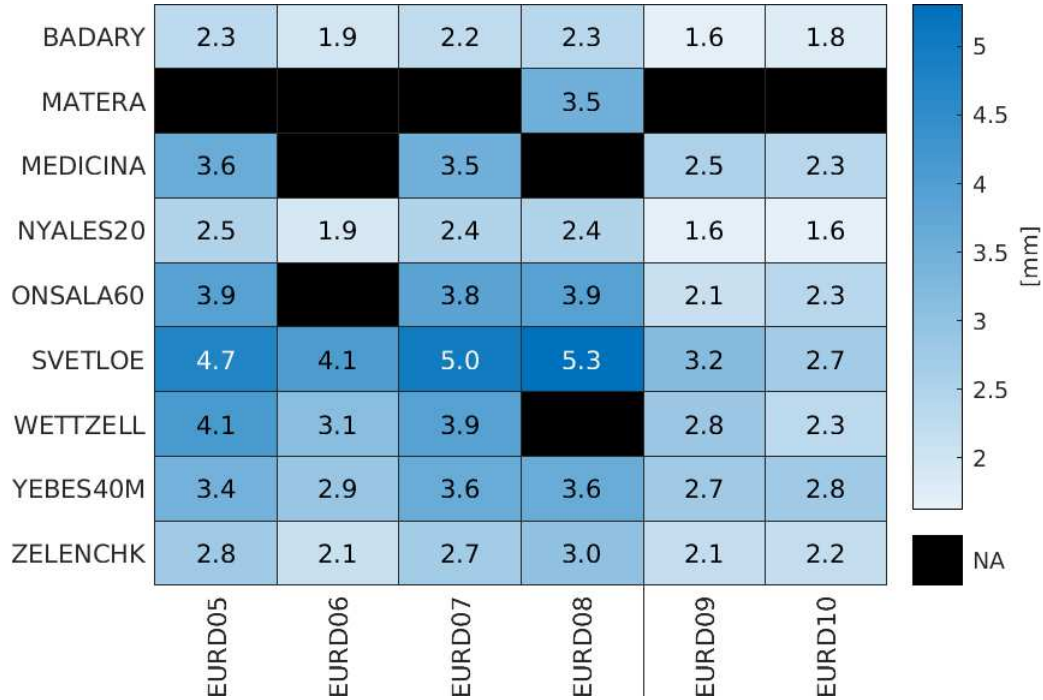


Figure 45: Simulated station coordinate repeatabilities of EURR&D sessions. A black box indicates that this station was not scheduled in this session.

comparing the sessions with an identical network (EURD05, EURD07, EURD09, and EURD10), clear improvements can be expected for the VieSched++ schedules.

6.2.2 Real observations

Figure 46 displays the number of scheduled observations and compares them with the number of correlated, recoverable and used observations as listed in the official IVS analysis reports. There are no official analysis reports available for EURD05 and EURD06. Unfortunately, BADARY did not participate in EURD10 although it was scheduled and MEDICINA missed a total of ≈ 6 hours due to software crashes in this session. This explains the big difference in scheduled observations compared to correlated observations for EURD10. However, no major issues are reported from stations participating in session EURD05, EURD07 and EURD09. Since these sessions are scheduled using the same anten-

6. RESULTS

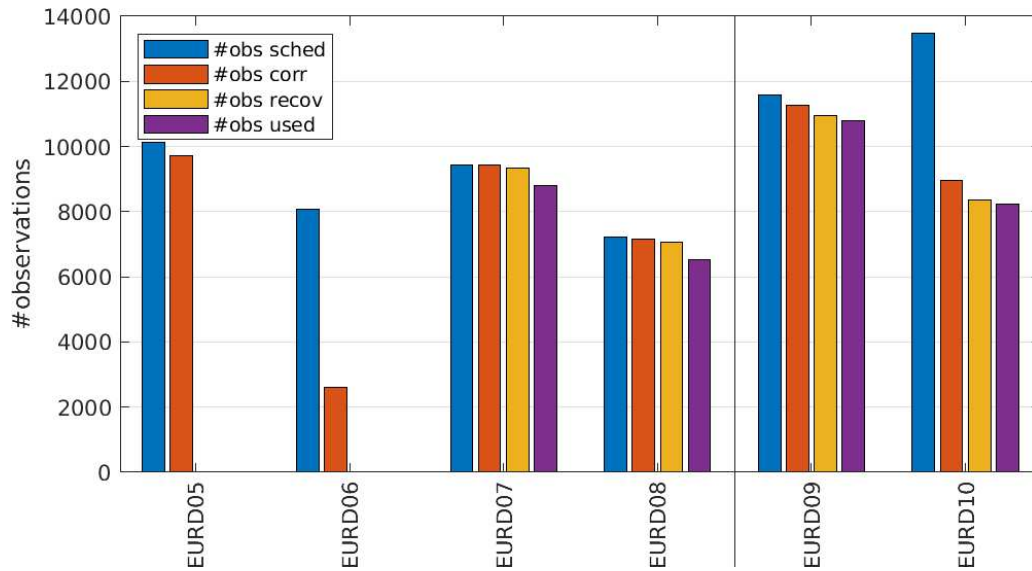


Figure 46: Number of observations scheduled, correlated, recoverable and used for the EURR&D sessions as listed in the official IVS analysis report.

nas with the same observing mode, direct comparisons of these three sessions are possible.

Figure 47 displays the EOP formal errors of the EURRD sessions. A clear improvement, especially for polar motion, can be seen for EURD09. Since BADARDY dropped out of EURD10 the improvement is smaller for EURD10 because BADARY provides the longest baselines in this session.

By taking the average formal errors of EURD05 and EURD07 and comparing it with the formal errors of EURD09, the improvement is a factor of three for polar motion, a factor of 2.5 for dUT1 and a factor of 1.4 for nutation.

Most importantly, Figure 48 displays the 3D-station coordinate formal errors. Similar to the T2 sessions, a clear improvement can be seen when comparing the schedules which are generated with VieSched++ with the previously submitted schedules. If the 3D-station coordinate formal errors of EURD05 and EURD07 are compared with the 3D-station coordinate formal errors of EURD09, the average improvement is almost a factor of three.

The real results outperform the expectations from the simulations in terms of EOPs and 3D-station coordinate accuracy. This indicates that the simulation strategy maybe

6. RESULTS

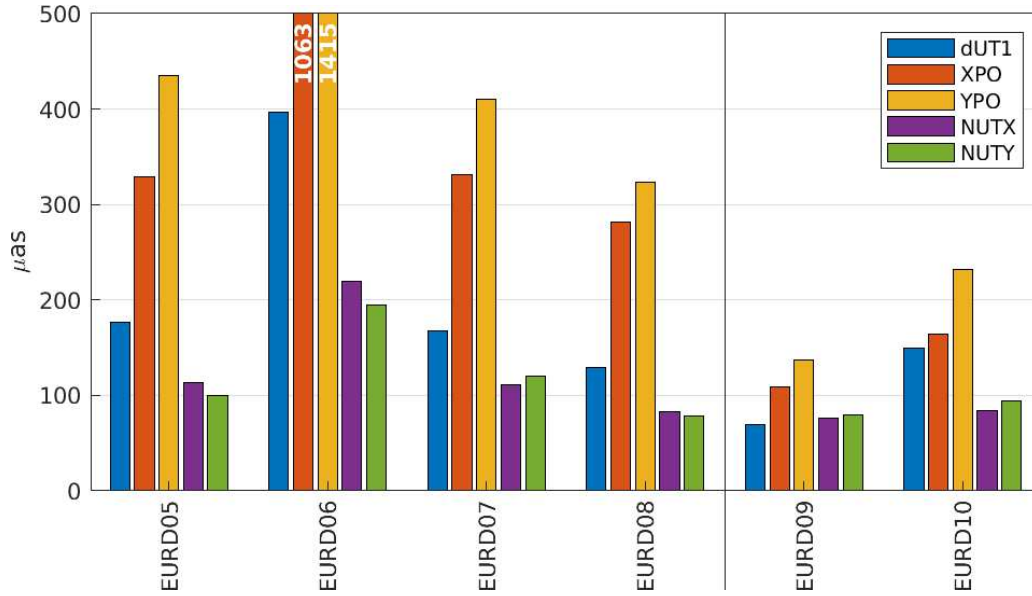


Figure 47: Formal errors of EOP estimates from EURR&D sessions.

has to be adjusted to provide more realistic values. Therefore, further research is necessary to improve the simulation. For example, the tropospheric wet delay of all stations is simulated using the same refractive index structure constant C_n . Individually adjusted C_n values should increase the simulation quality and provide more realistic results.

6.3 INT3

Starting in January 2019, VieSched++ is used to schedule the INT3 intensive sessions.

The goal of the INT3 observing program is to provide high-quality dUT1 estimates with a short time delay. Therefore, the INT3 antenna network consists of only three to five antennas, visualized in Figure 49 and the session duration is only one hour. Since long baselines with an east-west orientation are most sensitive for dUT1, the network geometry tries to focus on providing these baselines. Although the time delay between the observations and the result is critical for the success of intensive sessions and the data transfer is one bottleneck in this process, the observations are recorded with a relatively high recording rate of 1 Gbit/s for INT3.

The intensive sessions are not analyzed as described in section 4.1.2 to minimize the number of estimated parameters. This is necessary because most of the times only a small

6. RESULTS

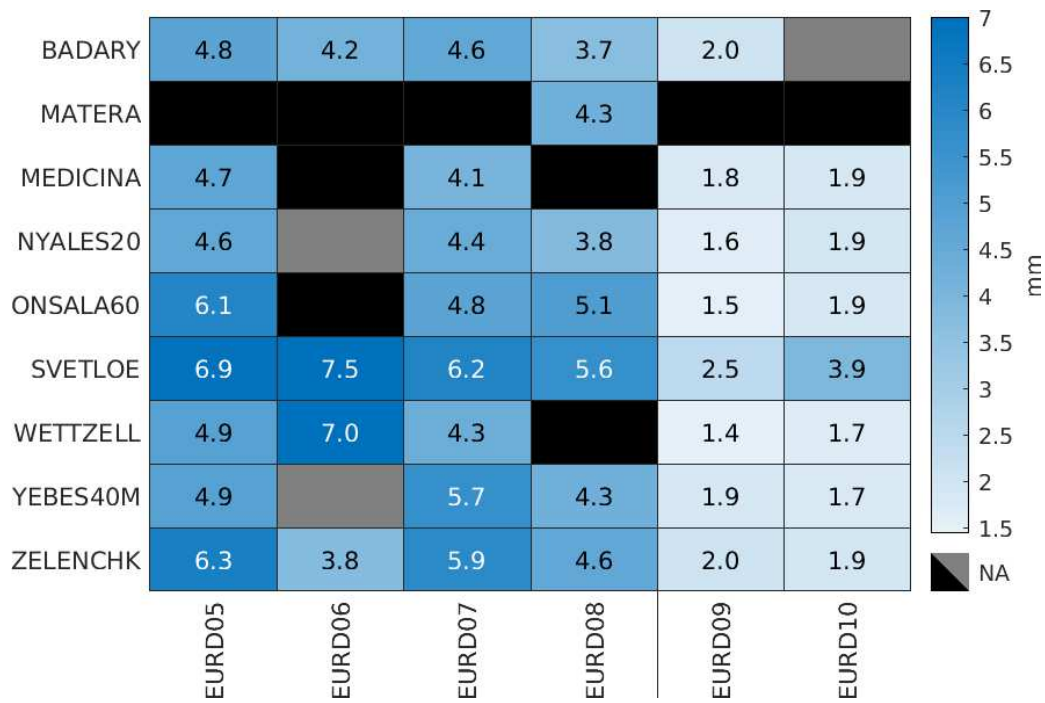


Figure 48: Formal errors of 3D-station coordinate of EURR&D sessions. A black box indicates that this antenna was not scheduled in this session. A gray box indicates that this antenna was scheduled but was not available or usable in the analysis.

number of observations is available for the parameter estimation.

In this section, the dUT1 formal errors are not estimated using VieVS. Instead, the formal errors from the official IVS analysis reports are taken for comparison.

The VieSched++ intensive schedules are generated using the following steps: First, a trial schedule is generated with very high weight on the sky-coverage weight factor (see section 5.4.2) and very little weight on the duration weight factor (see section 5.4.1) to generate a schedule with a very good sky-coverage containing many different sources. By using the VieSched++ Analyzer, a tool that can visualize schedules graphically, multiple sources which are near the two edges of the commonly visible sky area are selected since it is assumed that these sources contribute the most to the estimation of dUT1 (Uumila et al., 2012).

Afterward, the final schedule is generated using the following procedure: The sources located in one corner of the commonly visible sky area are given a very high weight. This

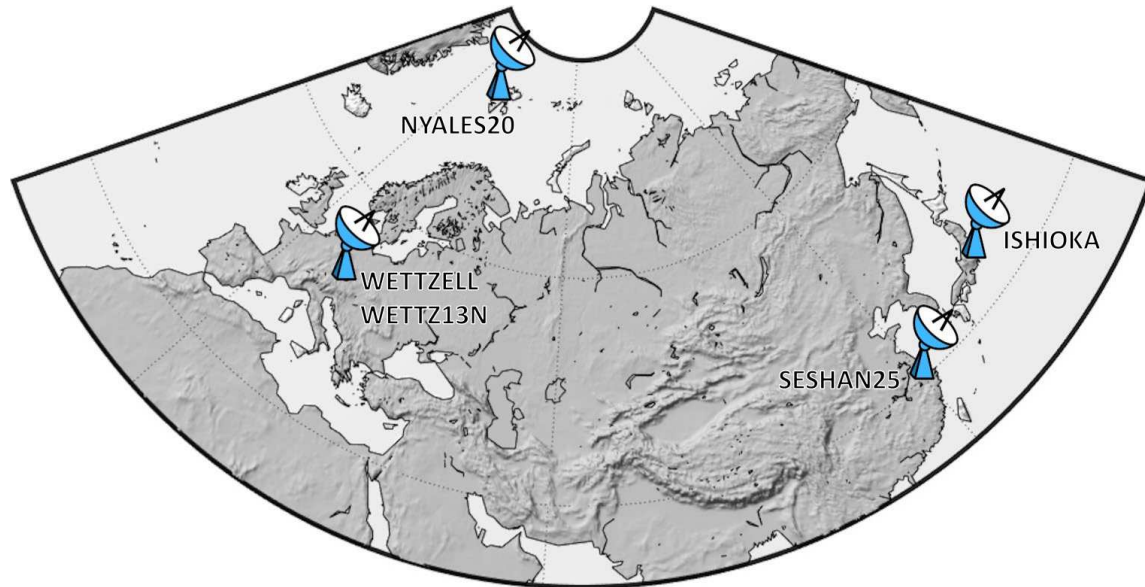


Figure 49: Antennas participating in recent INT3 sessions.

ensures, that these sources are observed at the start of the session. Additionally, the sources from the other corner of the commonly visible sky area get a very high weight, but only starting 15 minutes deep into the session (see section 5.8). The minimum time between two scans to the same source is set to 30 minutes for all sources. Furthermore, the weight factors are changed to a very low weight on the sky-coverage weight factor and a very high weight on the duration weight factor 5.4.1.

This results in a situation, where the schedule starts by observing the sources at one corner of the commonly visible sky due to the high weight of these sources. Since the duration weight factor is dominant, the following scans are scheduled to strong sources close to each other. This ensures a high number of observations and little slew time. After 15 minutes, the weight of the sources at the other side of the commonly visible sky has increased. This ensures, that the next scans are scheduled at this corner followed by scans to strong sources near this area. After 30 minutes the minimum time between two scans to the same source is reached for the sources located at the first corner of the commonly visible sky, resulting in new observations to these sources due to their high weight. After 45 minutes the same happens for the second corner.

Therefore, the schedule is specially designed to observe sources near the corners of the commonly visible sky area twice per schedule while providing a high number of observations

6. RESULTS

due to the high weight on the duration weight factor.

Figure 50 displays the number of schedule observations for all INT3 sessions in 2018 and 2019. Similar to 24-hour sessions, the number of observations increases with VieSched++

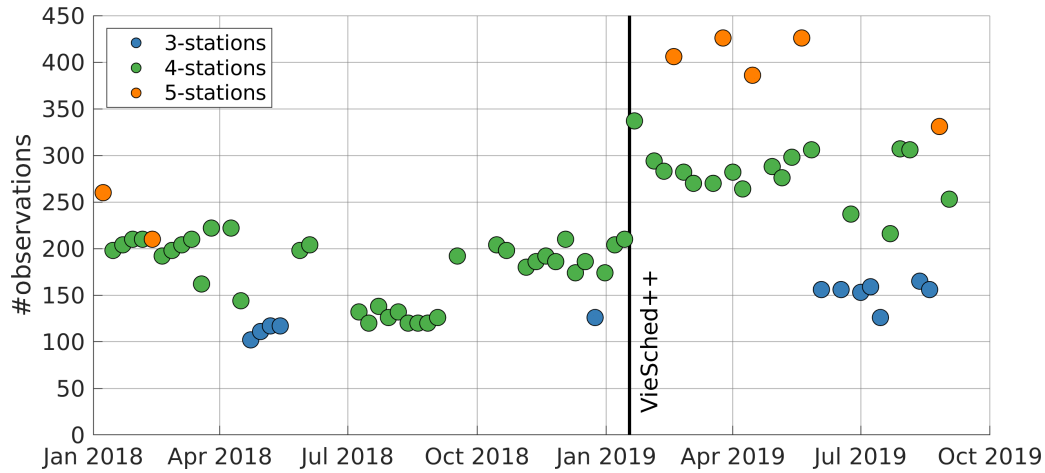


Figure 50: Number of observations for INT3 sessions scheduled in 2018 and 2019.

compared to previous schedules. Some outliers exist, which can be explained through the test of different source lists.

Figure 51 displays the UT1 formal error accuracy according to IVS analysis reports for all intensive sessions from mid-2017. It can be seen that sessions with a high number of stations and a higher recording rate lead to better results. The UT1 formal error is only shown up to $30\mu s$.

For a better visibility, Figure 52 displays the same as Figure 51 but highlights the INT3 observing program. The legend is the same as in Figure 52. The INT3 observing program provides the highest accuracy for UT1 estimates of all intensive programs. A yellow line marks the time, where the scheduling software is changed to VieSched++. The accuracy of the UT1 estimates is more or less constant since January 2019. As expected, the three-station networks tend to have worse accuracy than the four or five-station networks.

A situation, where the accuracy is worse over a longer period, as it was the case in mid-2018, is so far avoided with the use of VieSched++. The reason for the accuracy drop in mid-2018 is unclear. However, this period coincided with a drop in the number of observations as can be seen in Figure 50.

6. RESULTS

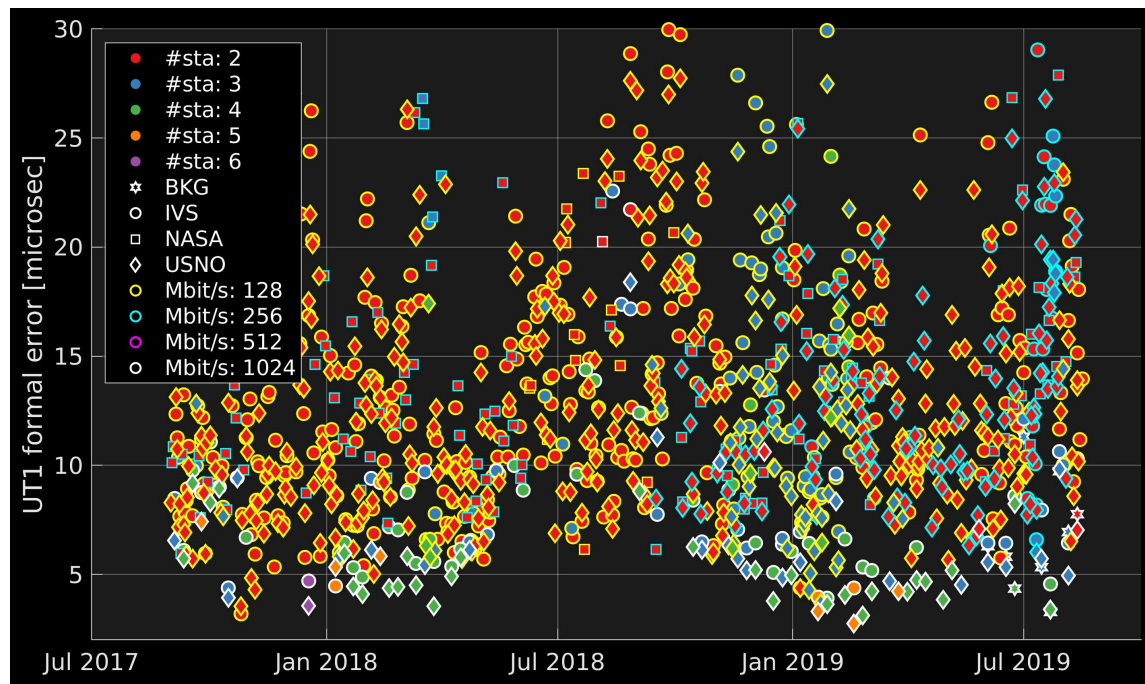


Figure 51: UT1 formal error accuracy according to IVS analysis reports for all intensive sessions.

A more detailed analysis of the INT3 results will be provided in a later work when more data is available.

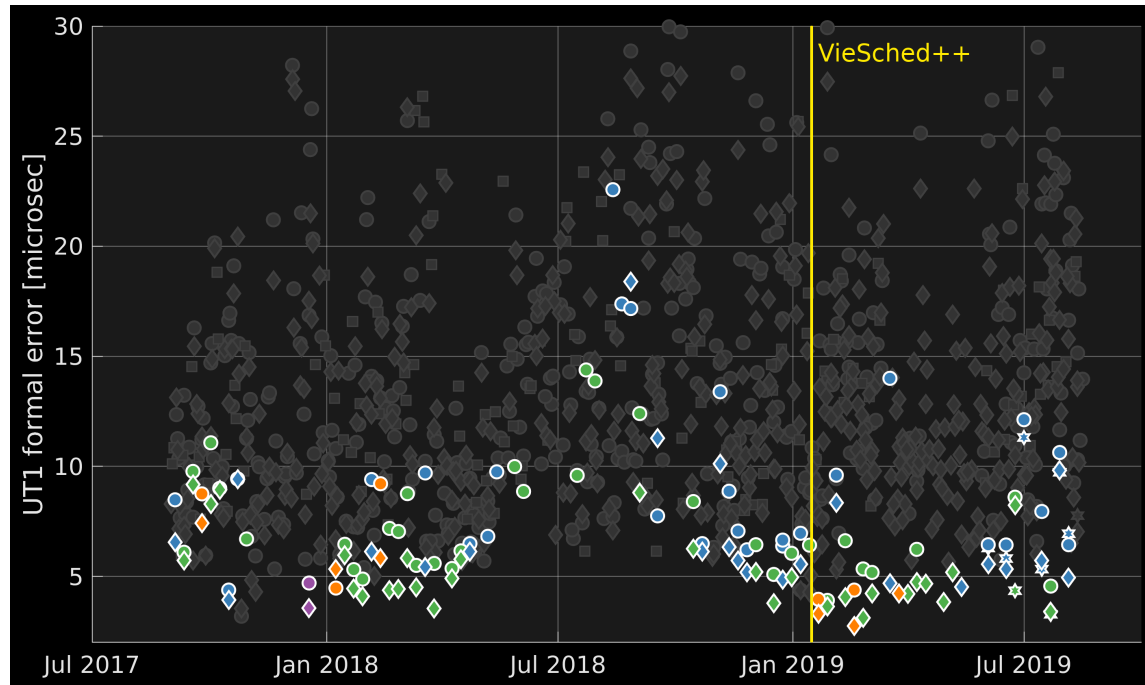


Figure 52: UT1 formal error accuracy according to IVS analysis reports for all INT3 sessions. The legend is identical as in Figure 51.

7 VGOS simulation study

In this section, results of simulation studies aiming to optimize a schedule for the VGOS session VT9175 are presented, similar as in [Schartner and Böhm \(2019a\)](#). At the time when this study was done, VT9175 was the most recent VGOS session. It consists of six stations, displayed in Figure 53. The antennas are located in Europe and North-America including Hawaii. Since the network lacks stations in the southern hemisphere and Asia, it cannot be seen as a global network. While four of the six participating antennas are fast slewing, GGAO12M and WESTFORD have slower slew rates. Additionally, the azimuth cable-wrap span (see section 3.4.1) of WESTFORD is only 360 degrees, which is uncommon for geodetic VLBI antennas and adds difficulty in scheduling this antenna since the slew directions are more restricted.

Table 10 lists the key attributes of the participating antennas.

The simulation study is performed using the VieSched++ multi-scheduling tool (see

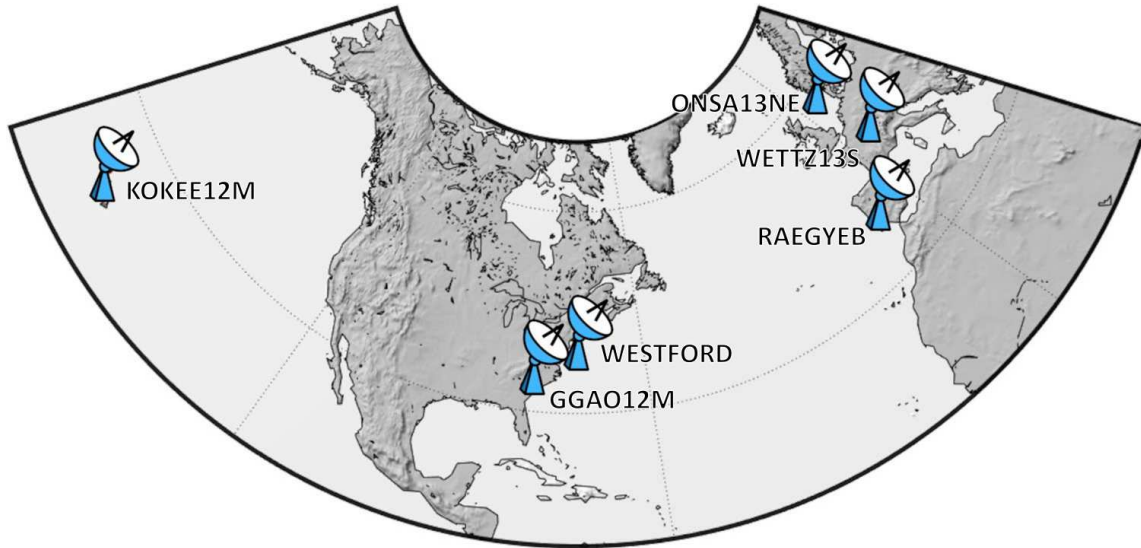


Figure 53: VT9175 antenna network.

Table 10: Antennas participating in VT9175 and their key attributes for scheduling.

station	slew rate az [deg/min]	slew rate el [deg/min]	azimuth span [deg]
GGAO12M	300	66	540
KOKEE12M	720	300	500
ONSA13NE	720	360	540
RAEGYEB	720	360	480
WESTFORD	200	120	360
WETTZ13S	720	360	540

section 5.6) in conjunction with Monte-Carlo simulations using VieVS. Several hundred schedules are generated and each schedule is simulated 1000 times. The troposphere is simulated using a refractive index structure constant C_n of $2.0 \times 10^{-7} \text{ m}^{-1/3}$, the clock with an ASD of $1 \times 10^{-14} \text{ s}$ after 50 minutes and 4 picoseconds of white noise are added as discussed in [Pany et al. \(2011\)](#), [Petrachenko et al. \(2009\)](#).

The analysis is done as described in section 4.1.2 but the tropospheric zenith wet delay is estimated every 15 minutes and the tropospheric north and east gradients are estimated every 30 minutes.

The schedules are generated using a constant observing time of 30 seconds as it is the

case for the official VGOS schedules. The slew rate is not fixed to a constant value but is instead calculated based on the real slew rates of the antennas. The minimum number of scans per source is set to three through the iterative source selection (see section 5.7). The VieSched++ multi-scheduling tool is used to vary four weight factors, namely the duration weight factor (see section 5.4.1), the number of observations weight factor (see section 5.4.3), the sky-coverage weight factor (see section 5.4.2) and the idle time weight factor (see section 5.4.4). Additionally, different sky-coverage definitions (see section 5.4.2), the impact of enabling subnetting (see section 3.7.1), and the effect of a minimum slew distance between two scans is investigated as discussed in [Schartner and Böhm \(2019a\)](#).

For the first three weight factors, the tested values are $\{0, 0.33, 0.67, 1\}$, while for the idle time weight factor only the values $\{0.5, 1\}$ with an interval of 300 seconds are tested. Since VGOS sessions are assumed to observe a scan every minute, the idle time weight factor mostly acts as a safety net to prefer scheduling scans with an antenna if it did not participate in the last couple of scans. This makes sure that all antennas are observing regularly and is important for the station KOKEE12M since its location is remote.

The sky-coverage definition is tested with an influence distance of $\{15, 30, 45\}$ degrees and an influence time of $\{900, 1800, 3600\}$ seconds, see section 5.4.2 and equation (27a) and (27b).

All previous studies reveal that the use of subnetting is beneficial, even for this regional network. Since the introduction of a required minimum slew distance does not lead to a better schedule, (as it will be discussed in section 7.1) only results with no additional minimum slew distance and with subnetting are further discussed in this section.

The following figures visualize the results of 1152 schedules, generated by using combinations of all multi-scheduling parameters as described above. Figure 54 visualizes the number of observations, number of scans and the sky-coverage score with 37 areas after 30 minutes (see section 5.13 and Figure 35). In blue, a histogram of the result of all 1152 schedules is visualized. One of the 1152 schedules is highlighted as the “selected” schedule, meaning this is the result from the schedule which would have been sent to the stations as the official schedule for observation. It is selected based on the repeatability values of the geodetic results from the Monte-Carlo simulations. The key scheduling parameters for this selected schedule are summarized in Table 11.

Figure 54 reveals that the number of scheduled observations is between 10 000 and 17 000 for most sessions. The number of observations of the selected schedule is 13 066 and thus located in the middle of the total range. The situation is similar for the number of

7. VGOS SIMULATION STUDY

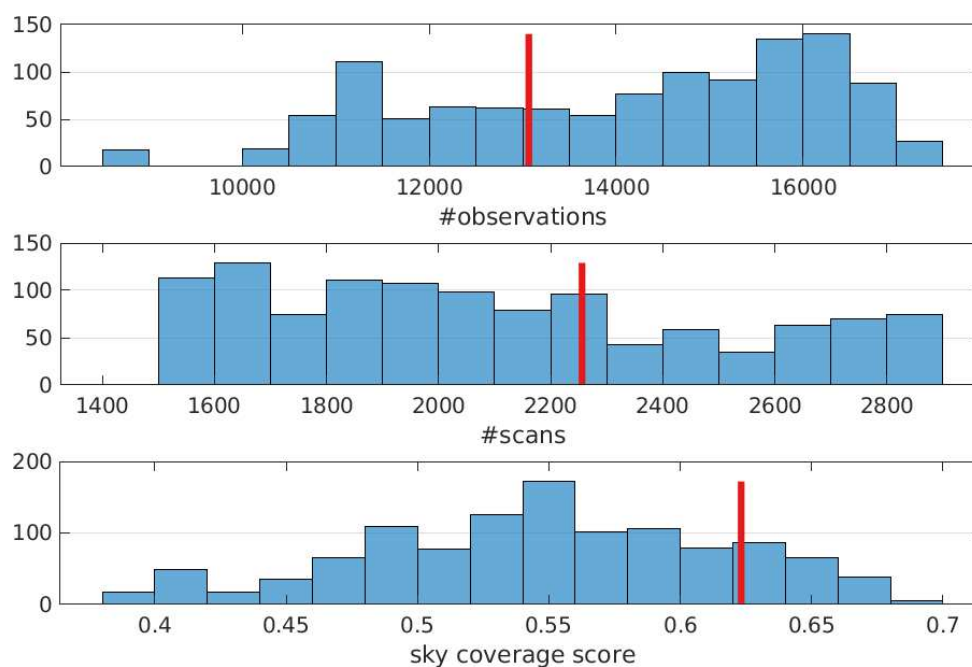


Figure 54: Histogram of scheduling statistics for all generated schedules (Schartner and Böhm, 2019a). The selected schedule is highlighted in red. The sky-coverage score is calculated using 37 areas and 30 minutes.

Table 11: Key scheduling parameters used to generate the optimized schedule based on the results from the repeatabilities.

parameter	value	unit
sky-coverage weight factor	0.67	
number of observations weight factor	0.33	
duration weight factor	0.67	
idle time weight factor	1.00	
sky-coverage influence distance	45	[deg]
sky-coverage influence time	1800	[s]
sky-coverage transfer functions	half cosine	
minimum slew distance	0	[deg]
considering subnetting	yes	
minimum scans per source	3	

scans per session, where the total range is between 1500 and 2900 scans while the number of scans for the selected schedule is 2256. Surprisingly, the selected schedule providing the

7. VGOS SIMULATION STUDY

best geodetic results in terms of repeatability values does not have the highest number of observations. However, when looking at the sky-coverage score calculated with 37 areas and 30 minutes the total range is between 0.4 and 0.7 and the selected schedule is located at 0.62. This value is close to the maximum of the total range.

As already discussed in section 3 the challenge of generating a good schedule is to find a good compromise between a high number of observations and a good sky-coverage. Based on the simulations, it seems like a good sky-coverage is more important than a high number of observations.

Figure 55 visualizes how the antenna time is spend during the VGOS sessions. The

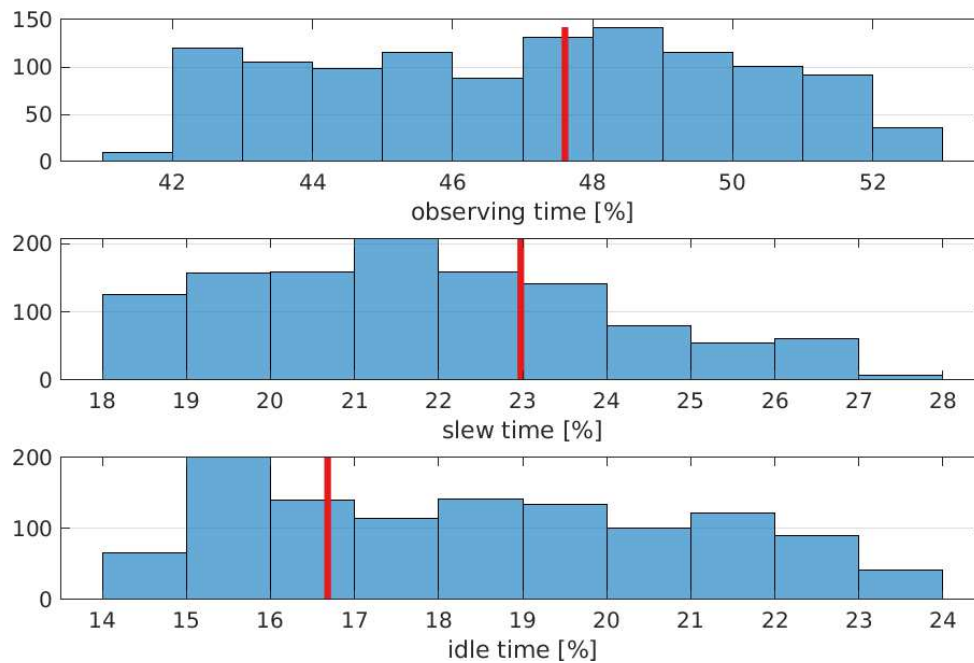


Figure 55: Histogram of the time spent during the VGOS sessions for all generated schedules (Schartner and Böhm, 2019a). The selected schedule is highlighted in red.

total observing time is between 41 and 53 percent for all sessions, while the slew time is between 18 and 28 percent and the idle time is between 14 and 24 percent. The selected schedule is located in the middle of the total range for observing and slew time and on the lower end in terms of idle time. Figure 55 does not visualize calibration and overhead time for the field system commands since these times are constant for each scan. The relatively high observing time can be explained by the fixed scan duration of 30 seconds.

7. VGOS SIMULATION STUDY

It is assumed, that this time reduces in the future when the recording rate of the VGOS sessions is increased and the required observing time is calculated based on the source flux density and the antenna SEFD values as described in section 5.3.4. It is important to note, that the idle time is relatively high compared to other sessions generated with VieSched++ because the occurring idle time is not used to extend the observing time as discussed in section 3.7.4 since this is only a simulation study and it is also not done in reality for VGOS sessions.

Figure 56 visualizes the estimated repeatability values of the geodetic parameters based on the Monte-Carlo simulations. The result of the EOP estimates and the 3D-station coordinates defined through equation (54) are displayed. The range of the 3D-station

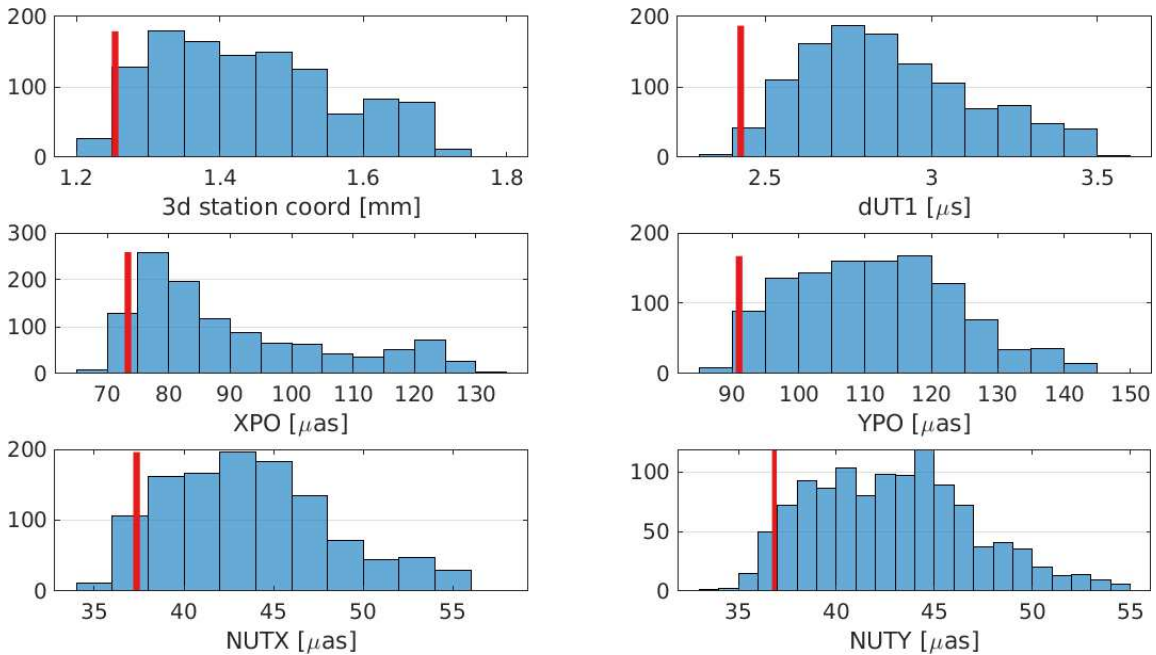


Figure 56: Histogram of the estimated repeatabilities for geodetic parameters based on Monte-Carlo simulations (Schartner and Böhm, 2019a). The selected schedule is highlighted in red.

coordinates is between 1.2 and 1.8 millimeters, which is close to the GGOS goal of 1 millimeter (Plag and Pearlman, 2009). It can be seen that the selected schedule, which is highlighted in red, provides very good estimates for all parameters. The schedule is selected based on these six parameters. If the dedicated goal of the session would be narrowed down

to simply provide high-quality station coordinates or one of the EOPs, the selection process could be adjusted for additional small improvement.

Figure 57 plots the number of observations against the sky-coverage scores and visualizes the expected EOP and station coordinate accuracy. This time, the selected schedule is highlighted as a green star. The shape of the dots indicates, that a high number of observations lead to a worse sky-coverage and vice versa as already discussed several times.

Surprisingly, the location of the selected schedule is not at the top-right edge, meaning there would be schedules which provide a better sky-coverage while having more observations. This indicates, that neither the number of observations nor the sky-coverage are perfect metrics for comparing and selecting schedules with the highest quality. Since scheduling is a complex optimization process including a multitude of different parameters and requirements, a simplification through either of these two metrics is not suitable for the highest quality. Instead, it is necessary to perform simulations to compare and select schedules based on these results.

Additionally, Figure 57 depicts that the highest precision of different geodetic parameters is achieved by using different schedules with different properties. This is especially visible for polar motion in the x-direction (XPO) where the area of highest accuracy (dark blue) is located in a different position as, for example, for the 3D-station coordinates.

Similar to Figure 57, Figure 58 plots the number of observations against the sky-coverage scores but it color-codes the values of the weight factors which were used to generate these schedules. When looking at the number of observations weight factor values, a clear trend can be seen. As expected, the number of observations rises if this optimization criterion gets a high relative weight. In case the number of observations weight factor is set to zero, less than 12 000 observations are scheduled. The maximum number of observations is achieved if the number of observations weight factor is set to a high value. However, this also leads to the poorest sky-coverage. It is necessary to note, that this is only the case for these regional VGOS networks like VT9175. Otherwise, a combination of high weight for the duration optimization criterion and high weight for the number of observations optimization criterion is needed to achieve the highest number of observations.

As noted before, the idle time weight factor is mainly used as a safety net to make sure that all antennas observe regularly. The one outlier with a poor sky-coverage score and a low number of observations on the bottom left of Figure 57 and 58 can be explained by a

7. VGOS SIMULATION STUDY

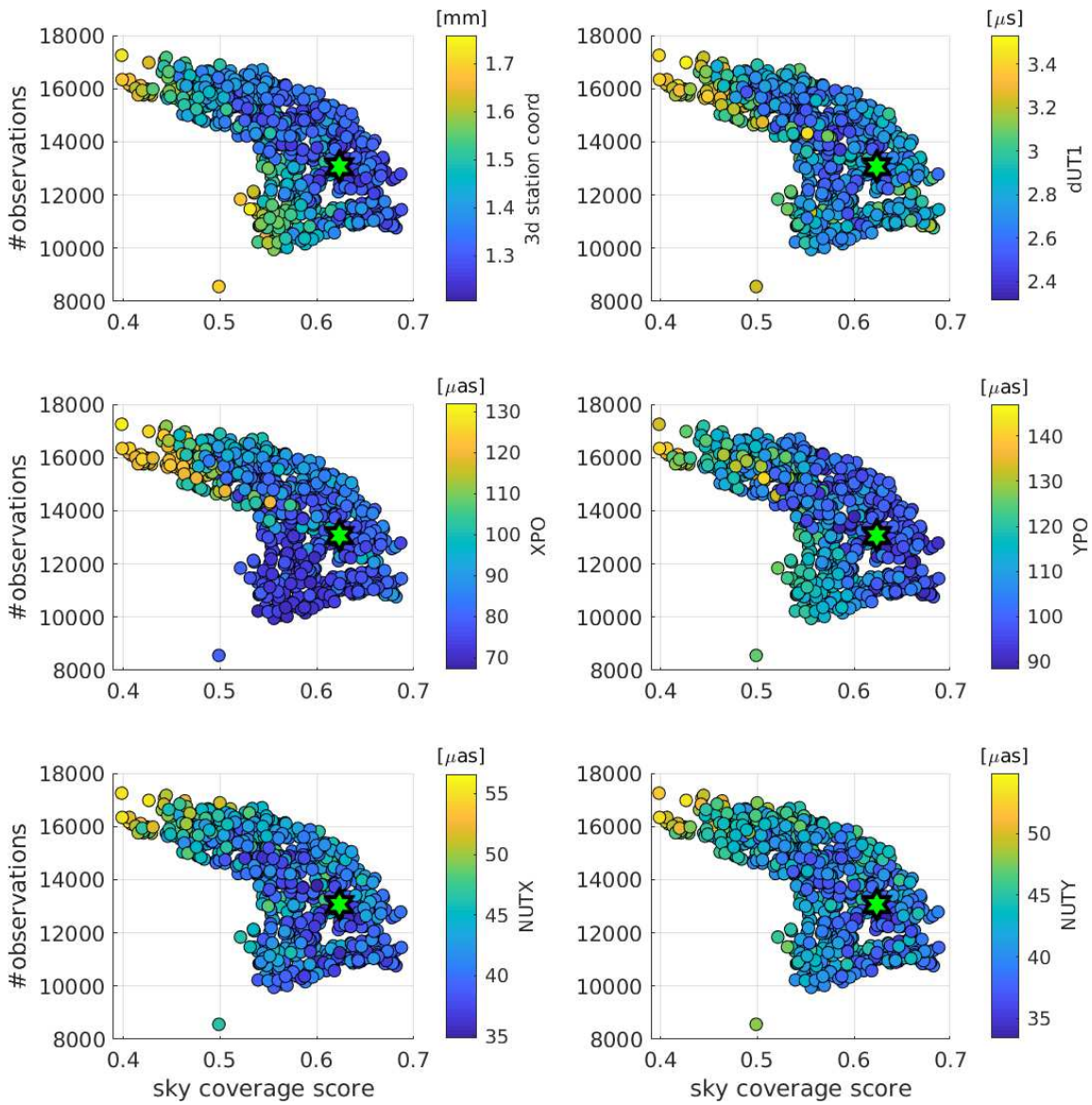


Figure 57: Number of observations versus sky-coverage score. The 3D-station coordinates and EOP repeatabilities are color-coded. The selected schedule is highlighted with a green star.

poor combination of weight factors, where only the idle time optimization criterion is used during the scan selection procedure, while all other weight factors have a value of zero.

A small positive correlation between the sky-coverage weight factor value and the sky-

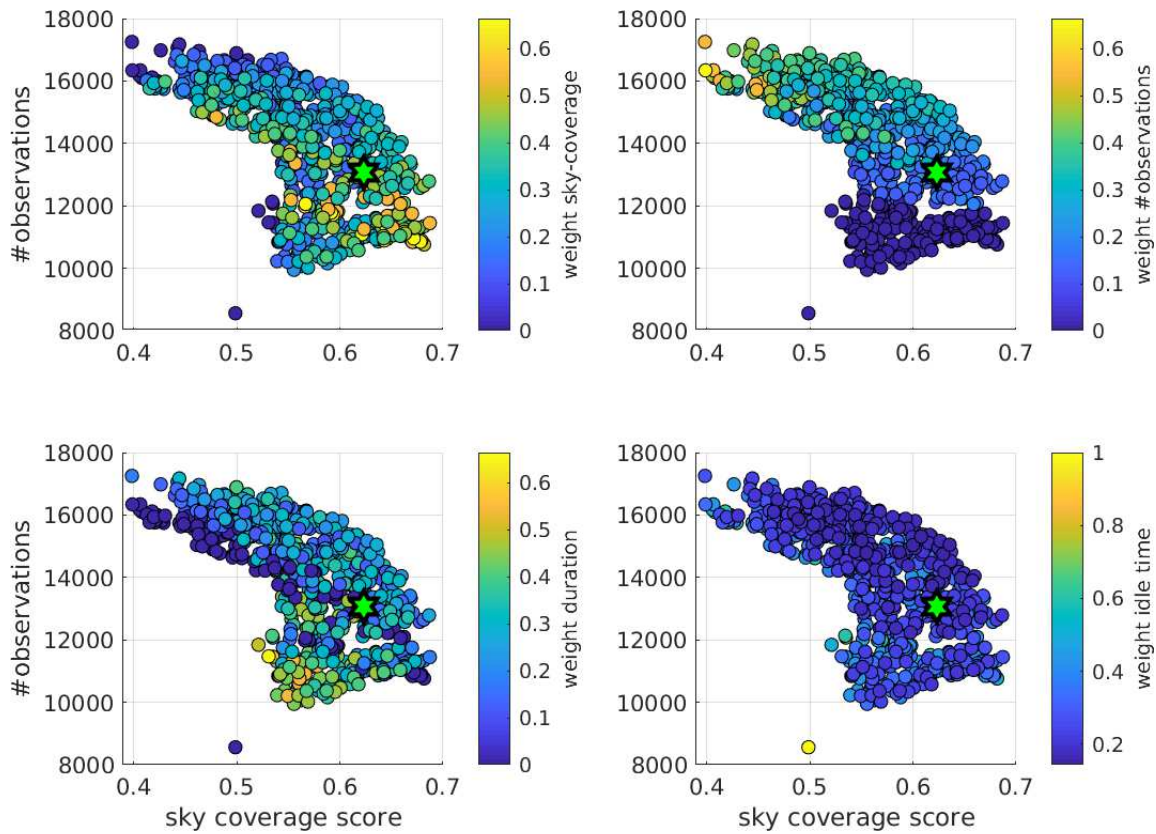


Figure 58: Number of observations versus sky-coverage score (Schartner and Böhm, 2019a). The weight factor values are color-coded. The selected schedule is highlighted with a green star.

coverage score can be seen. However, since other effects such as the number of scans also play an important role in the sky-coverage score this correlation is not that strong.

It can also be seen, that the duration weight factor plays a role in the total number of observations, although its impact is smaller compared to the number of observations weight factor.

7.1 Optimizing through minimum slew distance

The introduction of a minimum required slew distance between two consecutive scans is an alternative way to achieve a good sky-coverage and is used in the official VGOS schedules.

To test the impact of this approach with VieSched++, another simulation study is

7. VGOS SIMULATION STUDY

performed. In this study, a required minimum slew distance between 0 and 60 degrees is used in 10-degree steps. Based on this restriction, schedules are generated. Per minimum required slew distance, 64 different schedules are generated using different weight factor ratios as visualized in Figure 59. The 64 different schedules are generated to avoid effects on

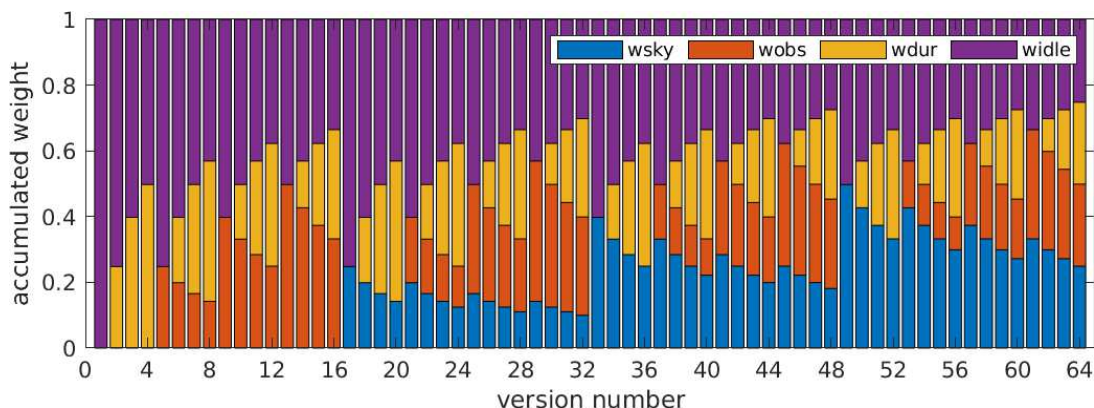


Figure 59: Ratio of weight factors used to generate the VT9175 schedules (Schartner and Böhm, 2019a).

the results which might occur based on bad optimization conditions for the scan selection. It is expected, that the introduction of a required minimum slew distance between scans has an influence on the optimal scheduling parameters and thus on the weight factors. Since the study aims to analyze the impact of a minimum slew distance on the schedule these additional influences should be minimized as much as possible. Together, this leads to a total of 448 investigated schedules.

Figure 60 visualizes the number of observations as well as the expected average 3D-station coordinate accuracy based on the repeatability values from the Monte-Carlo simulations. The different required minimum slew distances between two scans are color-coded. As expected, the number of observations lowers in case the minimum slew distance rises. This makes sense since the stations have to slew longer distances and have less time to observe. However, the difference between 0 and 50 degrees minimum slew distance is oftentimes not that big. The difference between the different versions, visible through a prominent zig-zag pattern, is higher than the difference between the minimum slew distance. This means that the weight factor has a higher influence on the result since the versions differ based on the weight factor ratios.

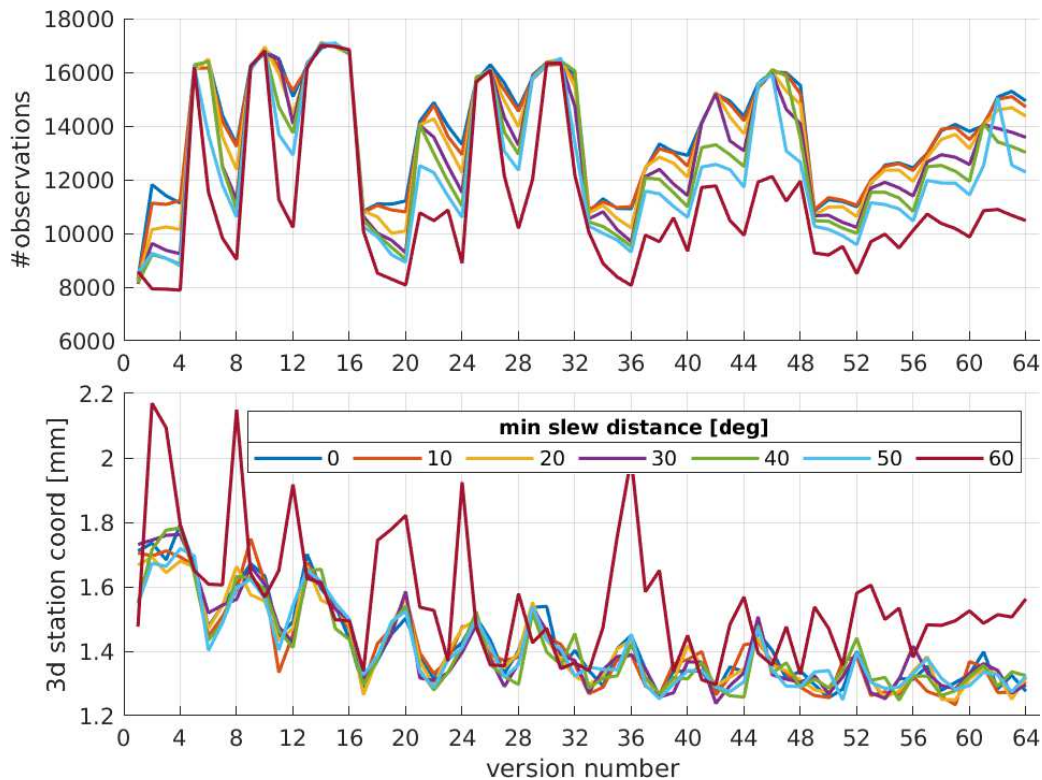


Figure 60: Impact of different minimum slew distances on geodetic results (Schartner and Böhm, 2019a). The abscissa lists the version number of the corresponding weight factor ratio visualized in Figure 59.

When looking at the estimated 3D-station coordinate repeatabilities in Figure 60, no improvement can be seen between 0 and 50 degrees minimum slew distance. In the case of 60 degrees minimum slew distance, a significant decrease of the accuracy is visible. Therefore, it can be concluded that the introduction of a required minimum slew distance between consecutive scans does not lead to an improvement of the schedule.

7.2 Optimizing through sky-coverage definitions

Since tropospheric time delays are considered one of the dominant error source for VGOS sessions, see Pany et al. (2011) and Petrachenko et al. (2009), a sophisticated definition of the sky-coverage implementation is necessary for generating high-quality VGOS schedules. Therefore, different definitions through the influence distance and time (see section 5.4.2)

7. VGOS SIMULATION STUDY

are tested.

In this study, nine different combinations of sky-coverage influence distances and times are investigated. The tested influence distance values are 15, 30, 45 degrees and the tested influence times are 900, 1800, 3600 seconds. Similar as for the minimum required slew distance study (see section 7.1), 64 different weight factors are investigated per sky-coverage definition, leading to a total of 576 schedules.

Figure 61 visualizes the results in terms of the number of observations and expected 3D-station coordinate repeatability per session. The sky-coverage influence time is color-coded

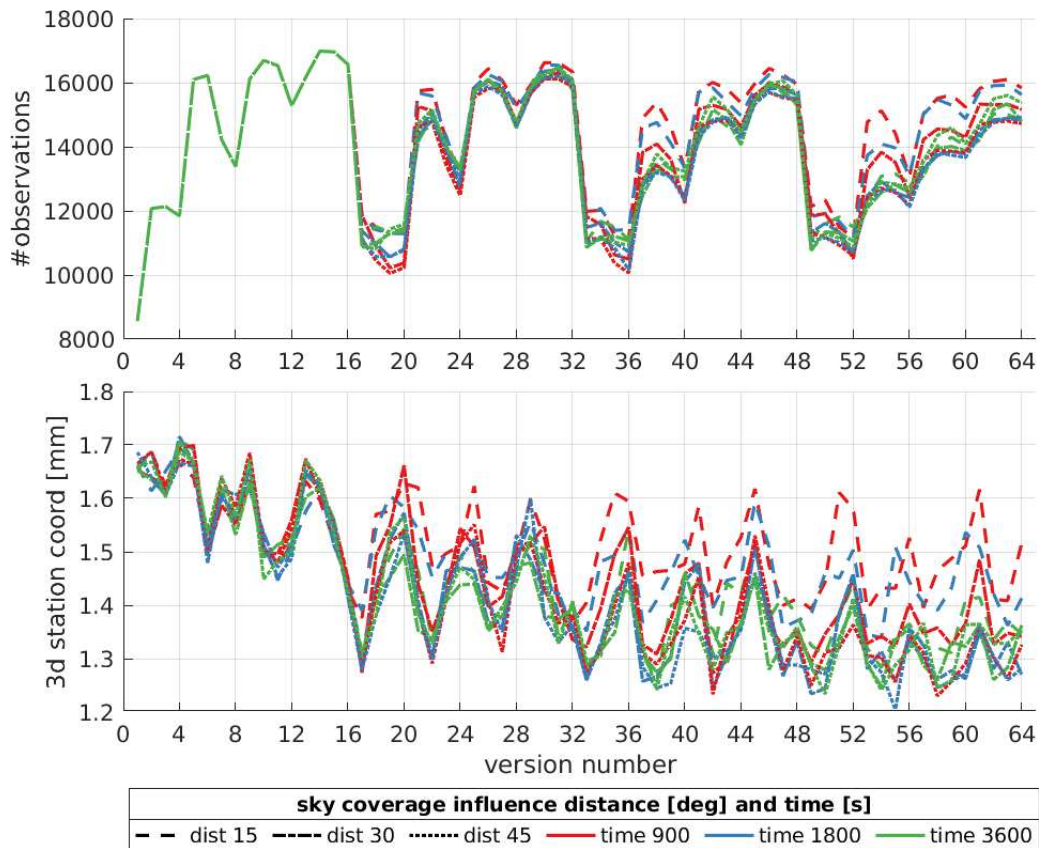


Figure 61: Impact of different sky-coverage definitions on geodetic results (Schartner and Böhm, 2019a). The abscissa lists the version number of the corresponding weight factor ratio visualized in Figure 59.

while the sky-coverage influence distance is distinguished by the line style.

When looking at the total number of observations in Figure 61, no difference can be seen

between the different sky-coverage definitions for the first 16 versions. This makes sense since the first 16 versions are generated with zero weight for the sky-coverage optimization criterion as visualized in Figure 59. In terms of the number of observations, even for the remaining versions, no big differences can be seen between the individual sky-coverage definitions. The only noticeable difference is, that the dashed lines which represent a sky-coverage influence distance of 15 degrees seems to lead to more observations. This can be explained through the shorter slew distances which lead to more leftover time for observations. However, a strong zig-zag pattern can be seen, which indicates that the weight factor ratios are again the dominant scheduling input parameters.

When looking at the expected 3D-station coordinate repeatability values in Figure 61, again a strong zig-zag pattern can be seen. The difference between the individual sky-coverage definitions is rather small, with the exception that the dashed lines, which represent a sky-coverage influence distance of 15 degrees, tend to produce worse schedules although these definitions lead to the highest number of observations. Therefore, it can be concluded that a sky-coverage influence distance of only 15 degrees is not enough for VGOS sessions.

Since the first 16 versions lead to completely identical schedules in this study, their 3D-station coordinate repeatability values should, in theory, be identical as well and can be used to validate the simulation approach. The results of the 3D-station coordinate repeatability values visualized in Figure 61 agree quite well, which leads to the conclusion that the 1000 simulations provide robust repeatability values.

7.3 Optimizing through weight factors

When looking at Figure 60 and Figure 61, the difference between the individual versions (abscissa) is more prominent as the difference between the tested parameters (lines). Since the individual versions differ only in terms of weight factor ratio, it can be concluded that a proper selection of well-suited weight factors is most important for the generation of high-quality VGOS sessions. The same is true for SX-sessions, as discussed in [Schartner et al. \(2017\)](#) and [Schartner and Böhm \(2019c\)](#).

When looking at Figure 60 and Figure 61, it can be seen that the accuracy of the 3D-station coordinate repeatability tends to decrease with a higher version number. A higher version number tends to put more weight on the sky-coverage optimization criterion, as it can be seen in Figure 59. Since the troposphere is the dominant error source in

7. VGOS SIMULATION STUDY

these simulations, a high weight on the sky-coverage optimization criterion which aims to help to estimate tropospheric time delays is beneficial. To further confirm this statement, the correlations between some selected scheduling input parameters with the repeatability values of geodetic parameters are calculated and displayed in Figure 62. The ratios of the

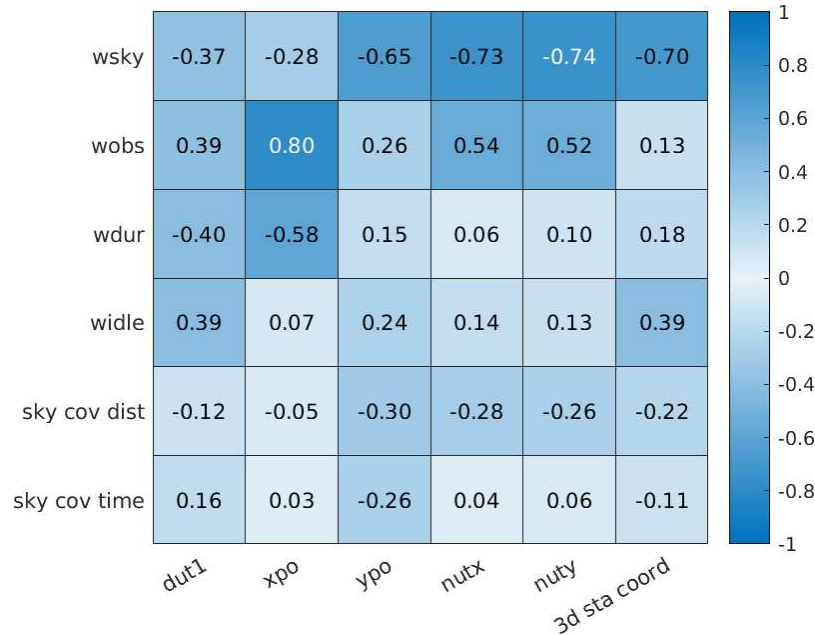


Figure 62: Correlations between scheduling parameters including weight factors and sky-coverage definitions with geodetic results (Schartner and Böhm, 2019a).

four tested weight factors and the two sky-coverage definition parameters are correlated against the repeatability values from the EOP accuracy and the 3D-station coordinate accuracy. A correlation close to zero would indicate, that this scheduling input parameter has no impact on the achieved geodetic result, while a correlation of plus or minus one would mean that this geodetic result is heavily influenced by the scheduling parameters. It can be seen that for the 3D-station coordinates, the sky-coverage weight factor has the highest influence with a correlation of -0.7.

In general, the correlation of the geodetic results with the weight factors is higher than the correlation with the sky-coverage definitions. This further confirms, that a proper selection of good weight factors is the dominant requirement for the generation of a high-quality schedule.

8 Summary and Conclusion

The generation of geodetic VLBI schedules is a complex challenge and sophisticated software is needed to get the best out of any session. VieSched++ is a high-quality scheduling software capable to fully optimize VLBI schedules. The software is written in modern C++ using an object-oriented software design. It is easy to install through a setup program for Windows and Ubuntu and easy to use via an intuitive GUI.

In the heart, VieSched++ works similarly as existing scheduling software, such as the popular “sked” software, which is developed and maintained by the Goddard Space Flight Center. It generates schedules on a scan-by-scan basis. First, all possible scans at a certain time are created. These scans are investigated based on so-called optimization criteria, and based on these optimization criteria a score is calculated for each scan. Then, the scan with the highest score is selected and scheduled and the whole process starts over again.

Additionally, VieSched++ uses many new approaches. For example, it is selecting its scans recursively, instead of generating the schedule in consecutive time order. Furthermore, all algorithms and optimization criteria are developed from scratch and great care was taken to be able to generate high-quality schedules. An iterative source selection is used to make sure that only the best sources for this session are observed. Although the main purpose of VieSched++ is the generation of high-quality geodetic VLBI sessions, additional algorithms for the optimization of astrometric purposes are also implemented.

Since scheduling is a complex task, the generation of high-quality schedules cannot be narrowed down to a simple rule or recommendation. Instead, every session has to be treated and optimized individually since the boundary conditions such as the station network and source strength changes constantly. For this purpose, the so-called multi-scheduling feature is implemented. With the multi-scheduling feature, multiple schedules are generated automatically and efficiently by using different scheduling input parameters. These schedules can then be used in additional software such as VieVS to carry out large scale Monte-Carlo simulations. Based on the results from these simulations the best schedule for a session can be selected based on real simulation results instead of raw scheduling statistics which are very hard to interpret. This process is fully automated in VieSched++ and VieVS and it runs with multi-core support to reduce the run time significantly.

VieSched++ is already successfully used to generate official schedules for the IVS. It is used to schedule the official T2, EURR&D, EUR, OHG, CRF, CRDS and INT3 observing

8. SUMMARY AND CONCLUSION

programs as well as some sessions which are not organized by the IVS. First results with these schedules show a significant increase in the accuracy of these programs through the optimized schedules which were used.

The number of observations for the T2 observing program has increased by a factor of two to three through the use of VieSched++ and the formal errors of the station coordinates are decreased on average by a factor of two. Additionally, the EOP formal errors are significantly reduced.

For the EURR&D observing program, big improvements in terms of sky-coverage, as well as improvements in terms of the number of observations, could be achieved. This leads to a reduction of the station coordinate formal errors by a factor of three. The same could be achieved for the polar motion formal errors.

With the INT3 observing program, VieSched++ is used to schedule the most accurate intensive sessions in the IVS.

Many additional sessions are already scheduled using VieSched++ but are not yet correlated and ready for analysis. However, simulations show that further improvements can be expected.

The multi-scheduling feature combined with the possibility to run VieSched++ in a batch mode without the GUI makes VieSched++ a perfect software for large scale simulation studies. In this work, one of these studies about the optimization of VGOS schedules is presented. Since VGOS is the future of geodetic VLBI, great care should be taken to provide high-quality VGOS schedules. It is shown, that a proper definition of the weight factors is the key for the generation of high-quality VGOS schedules.

9 Outlook

Through the ongoing development and improvement of VGOS, geodetic VLBI is changing rapidly and new challenges and opportunities arise. This is especially true for scheduling, since the new fast slewing antennas open new possibilities. So far, brute force approaches still yield the best results for geodetic VLBI scheduling. Following this, VieSched++ is well equipped for the future development of VLBI. It is capable to generate hundreds of schedules efficiently and no restrictions regarding the station network size or in terms of observing mode such as the number of observed bands exist. Moreover, preparations and initial tests are made for many additional features such as mixed-mode schedules or special scan alignments. Additionally, the object-oriented software design allows a simple extension and improvement of the software.

In the future, it is planned to include observations to artificial VLBI targets, such as satellites into the software. The idea is, to schedule these scans during the a priori phase and use the recursive scan selection in between these satellite scans to fill this time with observations to quasars. VieSched++ already supports the definition of multiple observing modes, which will be useful for the observation of satellites. Additionally, the recursive scan selection already works as intended. The missing piece is the proper implementation of satellite observations.

Another point for the future is the sophisticated implementation of the VGOS observing mode and scheduling files. Although preparations for this are already made, the problem lays in the lack of standards and official scheduling output formats which support all requirements for VGOS. The proper implementation of VGOS observations will be implemented as soon as the proper standards and file formats exist. However, VieSched++ is already capable to schedule VGOS observations as it is currently done by the IVS.

In terms of real observations, one goal is to use VieSched++ for more observing programs in the future and to get more people of the geodetic VLBI community to use the software. Initial simulations and tests show that big improvements can be expected for most observing programs such as R4 and VGOS. In both cases, it is possible to almost double the number of observations and improve the sky-coverage as it was done for T2 and EURR&D. Although the GUI is already of high quality and high-quality schedules can be generated with very little learning effort, further improvement is being considered to simplify the scheduling generation process even further allowing more people to use the

9. OUTLOOK

software. Additionally, a VieVS YouTube channel exists, which hosts videos about how to use VieSched++ and how to generate high-quality schedules. The VieVS YouTube channel can be reached via [this](#) link.

References

- Altamimi, Z., Rebischung, P., Métivier, L., and Collilieux, X. (2016). ITRF2014: A new release of the International Terrestrial Reference Frame modeling nonlinear station motions. *Journal of Geophysical Research: Solid Earth*, 121(8):6109–6131.
- Anderson, J. M. and Xu, M. H. (2018). Source Structure and Measurement Noise Are as Important as All Other Residual Sources in Geodetic VLBI Combined. *Journal of Geophysical Research: Solid Earth*, 123(11):10,162–10,190.
- Baver, K. and Gipson, J. (2013). Refining the Uniform Sky Strategy for IVS-INT01 Scheduling. In Zubko, N. and Poutanen, M., editors, *Proceedings of the 21st European VLBI Group for Geodesy and Astrometry Working Meeting*, pages 205–210.
- Baver, K. and Gipson, J. (2014). Balancing Sky Coverage and Source Strength in the Improvement of the IVS-INT01 Sessions. In Behrend, D., Baver, K. D., and Armstrong, K. L., editors, *International VLBI Service for Geodesy and Astrometry 2014 General Meeting Proceedings: “VGOS: The New VLBI Network”*, Eds. Dirk Behrend, Karen D. Baver, Kyla L. Armstrong, Science Press, Beijing, China, ISBN 978-7-03-042974-2, 2014, p. 267-271, pages 267–271.
- Baver, K., Gipson, J., Carter, M. S., and Kingham, K. (2012). Assessment of the First Use of the Uniform Sky Strategy in Scheduling the Operational IVS-INT01 Sessions. In Behrend, D. and Baver, K. D., editors, *International VLBI Service for Geodesy and Astrometry 2012 General Meeting Proceedings*, pages 251–255.
- Baver, K. D. and Gipson, J. M. (2018). Selected Results from Testing the IVS INT01 BA 50 Balanced Scheduling Strategy. *AGU Fall Meeting Abstracts*.
- Behrend, D. (2015). Continuous VLBI Scheduling: The CONT14 Example. In Haas, R. and Colomer, F., editors, *Proceedings of the 22nd European VLBI Group for Geodesy and Astrometry Working Meeting*, pages 145–149.
- Böhm, J., Böhm, S., Boisits, J., Girdiuk, A., Gruber, J., Hellerschmied, A., Krásná, H., Landskron, D., Madzak, M., Mayer, D., McCallum, J., McCallum, L., Schartner, M., and Teke, K. (2018). Vienna VLBI and Satellite Software (VieVS) for Geodesy and Astrometry. *Publications of the Astronomical Society of the Pacific*, 130(986):044503.

REFERENCES

- Böhm, J., Böhm, S., Nilsson, T., Pany, A., Plank, L., Spicakova, H., Teke, K., and Schuh, H. (2012). The new vienna vlbi software views. In Kenyon, S., Pacino, M. C., and Marti, U., editors, *Geodesy for Planet Earth*, pages 1007–1011, Berlin, Heidelberg. Springer Berlin Heidelberg.
- Böhm, J., Werl, B., and Schuh, H. (2006). Troposphere mapping functions for GPS and very long baseline interferometry from European Centre for Medium-Range Weather Forecasts operational analysis data. *Journal of Geophysical Research (Solid Earth)*, 111:B02406.
- Brotten, N. W., Legg, T. H., Locke, J. L., McLeish, C. W., Richards, R. S., Chisholm, R. M., Gush, H. P., Yen, J. L., and Galt, J. A. (1967). Long base line interferometry: A new technique. *Science*, 156(3782):1592–1593.
- Campbell, J. (2000). From Quasars to Benchmarks: VLBI Links Heaven and Earth. In *International VLBI Service for Geodesy and Astrometry 2000 General Meeting Proceedings*.
- Capitaine, N., Mathews, P. M., Dehant, V., Wallace, P. T., and Lambert, S. B. (2009). On the iau 2000/2006 precession–nutaton and comparison with other models and vlbi observations. *Celestial Mechanics and Dynamical Astronomy*, 103(2):179–190.
- Deller, A. T., Brisken, W. F., Phillips, C. J., Morgan, J., Aref, W., Cappallo, R., Middelberg, E., Romney, J., Rottmann, H., Tingay, S. J., and Wayth, R. (2011). DiFX-2: A more flexible, efficient, robust, and powerful software correlator. *Publications of the Astronomical Society of the Pacific*, 123(901):275–287.
- Deller, A. T., Tingay, S. J., Bailes, M., and West, C. (2007). DiFX: A software correlator for very long baseline interferometry using multiprocessor computing environments. *Publications of the Astronomical Society of the Pacific*, 119(853):318–336.
- Fey, A. L., Gordon, D., Jacobs, C. S., Ma, C., Gaume, R. A., Arias, E. F., Bianco, G., Boboltz, D. A., Böckmann, S., Bolotin, S., Charlot, P., Collioud, A., Engelhardt, G., Gipson, J., Gontier, A.-M., Heinkelmann, R., Kurdubov, S., Lambert, S., Lytvyn, S., MacMillan, D. S., Malkin, Z., Nothnagel, A., Ojha, R., Skurikhina, E., Sokolova, J., Souchay, J., Sovers, O. J., Tesmer, V., Titov, O., Wang, G., and Zharov, V. (2015). The Second Realization of the International Celestial Reference Frame by Very Long Baseline Interferometry. *The Astronomical Journal*, 150:58.

REFERENCES

- Gipson, J. (2010). An Introduction to Sked. In Navarro, R., Rogstad, S., Goodhart, C. E., Sigman, E., Soriano, M., Wang, D., White, L. A., and Jacobs, C. S., editors, *International VLBI Service for Geodesy and Astrometry 2010 General Meeting Proceedings*, pages 77–84.
- Gipson, J. (2016). *Sked VLBI Scheduling Software*. NVI, Inc. NASA/Goddard Space Flight Center.
- Gipson, J. and Baver, K. (2016). Improvement of the IVS-INT01 sessions by source selection: development and evaluation of the maximal source strategy. *Journal of Geodesy*, 90:287–303.
- Gold, T. (1967). Radio method for the precise measurement of the rotation period of the earth. *Science*, 157(3786):302–304.
- Hellerschmied, A. (2018). Satellite observations with VLBI. *Geowissenschaftliche Mitteilungen*, 102(102).
- Hellerschmied, A., Böhm, J., Kwak, Y., McCallum, J., and Plank, L. (2016). VLBI observations of GNSS satellites on the baseline Hobart-Ceduna. In *EGU General Assembly Conference Abstracts*, volume 18 of *EGU General Assembly Conference Abstracts*, pages EPSC2016–8895.
- Hellerschmied, A., Böhm, J., Neidhardt, A., Kodet, J., Haas, R., and Plank, L. (2017). Scheduling VLBI observations to satellites with VieVS. In van Dam, T., editor, *REFAG 2014*, pages 59–64, Cham. Springer International Publishing.
- Herring, T. A., Davis, J. L., and Shapiro, I. I. (1990). Geodesy by radio interferometry: The application of Kalman Filtering to the analysis of Very Long Baseline Interferometry data. *Journal of Geophysical Research: Solid Earth*, 95(B8):12561–12581.
- Herring, T. A., Shapiro, I. I., Clark, T. A., Ma, C., Ryan, J. W., Schupler, B. R., Knight, C. A., Lundqvist, G., Shaffer, D. B., Vandenberg, N. R., Corey, B. E., Hinteregger, H. F., Rogers, A. E. E., Webber, J. C., Whitney, A. R., Elgered, G., Romang, B. O., and Davis, J. L. (1986). Geodesy by radio interferometry: Evidence for contemporary plate motion. *Journal of Geophysical Research: Solid Earth*, 91(B8):8341–8347.

REFERENCES

- Hinteregger, H. F., Shapiro, I. I., Robertson, D. S., Knight, C. A., Ergas, R. A., Whitney, A. R., Rogers, A. E. E., Moran, J. M., Clark, T. A., and Burke, B. F. (1972). Precision geodesy via radio interferometry. *Science*, 178(4059):396–398.
- Hobiger, T., Kondo, T., and Schuh, H. (2006). Very long baseline interferometry as a tool to probe the ionosphere. *Radio Science*, 41(1).
- Kellermann, K. and Moran, M. (2001). The Development of High-Resolution Imaging in Radio Astronomy 1. *Annu. Rev. Astron. Astrophys*, 39:457–509.
- Krásná, H., Böhm, J., Plank, L., Nilsson, T., and Schuh, H. (2014). Atmospheric effects on vlbi-derived terrestrial and celestial reference frames. In Rizos, C. and Willis, P., editors, *Earth on the Edge: Science for a Sustainable Planet*, pages 203–208, Berlin, Heidelberg. Springer Berlin Heidelberg.
- Leek, J., Artz, T., and Nothnagel, A. (2015). Optimized scheduling of VLBI ut1 intensive sessions for twin telescopes employing impact factor analysis. *Journal of Geodesy*, 89(9):911–924.
- Ling, B. S. (2011). *The Boost C++ Libraries*. XML Press.
- Lovell, J., Plank, L., McCallum, J., Shabala, S., and Mayer, D. (2016). Prototyping Automation and Dynamic Observing with the AuScope Array. In Behrend, D., Baver, K. D., and Armstrong, K. L., editors, *International VLBI Service for Geodesy and Astrometry 2016 General Meeting Proceedings*, pages 92–95.
- Matveenko, L. I., Kardashev, N. S., and Sholomitskii, G. B. (1965). Large base-line radio interferometers. *Soviet Radiophysics*, 8(4):461–463.
- Mayer, D. (2018). VLBI celestial reference frames and assessment with Gaia. *Geowissenschaftliche Mitteilungen*, 103(103).
- McCallum, L., Mayer, D., Le Bail, K., Schartner, M., McCallum, J., Lovell, J., Titov, O., Shu, F., and Gulyaev, S. (2017). Star scheduling mode—a new observing strategy for monitoring weak southern radio sources with the auscope VLBI array. *Publications of the Astronomical Society of Australia*, 34:e063.
- Metropolis, N. and Ulam, S. (1949). The Monte Carlo Method. *Journal of the American Statistical Association*, 44(247):335–341.

REFERENCES

- Moran, J. M., Crowther, P. P., Burke, B. F., Barrett, A. H., Rogers, A. E. E., Ball, J. A., Carter, J. C., and Bare, C. C. (1967). Spectral line interferometry with independent time standards at stations separated by 845 kilometers. *Science*, 157(3789):676–677.
- Niell, A., Barrett, J., Burns, A., Cappallo, R., Corey, B., Derome, M., Eckert, C., Elosegui, P., McWhirter, R., Poirier, M., Rajagopalan, G., Rogers, A., Ruzsczyk, C., SooHoo, J., Titus, M., Whitney, A., Behrend, D., Bolotin, S., Gipson, J., and Petrachenko, B. (2018). Demonstration of a Broadband Very Long Baseline Interferometer System: A New Instrument for High-Precision Space Geodesy. *Radio Science*, 53.
- Niell, A., Whitney, A., Petrachenko, B., Schlüter, W., Vandenberg, N., Hase, H., Koyama, Y., Ma, C., Schuh, H., and Tuccari, G. (2005). VLBI2010: current and future requirements for geodetic VLBI systems. Tech. Rep.
- Nilsson, T., Haas, R., and Elgered, G. (2007). Simulations of atmospheric path delays using turbulence models. In Böhm, J., Pany, A., and Schuh, H., editors, *Proceedings of the 18th European VLBI for Geodesy and Astrometry Work Meeting*, pages 175–180.
- Nothnagel, A. (2019). *Very Long Baseline Interferometry*, pages 1–58. Springer Berlin Heidelberg, Berlin, Heidelberg.
- Nothnagel, A., Artz, T., Behrend, D., and Malkin, Z. (2017). International VLBI Service for Geodesy and Astrometry. *Journal of Geodesy*, 91(7):711–721.
- Pany, A., Böhm, J., MacMillan, D., Schuh, H., Nilsson, T., and Wresnik, J. (2011). Monte Carlo simulations of the impact of troposphere, clock and measurement errors on the repeatability of VLBI positions. *Journal of Geodesy*, 85(1):39–50.
- Petit, G. and Luzum, B. (2010). *IERS conventions 2010 (IERS Technical Note No. 36)*, volume 36. IERS Conventions Centre.
- Petrachenko, B., Niell, A., Behrend, D., Corey, B., Böhm, J., Charlot, P., Collioud, A., Gipson, J., Haas, R., Hobiger, T., Koyama, Y., MacMillan, D., Malkin, Z., Nilsson, T., Pany, A., Tuccari, G., Whitney, A., and Wresnik, J. (2009). Design Aspects of the VLBI2010 System. Progress Report of the IVS VLBI2010 Committee, June 2009. NASA/TM-2009-214180, 2009, 62 pages.

REFERENCES

- Petrachenko, W. T., Niell, A. E., Corey, B. E., Behrend, D., Schuh, H., and Wresnik, J. (2012). VLBI2010: Next Generation VLBI System for Geodesy and Astrometry. *International Association of Geodesy Symposia Volume 136, 2012*, pp 999-1005, 136.
- Petrov, L., Gordon, D., Gipson, J., MacMillan, D., Ma, C., Fomalont, E., Walker, R. C., and Carabajal, C. (2009). Precise geodesy with the Very Long Baseline Array. *Journal of Geodesy*, 83(9):859–876.
- Plag, H.-P. and Pearlman, M. (2009). *Global geodetic observing system: Meeting the requirements of a global society on a changing planet in 2020*. Springer-Verlag Berlin Heidelberg.
- Plank, L., E.J. Lovell, J., S. Shabala, S., Böhm, J., and Titov, O. (2015). Challenges for geodetic VLBI in the southern hemisphere. *Advances in Space Research*, 85.
- Plank, L., Lovell, J. E. J., McCallum, J. N., Mayer, D., Reynolds, C., Quick, J., Weston, S., Titov, O., Shabala, S. S., Böhm, J., Natusch, T., Nickola, M., and Gulyaev, S. (2017). The austral VLBI observing program. *Journal of Geodesy*, 91(7):803–817.
- Rogers, A. E. E. (1970). Very long baseline interferometry with large effective bandwidth for phase-delay measurements. *Radio Science*, 5(10):1239–1247.
- Salzberg, I. (1967). Mathematical relationships of the MFOD ANTENNA axes. Tech. Rep. 67N39334, NASA Goddard Space Flight Center, Greenbelt, MD, United States, report/Patent Number: NASA-TM-X-55956, X-553-67-213, Document ID: 19670030005.
- Schartner, M. and Böhm, J. (2019a). Optimizing schedules for the VLBI Global Observing System. *Journal of Geodesy - submitted*.
- Schartner, M. and Böhm, J. (2019b). VieSched++: A new Scheduling Tool in VieVS. In *International VLBI Service for Geodesy and Astrometry 2018 General Meeting Proceedings - in press*.
- Schartner, M. and Böhm, J. (2019c). VieSched++: A New VLBI Scheduling Software for Geodesy and Astrometry. *Publications of the Astronomical Society of the Pacific*, 131(1002):084501.

REFERENCES

- Schartner, M., Böhm, J., Mayer, D., McCallum, L., and Hellerschmied, A. (2017). Recent Developments in Scheduling with VieVS. In *Proceedings of the 23rd European VLBI Group for Geodesy and Astrometry Working Meeting*, pages 113–116.
- Schlüter, W. and Behrend, D. (2007). The International VLBI Service for Geodesy and Astrometry (IVS): current capabilities and future prospects. *Journal of Geodesy*, 81(6):379–387.
- Schuh, H. and Böhm, J. (2013). *Very Long Baseline Interferometry for Geodesy and Astrometry*, pages 339–376. Springer Berlin Heidelberg, Berlin, Heidelberg.
- Shapiro, I. I. and Knight, C. A. (1970). *Geophysical Applications of Long-Baseline Radio Interferometry*, pages 284–301. Springer Netherlands, Dordrecht.
- Shapiro, I. I., Robertson, D. S., Knight, C. A., Counselman, C. C., Rogers, A. E. E., Hinteregger, H. F., Lippincott, S., Whitney, A. R., Clark, T. A., Niell, A. E., and Spitzmesser, D. J. (1974). Transcontinental baselines and the rotation of the earth measured by radio interferometry. *Science*, 186(4167):920–922.
- SOFA (2019). IAU SOFA Software Collection.
- Sovers, O. J., Fanselow, J. L., and Jacobs, C. S. (1998). Astrometry and geodesy with radio interferometry: experiments, models, results. *Rev. Mod. Phys.*, 70:1393–1454.
- Spicakova, H., Boehm, J., Boehm, S., Nilsson, T., Pany, A., Plank, L., Teke, K., and Schuh, H. (2010). Estimation of geodetic and geodynamical parameters with views. In Navarro, R., Rogstad, S., Goodhart, C. E., Sigman, E., Soriano, M., Wang, D., White, L. A., and Jacobs, C. S., editors, *International VLBI Service for Geodesy and Astrometry 2010 General Meeting Proceedings*, pages 202–206.
- Sun, J. (2013). VLBI scheduling strategies with respect to VLBI2010. *Geowissenschaftliche Mitteilungen*, 92(92).
- Sun, J., Böhm, J., Nilsson, T., Krásná, H., Böhm, S., and Schuh, H. (2014). New VLBI2010 scheduling strategies and implications on the terrestrial reference frames. *Journal of Geodesy*, 88.
- Teke, K. (2011). Sub-daily parameter estimation in VLBI data analysis. *Geowissenschaftliche Mitteilungen*, 87(87).

REFERENCES

- Titov, O., Girdiuk, A., Lambert, S. B., Lovell, J., McCallum, J., Shabala, S., McCallum, L., Mayer, D., Schartner, M., de Witt, A., Shu, F., Melnikov, A., Ivanov, D., Mikhailov, A., Yi, S., Soja, B., Xia, B., and Jiang, T. (2018). Testing general relativity with geodetic VLBI. What a single, specially designed experiment can teach us. *A&A*, 618:A8.
- Treuhaft, R. N. and Lanyi, G. E. (1987). The effect of the dynamic wet troposphere on radio interferometric measurements. *Radio Science*, 22(2):251–265.
- Uunila, M., Nothnagel, A., and Leek, J. (2012). Influence of Source Constellations on UT1 Derived from IVS INT1 Sessions. In Behrend, D. and Baver, K. D., editors, *International VLBI Service for Geodesy and Astrometry 2012 General Meeting Proceedings*, pages 395–399.
- Vandenberg, N. (1997). *sked's Catalogs Program Reference Manual*. NVI, Inc. NASA/-Goddard Space Flight Center.
- Vandenberg, N. (1999). *sked: Interactive/Automatic Scheduling Program*. NVI, Inc. NASA/Goddard Space Flight Center.
- Walker, R. (2018). *The SCHED user manual*.